THE AMERICAN JOURNAL OF PATHOLOGY

VOLUME XXXV JANUARY-FEBRUARY, 1959 NUMBER 1

POLYOSTOTIC HYPEROSTOSIS IN THE FEMALE PARAKEET*

HANS G. SCHLUMBERGER, M. D.

From the Department of Pathology, Medical Center, University of Arkansas, Little Rock, Ark.

The striking deposition of medullary bone that occurs in female birds during the preovulatory stage of the egg-laying cycle was first reported in 1934 by Kyes and Potter.[1] The pigeon, the bird in which these changes were observed, has been extensively studied by several investigators.[2-4] With minor variations these findings have been confirmed in the chicken,[5] duck,[6] quail,[7] and sparrow.[7,8] The literature has been ably reviewed by the Silberbergs.[9]

During the past 3 years, over 1,300 Shell Parakeets, *Melopsittacus undulatus,* have been subjected to gross and histologic examination in this laboratory. It was noted that in the female parakeet medullary bone formation similar to that described in other birds occurs during the egg-laying cycle (Figs. 1 and 2). In addition, a remarkable exophytic overgrowth of bone was encountered in 21 of the hens (Table I). None of these birds was in active egg production at the time of necropsy.

MATERIAL AND METHODS

The birds were received during the period November, 1954, to April, 1958, from all sections of the United States and were genetically unrelated. Roentgenograms were made post mortem since in most instances the lesions were discovered at necropsy. Tissues were fixed in 10 per cent formalin, the bones were decalcified in a mixture of 10 per cent sodium citrate and 25 per cent formic acid. Stains were hematoxylin and eosin and Giemsa. For x-ray diffraction studies, the cortex from femurs of male birds provided normal bone; medullary bone was obtained from the femurs of hens during the preovulatory period. The cortex was ground away leaving the medullary bone intact. Specimens

* Supported by grants from the National Institutes of Health (C-3434) and the American Cancer Society (E-41).

Received for publication, June 16, 1958.

TABLE I

Female Parakeets Showing Hyperostosis

Bird no.	Age (yrs.)	Pituitary wt. (mg.)	Sites of hyperostosis												Remarks
			Skull	Sternum	Sacrum	Pelvis	Vertebrae	Ribs	Coracoid	Humerus	Radius	Ulna	Femur	Tibiotarsus	Hyoid	
1			+	+	+											Eggs retained in abdomen.
2								+	+						+	
3			+						+	+						Fatty liver; both coracoids affected.
4			+	+	+			+		+						
5			+	+	+	+		+	+	+			+	+		Paralysis of leg due to bony overgrowth at intervertebral foramen; 3 ribs, both coracoids.
6		0.95	+	+	+											
7	2	0.45		+	+	+	+	+								Paralysis of leg due to bony overgrowth at intervertebral foramen; 4th and 5th thoracic vertebrae.
8	2	0.75	+	+												Broke every egg she ever laid.
9			+	+		+				+						Serum alkaline phosphatase 52.7 K-A units, serum phosphorus 3.2 mg. %.
10	4	0.75	+	+	+				+							Pecked and killed her babies; both coracoids.
11		0.8		+												Small ovary with multiple cysts; islet cell tumor of pancreas.
12					+	+	+		+	+	+	+				1st to 4th cervical vertebrae and both ulnas.
13	4			+			+	+								
14	2		+	+	+	+		+								Cere half brown, half blue; blind due to bone overgrowth at optic foramens; hyperplastic thyroid.
15	4		+							+						
16	3				+											Small cysts in ovary; renal adenocarcinoma invading sacral exostosis; 7 clutches; raised 25 babies in 3 seasons.
17				+	+											
18	5			+	+		+		+	+						Serum calcium, 8.0 mg. %; alkaline phosphatase 165 K-A units.
19				+	+	+	+									Painted 2 times weekly for 7 mos. with 2% methylcholanthrene; fibrosarcoma in kidney and spleen; 10th to 12th cervical vertebrae.
20	2	1.25				+										Received 1,500 r. total body x-irradiation 567 days previously.
21		0.95	+		+	+			+							Received 2,750 r. x-irradiation 17 days previously; cystic ovary.

of cortex, medullary bone, and hyperostosis were thoroughly cleaned, washed and dried. Diffractograms of the powdered bone were prepared by Dr. Erwin Eichen in the Metallurgical Laboratory of Ohio State University.

To obtain enough blood for chemical analysis it was necessary to exsanguinate the birds by cardiac puncture. Total serum calcium was determined by the method of Clark and Collip[10]; total serum inorganic phosphate by the procedure of Fiske and Subbarow.[11] For serum alkaline phosphatase levels, expressed in King-Armstrong units, a modification of the method of Benotti, Rosenberg and Dewey[12] was used. Even with exsanguination, only 1.0 to 1.5 ml. of blood could be drawn from a single bird; therefore, no more than any two of these tests could be carried out on the same specimen.

Spontaneous Hyperostosis

Although these lesions were usually discovered at necropsy, in several cases the diagnosis was suspected in the living bird. One of these (no. 3) was kept under observation 2½ months, but no definite change in the size of the lesions could be recognized. A striking sign of hyperostosis noted in the live bird was exophthalmos due to the presence of bony masses growing from the orbital bones. When first seen, this was mistaken for the more frequently occurring retro-orbital extension of a pituitary tumor, a neoplasm that is quite common in the parakeet.[13] The exophthalmos may be partly obscured by overgrowth of the orbital ridges accompanied by a marked increase of the transverse diameter of the skull and of the interocular distance (Figs. 3 and 4). In one bird, blindness was due to pressure on the optic nerves, resulting from encroachment of bone on the optic foramens. Similar lesions affecting the intervertebral foramens led to paralysis of a leg in two cases. However, leg paralysis in the parakeet is more frequently the result of neural invasion by a renal cancer; indeed, in one instance both lesions were present. Bony masses occurring elsewhere than on the skull are usually hidden by feathers; occasionally large growths on the sternum may be felt during casual handling of the bird.

Because these were necropsy observations, blood chemical determinations were rarely made. In one bird (no. 9) the serum phosphorus of 3.2 mg. per hundred cc. was in the normal range; in another bird (no. 18) the serum calcium level was 8.0 mg. per hundred cc., also within normal limits. In both birds the alkaline phosphatase which in the non-laying female may be as high as 20 King-Armstrong (K-A) units, was elevated to 57.7 and 165 K-A units respectively.

Gross Description

The bones most often affected were those of the axial skeleton: sternum, sacrum, skull, ribs, vertebrae and hyoid, in descending order of frequency (Table I). Of the appendicular skeleton, the pelvis, coracoid, and humerus were more often involved than the femur, tibiotarsus, radius, and ulna. No lesions were encountered on the distal wing bones or those of the feet.

The distribution and some of the gross characteristics of the bony overgrowths may be seen in roentgenograms (Figs. 5 to 8, and 10). When the hyperostoses were small, large amounts of medullary bone were present (Fig. 5); with larger lesions this was less evident (Figs. 6 to 8). The affected ribs often showed a diffuse fusiform enlargement (Figs. 7 and 8) with a smooth surface (Fig. 9). A diffuse nodular thickening was also observed on the calvarium (Fig. 4); however, surface irregularities might be absent, and only a marked widening and increased density of the diploë noted (Fig. 10).

In the synsacrum (fused lumbar and sacral vertebrae), the hyperostosis was characteristically granular, sand-like in appearance, and extended vertically into the region of the kidneys. The largest bony masses were found on the sternum where they were usually multiple and reached a diameter of 2.5 cm. (Fig. 10). The surface was smooth, and the masses in some instances grew posteriorly into the thorax (Fig. 11) or anteriorly to displace the heavy pectoral muscles (Fig. 12). Although on first inspection all hyperostoses appeared intimately fused with the underlying bone, in some instances they could be pried free, following a line of cleavage between the osteophyte and normal bone.

No gross changes were observed in other organs which might be regarded as a characteristic accompaniment of the hyperostoses. No abnormalities were found in the lung that would link the hyperostoses to hypertrophic pulmonary osteoarthropathy. The pituitary, thyroids, and adrenals were normal, both by weight and microscopic structure. Despite careful examination, an ovarian abnormality was found in only 3 birds (nos. 11, 15, 21); in each of these the ovary bore numerous 2 to 5 mm. cysts. Associated neoplasms were found in 3 birds: an islet cell tumor of the pancreas (no. 11), a renal adenocarcinoma (no. 16), and a fibrosarcoma of the kidney and spleen (no. 19). In no instance has there been evidence of malignant change in the hyperostoses. Three cases of osteogenic sarcoma in parakeets examined in this laboratory failed to show hyperostosis on other bones.

Soft tissue calcifications such as occur in the lungs and kidneys in hypervitaminosis D were never seen, nor was there evidence of hypovitaminosis A in affected birds.

Microscopic Description

The histologic appearance of the hyperostoses was varied. The actively growing lesion was composed of irregular, interlacing trabeculae of bone and osteoid, with prominent cement lines attesting to the extent and rapidity of the structural changes (Fig. 13). At the periphery were several layers of elongate fusiform cells in process of differentiation into osteocytes (Fig. 14) and occasionally into chondrocytes (Fig. 15). The adjacent muscle showed none of the degenerative alterations and inflammatory cell infiltrations that characterize myositis ossificans (Fig. 14). In some areas fibrocytes and reticulum cells formed a prominent part of the lesion, and palisades of osteoblasts were apposed to the newly formed bone (Fig. 16). However, even in these regions of fibroblastic proliferation and bone formation there were foci of bone destruction, identified by the accumulation of multinucleate osteoclasts. Islands of hematopoietic tissue were also present.

In some hyperostoses active growth had apparently ceased; the bone was dense and did not take the deep blue color of young bone when stained with Giemsa stain. Most of the osteoblasts had become mature osteocytes incarcerated in the bone; only a few fibrocytes and reticulum cells remained in the narrow interstices that conveyed the nutrient vessels (Fig. 17). When examined with the polarizing microscope, the normal cortical bone of the parakeet shows double refraction due to the presence of broad bands of collagen fibers in linear orientation. In the hyperostoses, as well as in the medullary bone deposited during egg laying, double refraction was rarely seen, indicating lack of orientation of the collagen.

In many areas fusion between normal cortical bone and hyperostosis was such that the boundary between them could not be recognized. Occasionally, however, a broad cement line separated the two, and a cleft might appear during preparation of the tissue (Fig. 17). This is consistent with the observation that some of the hyperostoses could be pried free from the underlying bone.

Of particular interest was the observation that the degree of growth activity and bone formation in hyperostoses was not always a reflection of similar changes within the medullary cavity. In several instances in which there was very active bone formation in the hyperostoses, no medullary bone was present in shafts of the long bones.

X-Ray Diffraction Patterns

Because of the very rapid formation and subsequent destruction of medullary bone during the egg-laying cycle, it appeared possible that the composition of this provisional bone differed from that of the cortex. Some support for this was offered by Reed, Reed and Gardner,[14] who found that in medullary bone deposited within the femurs of mice receiving stilbestrol, the x-ray diffraction pattern carried some prominent lines characteristic of powdered egg shell ($Ca\ CO_3$). These were absent in diffractograms of normal cortical bone. These authors concluded that the medullary bone of the mice represented a progressive deposition of a disoriented mixture of $Ca\ CO_3$ and variable amounts of apatite.

The x-ray diffraction patterns obtained by Dr. E. Eichen with the parakeet bone submitted to him, whether of cortex, medulla, or a hyperostosis, were all identical and differed strikingly from that of parakeet egg shell (Fig. 18). In the diffractogram of each sample of bone, a single very faint line equivalent to the strongest line in the egg shell pattern probably represented a $Ca\ CO_3$ line.

The identity of the diffractograms of the normal cortical bone and that of the hyperostoses in parakeets is similar to the observations of others with human bone. Brandenberger and Schinz[15] observed that in a wide variety of bone lesions, including osteitis fibrosa cystica, osteomyelitis, rickets, Paget's disease, and osteopetrosis there was no abnormality of the x-ray diffraction pattern.

Experimental Induction of Hyperostoses

Hypervitaminosis D is often associated with soft tissue calcification and even bone formation. To determine its relation, if any, to hyperostosis in the parakeet, large doses of vitamin D_2 were administered to 4 female and 4 male birds. Each received two intramuscular injections of 50,000 units of vitamin D_2 at an interval of a week, followed one week later by a final injection of 100,000 units. Roentgenograms made after one month were negative. The birds were sacrificed when 3 months had elapsed since the last injection. Neither on the postmortem roentgenograms nor on gross and microscopic examination was there evidence of medullary or periosteal bone formation.

In view of the striking deposition of medullary bone in the hen parakeet during the egg-laying period, and because the hyperostoses have been found only in females, it appears likely that the induction of the bone lesion is associated with some hormonal disturbance, probably linked with estrogens.

Stilbestrol, when administered as 3 to 6 mg. pellets beneath the skin,

induces in parakeets of both sexes a prompt rise in serum calcium and alkaline phosphatase, but no significant change in the serum phosphorus. In birds bled 9 days after administration of 6 mg. of stilbestrol, the serum calcium averaged 36.0 mg. per hundred cc. of blood, with a range of 22.8 to 41.1 mg. Normal values are usually 8 to 10 mg., but may be as high as 17 mg. The same birds had an average inorganic serum phosphate level of 2.4 mg. with a range of 0.5 to 4.0 mg.; this is similar to that of untreated birds. The alkaline phosphatase levels were from 55.8 to 99.6 King-Armstrong units; the average was 74.2 units. In normal birds there was considerable variation, the values ranging from 8 to 20 K-A units.

Although medullary bone is more rapidly deposited in non-laying females receiving stilbestrol than it is in similarly treated males, the levels of serum calcium, inorganic phosphate, and alkaline phosphatase show no significant sex difference. Both sexes manifest a striking hyperlipemia, associated with an accumulation of fat in the liver cells and often with fatty dystrophy of cardiac and even skeletal muscle.

Among birds receiving stilbestrol, the early osseous changes were limited to the deposition of medullary bone, particularly in the femur. Histologically this was seen to begin in apposition to the inner surface of the cortical bone and was preceded and accompanied by focal hyperplasia of the endosteum and adjacent reticulum cells which subsequently became osteocytes (Fig. 19). Later the other long bones as well as the diploë of the calvarium showed similar changes.

Hyperostoses were not observed in any birds which lived less than 100 days after beginning treatment with stilbestrol. Among 16 parakeets that received a single 4.5 mg. pellet of stilbestrol, 4 of the 10 which survived over 100 days developed hyperostoses. Of 11 that were given 7 mg. of stilbestrol monthly and lived more than 100 days, 5 had hyperostoses; and among 6 birds that received 3 mg. of stilbestrol monthly for over 100 days, 3 showed hyperostoses. Male as well as female birds developed the lesions.

The overgrowths occurred most commonly on the ventral aspect of the sacrum, encroaching on the kidney bed (Fig. 20) and had the same granular appearance as those occurring spontaneously in this region. A similar alteration was frequently seen in the ribs, which appeared greatly widened; in two instances this was associated with the appearance of discrete nodules of bone (Figs. 21 to 23). In one case several small, well circumscribed hyperostoses that closely resembled the spontaneous lesion, were found on the sternum (Figs. 24 and 25). Histologically all of these lesions were identical with those encountered in untreated birds.

Although in several instances the birds were kept on stilbestrol over a year, in none did the hyperostoses approach the spontaneous lesions in size. That some factors in addition to excess estrogenic hormone may play a part was considered. Of these, chronic inflammation and the healing response appeared most promising.

Powdered magnesium silicate was introduced beneath the scalp over a portion of the calvarium where multiple incisions had been made in the periosteum. Nine male and 9 female parakeets so treated received a 7 mg. pellet of stilbestrol every 6 weeks. After 33 weeks the 7 surviving birds were killed and the calvarium examined grossly and microscopically for the presence of hyperostoses. None of these birds nor any of those that had died earlier showed bone lesions at the site of the silicate. A foreign body giant cell reaction was evident in the periosteum, but this was unaccompanied by bone formation.

To determine the possible role of fibroblastic proliferation and differentiation on the formation of hyperostoses, a study of this response in stilbestrol-treated birds was undertaken. At the beginning of the experiment, each of 18 birds received 4.5 mg. of stilbestrol; this was repeated at monthly intervals. The left tibiotarsus, and after 8 weeks the right humerus, of each bird was fractured. Healing was accompanied by extensive fibroblastic proliferation and metaplastic bone and cartilage formation, but the stilbestrol-induced medullary bone did not have any demonstrable effect on fracture healing. After a month most excess callus had been resorbed, and after 3 months the former fracture sites were difficult to recognize; no hyperostoses were present.

Discussion

Lesions similar to polyostotic hyperostosis of the parakeet have not been described in other birds. The well known "osteopetrosis" of chickens affects chiefly the bones of the extremities and is a manifestation of one variety of lymphomatosis.[16] In view of the probable relationship of parakeet hyperostoses to estrogenic hormones and associated changes in bone metabolism, the absence of this lesion in chickens becomes noteworthy. Chickens of some breeds, e.g. white Leghorn, may lay 300 eggs within a year and have continuously elevated serum lipid and calcium levels.[17] A possible clue may be sought in the fact that parakeets with hyperostosis were never under two years of age, and many were older. The most active reproductive period of these birds is at the end of the first year; thereafter, egg production declines. It is at this time that hyperostoses begin to appear; viz., at an age when most chickens have already been slaughtered.

Correlative material from mammals is not at hand, with the possible

exception of an interesting lesion observed in pregnant women. In the later stages of pregnancy, thin vascular sheets of lamellar bone have been found lining the inner table of the calvarium, particularly in the frontal and parietal regions. The lesion has been fully described by Greig[18] and recently reported by Haslhofer.[19] It does not occur in men. The concentration of estrogens increases during pregnancy, reaching a peak some time before the beginning of parturition. It is probable that the appearance of the endocranial osteophytes bears some relation to the concentration of estrogenic hormone.

Recently Dessauer, Fox and Gilbert[20] have reported that in viviparous Colubrid snakes the increase of serum calcium, magnesium, and proteins in females during estrus equals or is greater than that found in preovulatory birds. At some time during their evolution these reptiles probably laid eggs with shells, impregnated by calcium salts. Since this depository for calcium has been lost, it would be of interest to examine females of these species for the occurrence of hyperostoses.

The absence of hyperplasia of the parathyroid in birds with spontaneous hyperostoses and those receiving estrogen is consistent with experimental results observed in other animals. Riddle, Rauch and Smith[14] found that estrogens administered to parathyroidectomized pigeons produced an elevation of serum calcium similar to that in the intact animal. Benoit and Clavert[21] noted that estrogens still led to medullary bone formation in these birds, although mineralization was impaired. Using Ca^{45}, Manunta, Saroff and Turner[22] reported that in rats the role of estrogen in calcium metabolism was independent of parathyroid hormone. Recently McLean[23] has pointed out that in young animals the turnover of serum calcium may amount to 100 per cent per minute and that this rapid exchange between blood and bone is independent of the parathyroid glands. Such a rate of calcium transfer is consistent with the remarkable rapidity with which medullary bone is laid down and resorbed in birds such as the pigeon and parakeet during the period of egg laying.

Pituitary tumors were not encountered in parakeets with hyperostosis. A transplantable pituitary tumor that probably secretes a growth hormone[24] was inoculated into birds receiving stilbestrol. The transplants grew well, but no hyperostoses developed, although in human subjects with acromegaly some bony overgrowth is known to occur, particularly in the calvarium. Urist, Budy and McLean,[25] in their study of endosteal bone formation in estrogen-treated mice, observed that the osteogenic action of estrogen is neither enhanced nor inhibited by simultaneous treatment of the animals with preparations of anterior pituitary hormone. It may be noted parenthetically that

estrogen-treated mice, even in the presence of medullary bone formation, have normal levels of serum calcium, phosphorus, and alkaline phosphatase.

The hyperostoses have been found to occur spontaneously only in female parakeets. The absence of conspicuous ovarian abnormalities in hens bearing these overgrowths is disappointing. Although cysts were present in the ovaries of 3 birds, in the others no significant gross or microscopic lesions could be recognized. In some there was abnormal behavior, such as breaking eggs, pecking and killing babies; in one bird several eggs had been retained in the abdominal cavity. In no instance were the ovaries atrophic; the follicles, though small, were larger than those in the involuted gonad.

It is well known that the liver serves to inactivate estrogens. An impairment of this hepatic function would therefore lead to an increase in circulating estrogen. The livers of many parakeets bearing hyperostoses showed fatty vacuoles in the liver cells, a change which Campbell[26-28] has found in the female fowl. He suggested that this might account for the diminished efficiency of the liver of the hen in the bromsulphalein excretion test as compared to that of the cock. In several of the parakeet livers there were also occasional small inflammatory cell infiltrates in the interstitial tissue, but these were never striking. Biskind[29] has shown that the ability of the liver to inactivate estrogen is dependent upon an adequate vitamin intake. He pointed out that impairment of the estrogen-inactivating mechanism may occur in the absence of detectable morphologic alteration. In some instances, therefore, the hyperostoses in the parakeet may be a reflection of impaired liver function.

The role of estrogen in the induction of medullary bone in birds has been examined by numerous investigators.[9] The striking hyperlipemia often observed in estrogen-treated parakeets probably bears little relation to the serum calcium level, for Schjeide and Urist[30] reported that in similarly treated roosters the chylomicrons and lipoproteins bound less than 5 per cent of the serum calcium; most of it was associated with a phosphoprotein. Govaerts, Dallemagne and Melon,[31] who used Ca^{45} as an indicator, found that in the pigeon exogenous estrogen increased radiocalcium retention much more than the hormone physiologically secreted by the ovaries. This also raises the question whether a naturally occurring estrogen such as estrone behaves differently from an artificial one, e.g., stilbestrol. To determine this a dozen parakeets were injected with 3 mg. pellets of estrone and observed for two months. The production of medullary bone was similar to that found in stil-

bestrol-treated birds. Hyperostoses were not seen, but the time lapse was less than that usually necessary to produce these lesions even with stilbestrol.

The presence of medullary bone may be taken as evidence of estrogen stimulation in the bird; it was found in the long bones of all parakeets receiving stilbestrol. Its occurrence in birds with early spontaneous periosteal overgrowths serves to link these lesions with the estrogenic hormone. In cases with large hyperostoses there may be little medullary bone remaining; this suggests that estrogenic stimulation has greatly decreased. Whether the hyperostoses will continue to increase in size in the absence of such stimulation is not clear from the material available. However, medullary bone was absent occasionally from the long bones of a bird in which large hyperostoses were the site of striking osteoblastic activity. This would suggest that continued growth of the hyperostosis was not dependent on estrogenic stimulation. Support for this was also found in the presence of a normal serum calcium level of 8.0 mg. per hundred cc. of blood, associated with the strikingly high alkaline phosphatase of 165 K-A units (bird no. 18).

Summary

Among approximately 1,300 parakeets *Melopsittacus undulatus* necropsied during the past 3 years, 21 females aged 2 to 4 years had polyostotic hyperostoses; no males bore similar lesions. The skull, sternum, vertebrae, and sacrum were most often affected. The overgrowths ranged in size from 2 or 3 mm. to 2.5 cm. in diameter; some that arose from the retro-orbital bone led to exophthalmos. Nerve pressure by sacral exostoses produced leg paralysis.

During the egg-laying period, parakeet hens normally produce large amounts of endosteal bone in the humerus and femur. Similar changes were found in some of the birds with hyperostoses. This and the sex-linkage of the lesions suggests that an excess of estrogen may be a causative factor although no consistent ovarian abnormalities were observed.

Stilbestrol will induce endosteal bone formation, as well as lipemia and hypercalcemia. Slightly less than half of the birds receiving stilbestrol and surviving over 100 days developed small hyperostoses. The lesions were usually limited to the sacrum, but in two cases nodules were present on each of two ribs. Though only 2 to 5 mm. in diameter, these hyperostoses grossly and histologically resembled the spontaneous variety.

REFERENCES

1. Kyes, P., and Potter, T. S. Physiological marrow ossification in female pigeon. *Anat. Rec.*, 1934, **60**, 377–379.
2. Pfeiffer, C. A., and Gardner, W. U. Skeletal changes and blood serum calcium level in pigeons receiving estrogens. *Endocrinology*, 1938, **23**, 485–491.
3. Bloom, W.; Bloom, M. A., and McLean, F. C. Calcification and ossification. Medullary bone changes in the reproductive cycle of female pigeons. *Anat. Rec.*, 1941, **81**, 443–475.
4. Riddle, O.; Rauch, V. M., and Smith, G. C. Action of estrogen on plasma calcium and endosteal bone formation in parathyroidectomized pigeons. *Endocrinology*, 1945, **36**, 41–47.
5. Landauer, W.; Pfeiffer, C. A.; Gardner, W. U., and Man, E. B. Hypercalcification, -calcemia and -lipemia in chickens following administration of estrogens. *Proc. Soc. Exper. Biol. & Med.*, 1939, **41**, 80–82.
6. Landauer, W., and Zondek, B. Observations on the structure of bone in estrogen-treated cocks and drakes. *Am. J. Path.*, 1944, **20**, 179–209.
7. Ringoen, A. R. Deposition of medullary bone in the female English sparrow, *Passer domesticus* (Linnaeus), and the bob-white quail, *Colinus virginianus*. *J. Morphol.*, 1945, **77**, 265–280.
8. Pfeiffer, C. A.; Kirschbaum, A., and Gardner, W. U. Relation of estrogen to ossification and the levels of serum calcium and lipoid in the English sparrow, *Passer domesticus*. *Yale J. Biol. & Med.*, 1940, **13**, 279–284.
9. Silberberg, M., and Silberberg, R. Steroid Hormones and Bone. In: The Biochemistry and Physiology of Bone. Bourne, G. H. (ed.). Academic Press, Inc., New York, 1956, pp. 623–670.
10. Clark, E. P., and Collip, J. B. A study of the Tisdall method for the determination of blood serum calcium with a suggested modification. *J. Biol. Chem.*, 1925, **63**, 461–464.
11. Fiske, C. H., and Subbarow, Y. The colorimetric determination of phosphorus. *J. Biol. Chem.*, 1925, **66**, 375–400.
12. Benotti, J.; Rosenberg, L., and Dewey, B. Modification of the Gutman and Gutman method of estimating "acid" phosphatase activity. *J. Lab. & Clin. Med.*, 1946, **31**, 357–360.
13. Schlumberger, H. G. Neoplasia in the parakeet. I. Spontaneous chromophobe pituitary tumors. *Cancer Res.*, 1954, **14**, 237–245.
14. Reed, C. I.; Reed, B. P., and Gardner, W. U. The influence of estrogens on the crystal structure of bone as revealed by x-ray diffraction studies on the femora of mice. *Endocrinology*, 1946, **38**, 238–244.
15. Brandenberger, E., and Schinz, H. R. Über die Natur der Verkalkungen bei Mensch und Tier und das Verhalten der anorganischen Knochensubstanz im Falle der hauptsächlichen menschlichen Knochenkrankheiten. Benno-Schwabe & Co., Basel, 1946, 63 pp.
16. Jungherr, E. Studies in fowl paralysis. III. A condition resembling osteopetrosis (marble bone) in the common fowl. *Storrs Agr. Exp. Sta. Bull.*, 1938, **222**, 1–34.
17. Breneman, W. R. Reproduction in Birds: the Female. In: Comparative Physiology of Reproduction and the Effects of Sex Hormones in Vertebrates. Jones, I. C., and Eckstein, P. (eds.). Cambridge University Press, Cambridge, 1955, pp. 94–113.
18. Greig, D. M. On intracranial osteophytes. *Edinburgh M. J.*, 1928, **35**, 165–191, and 237–260.

19. Haslhofer, L. Zur Kenntnis des Schwangerschafts-Osteophyts am Schädeldach. *Wien. klin. Wchnschr.*, 1958, **70**, 297–299.

20. Dessauer, H. C.; Fox, W., and Gilbert, N. L. Plasma calcium, magnesium and protein of viviparous Colubrid snakes during estrous cycle. *Proc. Soc. Exper. Biol. & Med.*, 1956, **92**, 299–301.

21. Benoit, J., and Clavert, J. Osteogénèse folliculique chez les oiseaux. Influence des diverses glandes endocrines. *Compt. rend. l'Assoc. Anat.*, 1950, **37**, 533–535.

22. Manunta, G.; Saroff, J., and Turner, C. W. Relationship between estradiol and parathyroid on retention of Ca^{45} in bone and blood serum of rats. *Proc. Soc. Exper. Biol. & Med.*, 1957, **94**, 785–787.

23. McLean, F. C. The ultrastructure and function of bone. *Science*, 1958, **127**, 451–456.

24. Schlumberger, H. G. Neoplasia in the parakeet. II. Transplantation of the pituitary tumor. *Cancer Res.*, 1956, **16**, 149–153.

25. Urist, M. R.; Budy, A. M., and McLean, F. C. Endosteal bone formation in estrogen-treated mice. *J. Bone & Joint Surg.*, 1950, **32-A**, 143–162.

26. Campbell, J. G. Studies on the influence of sex hormones on the avian liver. I. Sexual differences in avian liver clearance curves. *J. Endocrinol.*, 1957, **15**, 339–345.

27. Campbell, J. G. Studies on the influence of sex hormones on the avian liver. II. Acute liver damage in the male fowl, and the protective effect of oestrogen, as determined by a liver function test. *J. Endocrinol.*, 1957, **15**, 346–350.

28. Campbell, J. G. Studies on the influence of sex hormones on the avian liver. III. Oestrogen-induced regeneration of the chronically damaged liver. *J. Endocrinol.*, 1957, **15**, 351–354.

29. Biskind, M. S. Nutritional therapy of endocrine disturbances. In: Vitamins & Hormones. Harris, R. S., and Thimann, K. V. (eds.). Academic Press, Inc., New York, 1946, Vol. 4, pp. 147–185.

30. Schjeide, O. A., and Urist, M. R. Proteins and calcium in serums of estrogen-treated roosters. *Science*, 1956, **124**, 1242–1244.

31. Govaerts, J.; Dallemagne, M. J., and Melon, J. Radiocalcium as an indicator in the study of the action of estradiol on calcium metabolism. *Endocrinology*, 1951, **48**, 443–452.

[*Illustrations follow*]

LEGENDS FOR FIGURES

FIG. 1. Sagittal section through femur of a female parakeet in resting phase of ovulatory cycle. Marrow cavity is filled with hematopoietic tissue. Giemsa stain. × 90.

FIG. 2. Sagittal section through femur of a 3-year-old female parakeet in egg-laying cycle. Most of the marrow cavity is occupied by darkly staining medullary bone. Giemsa stain. × 90.

FIG. 3. Exophthalmos and widened interocular space due to overgrowth of periorbital bone. Bird no. 3.

FIG. 4. Calvarium of bird shown in Figure 3, eyes and beak still present. Heavy periorbital ridges, greatly thickened, and irregular outer table.

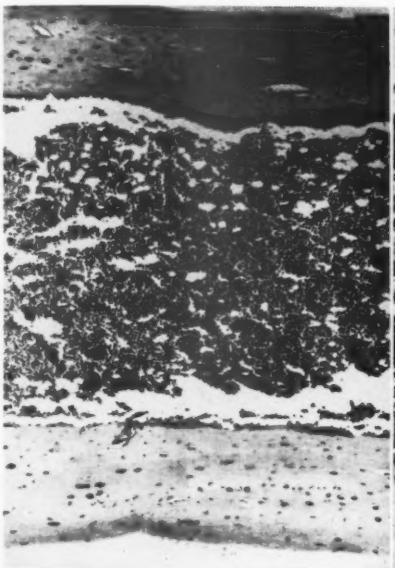

1

2

3

4

FIG. 5. Roentgenogram; sternum and portion of both coracoids removed, cervical vertebrae dislocated. Bones of wings and legs show extensive areas of increased density due to deposits of medullary bone. On left humerus is a small hyperostosis. For microscopic appearance, see Figure 17. Irregular hyperostosis on synsacrum, small nodule on right fifth rib. Bird no. 4. Natural size.

FIG. 6. Roentgenogram; massive hyperostosis of left coracoid, left radius and ulna, left ilium, cervical and lumbar vertebrae, and synsacrum. Small deposits of periosteal bone are seen on the right humerus. Bird no. 12. Natural size.

FIG. 7. Roentgenogram; sternum and coracoids removed. (For gross appearance of sternum, see Figure 11). Medullary bone in both humeri. Hyperostoses on third left rib, synsacrum, and right ilium. Bird no. 14. Natural size.

FIG. 8. Roentgenogram; cervical dislocation, sternum and right coracoid removed. Hyperostosis of anterior portion of mandible, massive involvement of hyoid bone. Hyperostosis of left coracoid, right seventh rib, synsacrum, and left ilium. Small periosteal deposits at distal end of right humerus and femur. Bird no. 2. Natural size.

FIG. 9. Same bird as in Figure 8, showing lesion of left coracoid and rib, synsacrum, and right ilium. × 1.5.

FIG. 10. Roentgenogram; bony thickening of skull and mandible. Massive hyperostoses on sternum, small bony overgrowths on left humerus and pelvis. Bird no. 9. Natural size.

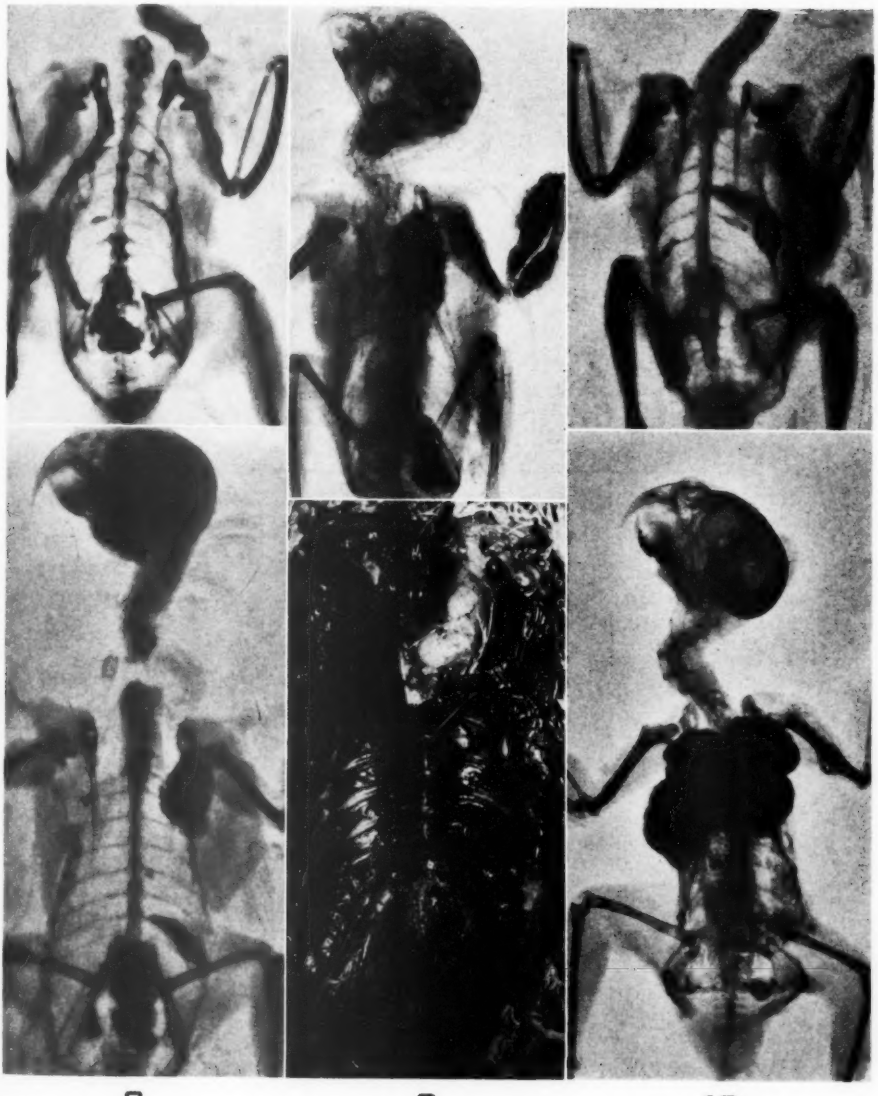

5

6, 7

8

9

10

FIG. 11. Inner aspect of sternum showing large hyperostoses. For rest of skeleton see Figure 7. Bird no. 14. × 2.7.

FIG. 12. Sagittal section through sternum and pectoral muscle. A large hyperostosis, of which a small part extends into the chest cavity; the largest portion has displaced and produced atrophy of the overlying muscle. Bird no. 11. × 2.4.

FIG. 13. Bone of hyperostosis showing prominent cement lines. Bird no. 14. Hematoxylin and eosin stain. × 240.

FIG. 14. Margin of hyperostosis showing peripheral layer of fibroblasts and attached skeletal muscle. Bird no. 14. Hematoxylin and eosin stain. × 240.

FIG. 15. Margin of hyperostosis; the peripheral layer of fibroblasts is in process of metaplastic change to cartilage. Bird no. 14. Hematoxylin and eosin stain. × 240.

FIG. 16. Active bone formation in hyperostosis evidenced by palisading of osteoblasts, proliferating fibroblasts and reticulum cells. A collection of osteoclasts may be seen adjacent to one of the bone trabeculae. Bird no. 14. Hematoxylin and eosin stain. × 260.

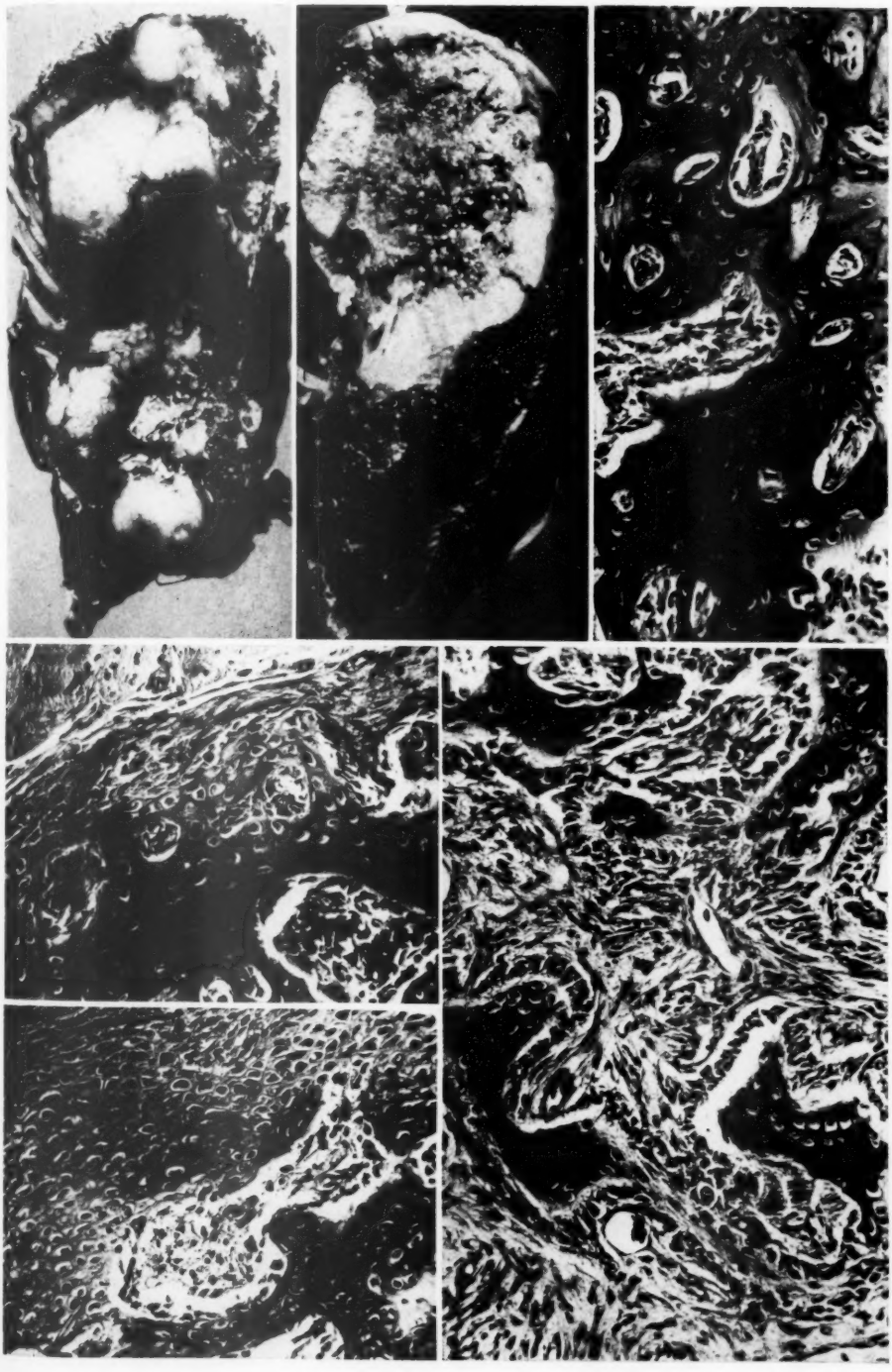
11
12, 13
14
16
15

FIG. 17. Small hyperostosis on humerus. The former separated partly from the underlying cortex during preparation of the slide. The bone of the hyperostosis, as well as the medullary bone seen near the right side of the figure, is dense, with little evidence of osteoblastic or osteoclastic activity. For appearance in roentgenogram see Figure 5. Bird no. 4. Hematoxylin and eosin stain. × 90.

FIG. 18. X-ray diffraction patterns of powdered bone and egg shell. Only the central portion of each diffractogram is reproduced. Reading from top to bottom: normal cortical bone, medullary bone from female during egg laying period, bone of hyperostosis, parakeet egg shell. The identity of the 3 bone patterns and the pronounced difference of the egg shell pattern is apparent.

FIG. 19. Early medullary bone formation in male parakeet 9 days after inoculation with 6 mg. of stilbestrol. Reticulum cell hyperplasia and appearance of osteoid ground substance adjacent to small endosteal osteophyte. Bird ST5-5. Hematoxylin and eosin stain. × 500.

FIG. 20. Transverse section through lateral portion of synsacrum. Dark gray areas are newly formed bone—hyperostosis. The circular light gray mass is kidney. A male bird that received 3 mg. of stilbestrol subcutaneously at intervals of a month, sacrificed 145 days after beginning of treatment. For roentgenogram see Figures 21 and 22. Bird ST 2-1. Giemsa stain. × 32.

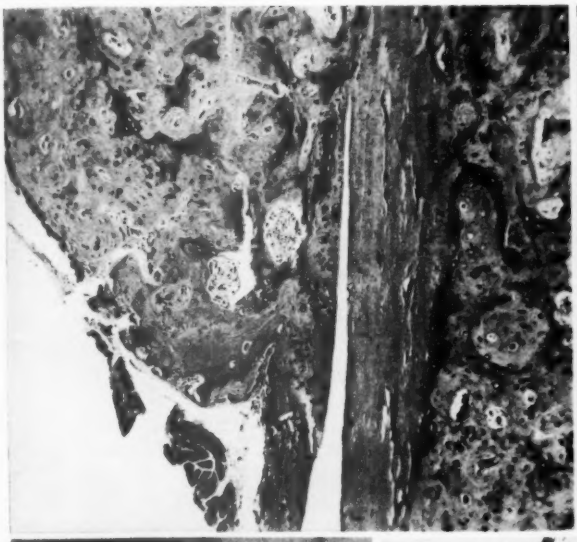

17

19

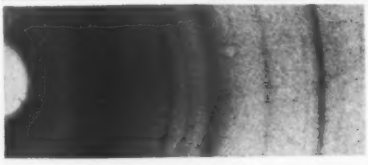

18

20

FIG. 21. Roentgenogram; sternum and portion of both coracoids removed. Stilbestrol-treated bird; for data see previous figure legend. Density of long bones is due to obliteration of marrow cavities by medullary bone. Diffuse periosteal bone formation about synsacrum and all ribs; small hyperostoses on right sixth and left seventh ribs. Bird ST 2-1.

FIG. 22. Enlargement of previous figure to show changes about ribs.

FIG. 23. Hyperostosis on fifth left rib. Female parakeet, 2 weeks after the last of 7 monthly subcutaneous implantations of a 7 mg. pellet of stilbestrol. Bird ST-9. × 6.

FIG. 24. Hyperostoses on inner aspect of sternum. Female parakeet, 3½ months after subcutaneous implantation of a 4.5 mg. pellet of stilbestrol. Bird ST 3-7. × 3.

FIG. 25. Section through smaller of the two hyperostoses shown in the previous figure. Hematopoietic tissue is present in the spaces between the bone trabeculae. The bony overgrowth has separated slightly from the underlying sternum. Hematoxylin and eosin stain. × 32.

21

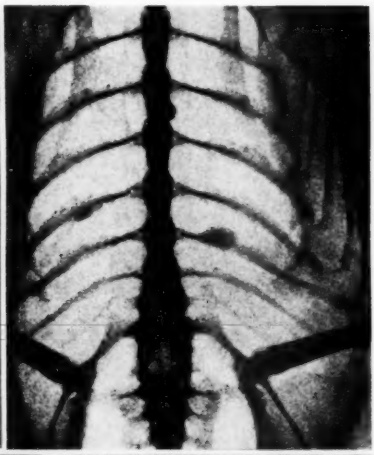

22

23

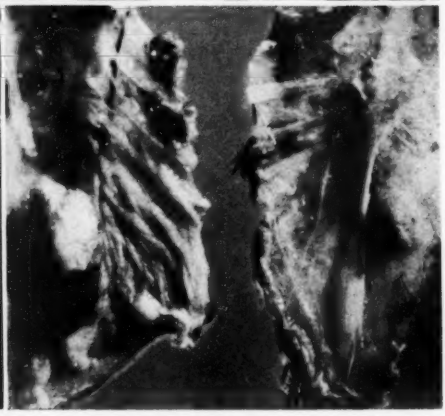

24

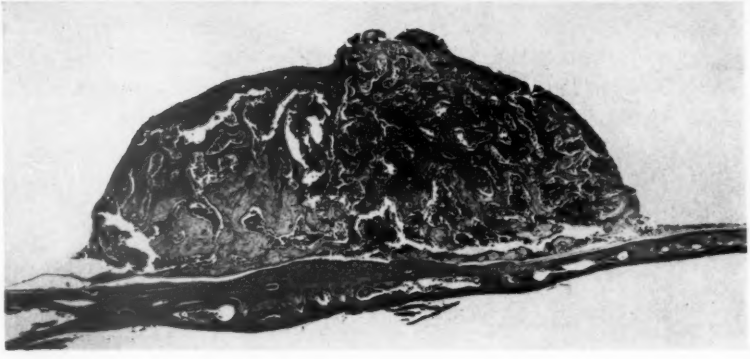

25

SUBACUTE GLOMERULONEPHRITIS *

JACOB CHURG, M.D. and EDITH GRISHMAN, M.D.
From the Department of Pathology, the Mount Sinai Hospital, New York, N.Y., and the Laboratories, Barnert Memorial Hospital, Paterson, N.J.

Subacute glomerulonephritis is the transitional phase between the acute and the chronic stages. As such, it provides an opportunity to examine the development of pathologic alterations which lead to eventual glomerular obsolescence and chronic renal failure. Clinically, subacute glomerulonephritis encompasses the period 2 to 12 months after the onset of illness, and is characterized by albuminuria, edema, hypertension, and uremia. The typical anatomic feature is a large, smooth, pale kidney, which, on microscopic examination, shows cellular proliferation and fibrosis in the glomerular tufts, epithelial crescents, and alteration of the capillary walls.

With recent advances in microscopic technique, it has become possible to study glomerular lesions in greater detail by means of thin (0.5 μ) sections stained by newer procedures or examined under the phase microscope. In a previous communication this technique was applied to the kidney in acute glomerulonephritis.[1] The present paper deals with observations in the various forms of subacute glomerulonephritis.

MATERIAL AND METHODS

The tissues were taken from the files of the Department of Pathology of the Mt. Sinai Hospital and the Barnert Memorial Hospital. Case 23 was obtained from the Newark Beth Israel Hospital through the courtesy of Dr. M. Kannerstein, and case 24 from the Knickerbocker Hospital, New York City, through the courtesy of Dr. W. Finkelstein.

Twenty-eight cases were examined. Most of these fulfilled both the clinical and the pathologic criteria outlined above. However, for the sake of completeness, one case with prominent epithelial crescents was also included. The patient had a very short history of only two weeks. At the other extreme, there were a number of patients (8) with manifestations of renal disorder of 14 months' to 3 years' duration but who presented the anatomic and histologic features of the subacute stage.

The methods employed have been described previously.[1] Kidney tissues from paraffin blocks were re-embedded in celloidin-paraffin

* Supported by research grant [A-918 (C) Path.] from the National Institute of Arthritis and Metabolic Diseases of the National Institutes of Health, United States Public Health Service, Bethesda, Md.

Presented at the Fifty-fourth Annual Meeting of the American Association of Pathologists and Bacteriologists, Washington, D.C., April 13, 1957.

Received for publication, June 30, 1958.

and cut serially at a thickness of 0.5 μ. Sections were stained with hematoxylin and eosin, the periodic acid-Schiff reagent (PAS),[2] a modified Mallory chromotrope-aniline blue stain (CAB),[3] and the periodic acid-silver methenamine method (PA-SM).[4] Some sections were also stained with PAS-colloidal iron by the method of Ritter and Oleson,[5] and some were examined by phase microscopy.[6]

Observations

Glomeruli

The two classical histologic characterizations of the lesion in subacute glomerulonephritis are designated as the extracapillary and intracapillary, or better, intercapillary, types. In recent years "membranous glomerulonephritis" has been added as a separate form. In our experiments the division into these 3 types is somewhat artificial, because many patients show various combinations of changes, including proliferation of epithelial cells with crescent formation, proliferation of intercapillary cells and fiber production, and alteration of the capillary walls. However, for the sake of clarity, these changes will be discussed separately.

Intercapillary Space. The intercapillary alterations in subacute glomerulonephritis are the direct continuation of those seen in the acute phase. The onset of the subacute stage is signaled by the deposition of fibers among the proliferated mononuclear cells in the intercapillary space (Fig. 1). At the beginning of this stage, mononuclear cells still predominate in this region; a small number of polymorphonuclear leukocytes may be evident, and there is a variable degree of edema (Fig. 3). The fibers are generally slender and tortuous, and stain red with the PAS and blue with the CAB stains. The entire intercapillary space is enlarged. The capillaries are shifted to the periphery of the lobule and are partly compressed (Fig. 1). They may contain a few red cells but are often empty. With progression of the disease, edema and leukocytes disappear completely, the mononuclear cells are fewer, and fibers increase in number and thickness. In many cases, hyaline material appears in the intercapillary space (Fig. 2). This substance stains red with PAS and pink to red with CAB. It appears to lie between the fibers, though often it fuses with them. Occasionally one gains the impression that the fibers themselves undergo hyaline transformation. Toward the end of the subacute stage, the intercapillary space becomes converted into a fibrous or fibro-hyaline mass containing but few cells. The size of the scar varies from case to case and from lobule to lobule. Some of the capillaries remain patent while others are completely collapsed.

Epithelial Cells and Bowman's Space. Proliferation of epithelial cells may occur early in the disease. Some of the patients dying within 2 to 4 weeks after the onset of acute glomerulonephritis reveal luxuriant epithelial crescents. Whether crescents appear early or late, their structure is the same. The proliferating cells are, as is well known, those of the parietal layer of Bowman's capsule. Thin fibers lying between the cells contribute toward formation of so-called pseudo-tubules. The fibers often appear to originate from the inner layer of Bowman's capsule and to branch among the epithelial cells (Fig. 14). This suggests that they are products of the basement membrane of Bowman's capsule rather than newly formed fibers. The membranes or fibers are at first thin and delicate, staining red with PAS and blue with CAB stains. However, they undergo rapid transformation, becoming thicker and less intensely eosinophilic, and losing their affinity for PAS. As the fibers increase in thickness, the epithelial cells decrease in number and eventually disappear, giving rise to so-called "fibrous crescents."

Not all fibrous crescents arise from the epithelial crescents. It is our impression that some of them are the result of repeated splitting, fibrosis, and hyalinization of Bowman's capsule. Alterations of this nature can be observed even in the acute stages of glomerulonephritis, and they are common in the subacute stage.

The visceral glomerular epithelium is often prominent in glomerulonephritis. Whether this is the result of actual multiplication or merely of swelling is difficult to state. These cells frequently contain hyaline droplets analogous to droplets observed in the epithelium of the tubules, or in the parietal epithelium of Bowman's capsule (Fig. 13). The hyaline droplets are usually accompanied by the appearance of hyalin in the intercapillary spaces.

Capillary Wall. Changes in the capillary wall may proceed in two directions. Attenuation of the basement membrane and even complete local disappearance sometimes accompany deposits of hyaline material in the capillary lumen. The hyaline appears to spill through a break in the wall into Bowman's space.

Much more frequently encountered is thickening of the capillary wall. This may be due to splitting or reduplication of the wall, so that internal to the basement membrane and separated by a space of varying width (pericapillary space) there is another membrane which varies in thickness and is sometimes discontinuous (Fig. 8). This second ("endothelial") membrane probably represents the innermost layer of the original basement membrane split off by extension of exudate from the intercapillary space, as observed in acute glomerulonephritis.[1] Connection between the intercapillary space and the peri-

capillary space can often be demonstrated (Fig. 10). The pericapillary space may contain a few cells but otherwise appears empty in sections (Fig. 8); in life it is probably filled with fluid or other substance that is easily washed out in processing tissue.

Splitting or reduplication of the wall is usually focal and variable. It rarely affects the whole glomerulus and rarely affects the majority of the glomeruli. If hyaline deposits are found in the intercapillary space, they may also be present in the pericapillary space. The hyalin is strongly eosinophilic, staining red with PAS and CAB. The affected capillary bears a considerable resemblance to the "wire loop" of lupus erythematosus (Fig. 10). Splitting of the capillary wall may also occur as a result of deposits of hyalin, causing separation of the endothelium (*membrana attenuata*)[7] from the basement membrane. This type of "wire-loop" thickening appears homogeneous with hematoxylin and eosin and PAS stains (Fig. 11), but the deposits can be clearly distinguished from the basement membrane by the PA-SM stain (Fig. 12).*

Another type of thickening of the capillary wall frequently associated with the nephrotic syndrome is the "membranous glomerulonephritis" described by Bell[8] (Figs. 3 to 6). The endothelium and basement membrane here appear little altered. However, between the basement membrane and the epithelial cells, there is a layer which can be quite wide (1 to 2 μ or more). This layer consists of two elements: hair-like or spike-like projections perpendicular to the basement membrane and spaced about 0.5 to 1.0 μ apart; and hyaline material deposited between these spikes. The spikes rest with their narrow points upon the basement membrane and widen toward the periphery. They sometimes appear to merge at their bases, creating a scalloped edge covering the hyaline deposit. The edge and the spikes stain red with PAS and blue with CAB. They are also strongly black with the PA-SM stain[4] and are blue when stained by the Ritter-Oleson procedure. The hyalin stains pale pink with PAS, red with CAB, and does not stain with PA-SM stains. Preliminary studies with electron microscopy suggest that the hyalin accumulates between the basement membrane and epithelial cells (podocytes) and that the spikes are in some way related to the epithelial trabeculae and foot processes. Within the cytoplasm and parallel to the basement membrane, one can frequently see a row of fine dots which stain red with the CAB stain. The significance of these dots is not clear at the present time.

* Though both the PAS and PA-SM stains are supposed to demonstrate the same chemical groupings, our experience has shown that there are consistent differences between the results obtained by the two methods which may serve differential staining purposes.

Endothelial Cells and Capillary Lumen. The endothelial cells often appear enlarged and have prominent nuclei. In some of the cases with manifestations of the nephrotic syndrome, the cytoplasm of the endothelium is markedly swollen and filled with fine vacuoles presumably because of lipid imbibition (case 25). The lumen of the partly collapsed capillaries is sometimes filled with homogeneous material which stains pale pink with eosin and PAS. Presumably this represents inspissated blood plasma.

In summary (Tables I and II), among the 28 examples examined, significant alterations (2+ or greater) in the various components of the glomerulus were distributed as follows: alteration of the intercapillary space, 19; crescent formation, 13; changes in the capillary wall, 17 (3 showed splitting; 7, splitting and hyaline deposit; and 7, membranous transformation). Vacuolization of endothelial cells was noted in one patient. These figures add to more than 28 because of frequent multiplicity of lesions. The actual distribution among the 28 cases was as follows: lesions predominantly intercapillary in location, 12 (8 with hyalinization and fibrosis; 4 with fibrosis alone); lesions predominantly extracapillary in location, 7; entirely or predominantly membranous, 5. Four cases were classified as mixed; cases 26 and 28 had combined extra- and intercapillary lesions of about equal intensity; case 26 also showed widespread splitting and deposit of hyalin in the capillary walls. Two other cases (25 and 27) exhibited mild membranous alterations and also epithelial crescent formation and intercapillary inflammation.

Renal Tubules and Stroma

A brief mention should be made of the tubular alterations encountered. These were characterized by the appearance of hyaline droplets, vacuolization of epithelium, and varying, generally moderate, degrees of atrophy. In many instances there was slight and occasionally even marked thickening and reduplication of the tubule basement membranes (Fig. 15). In some, the interstitial tissue showed slight to moderate inflammation.

Blood Vessels

As a rule, the arteries exhibited little abnormality. In a few instances, particularly in older patients, there was moderate to advanced arteriosclerosis. In specimens in which hyaline deposits appeared in glomeruli, arterioles were often affected by the same process (Fig. 16). In 3 patients there were thrombi in the renal veins; in one of these the thrombosis was bilateral. In two cases the thrombi were recent; in one the thrombus was old and recanalized. In all 3 cases

TABLE I

Summary of Alterations in Patients with Subacute Glomerulonephritis, Intercapillary and Extracapillary Types

Case no.	Sex	Age (yrs.)	Period of illness (mos.)	Blood pressure	Edema	Urine			Blood urea nitrogen (mg.)	Cholesterol (mg.)	Albumin/globulin ratio	Cause of death
						Specif. gravity	Albumin	Red blood cells				
1	M	4	14	160/90	3+	1034	4+	1+	8–17	880	1.7/2.7	Pneumococcus peritonitis; sepsis
2	M	12	24	160/64	0	1012	1+	0	N.D.	N.D.	N.D.	Pneumococcus
3	F	14	30	160/90	0	1016	4+	1+	50–110	280	N.D.	Meningococcus meningitis; uremia
4	F	29	3	170/104	1+	1020	3+	1+	36–85	240	2.5/1.6	Cardiac failure
5	F	10	3	200/110	2+	1018	3+	3+	125	300	2.1/1.9	Uremia
6	F	11	10	170/130	3+	1010	3+	1+	16–30	1000	1.7/1.9	Postop. heart fail
7	M	15	5	100/60	1+	1006	3+	±	238	N.D.	N.D.	Uremia
8	F	15	18	185/135	3+	1016	4+	1+	17–28	500	2.5/2.1	Pneumonia
9	M	21	12	176/116	1+	1012	3+	3+	98–180	N.D.	3.2/1.3	Uremia
10	M	21	2?	220/140	1+	1011	3+	1+	98–228	290	4.1/2.1	Uremia
11	M	35	18	190/110	3+	1017	4+	1+	50–396	600	2.3/2.9	Uremia; pneumo
12	M	38	18	135/110	±	1020	2+	1+	12–70	225	3.5/1.9	Cardiac failure;
13	F	8	3	170/110	2+	1020	4+	3+	156–234	N.D.	2.5/3.8	Uremia
14	M	10	½?	150/90	4+	1020	4+	3+	240	190	3.1/2.2	Uremia
15	M	36	2½	120/70	0	Low	3+	3+	146	N.D.	N.D.	Uremia
16	F	38	2½	160/86	0	1021	1+	2+	136	N.D.	N.D.	Uremia
17	M	41	12	170/70	3+	1012	1+	2+	15–64	230	2.4/2.0	Cerebral hemorrh
18	F	45	2½	175/90	2+	1012	3+	1+	70	N.D.	N.D.	Cardiac failure
19	F	49	9	110/80	3+	1020	+	+	56	N.D.	N.D.	Pneumonia

Numbers 1 to 4 (4 patients) represent intercapillary type without hyalinization. Numbers 5 to 12 (8 patients) represent intercapillary type with hyaline deposits. Numbers 13 to 19 (7 patients) represent extracapillary type.

the clinical course was marked by a nephrotic syndrome and there was membranous transformation of the glomerular capillary walls.

Clinico-pathologic Correlation

The salient clinical data and the main pathologic features are listed in Tables I and II. A few points relating to clinico-pathologic correlation are worthy of notice. The average age at the time of death was lowest in those in whom the lesions were predominantly intercapillary

TABLE I (continued)

Kidney	Obs. glom. (%)	Intercapillary space: Inflammation	Intercapillary space: Fibrosis	Intercapillary space: Hyalin	Capillary wall: Split	Capillary wall: Hyaline deposit	Capillary wall: Memb. trans.	Epith. cresc.	Remarks
y large, 275 gm. both; ale, smooth, yellow	10	2+	2+	0	0	0	0	1+	Nephrotic syndrome
ge, 310 gm. both; mooth	0	2+	3+	0	1+	0	0	0	Acute and chronic rheumatic heart disease
y large with yellow cks	10	4+	4+	0	1+	0	0	0	
gm. both; smooth, ale; many hemorrhages	0	2+	1+	0	4+	0	0	0	
ge, smooth	5	2+	2+	2+	2+	1+	0	2+	Nephrotic syndrome
ge, 280 gm. both; ne, yellow, granular	0	3+	4+	2+	2+	0	0	1+	Nephrotic syndrome; decapsulation
ge, smooth	50	2+	3+	3+	1+	1+	0	0	"Familial" type; few "wire loops"
y large, 575 gm. both; mooth, yellow	<2	3+	2+	2+	1+ to 4+	0 to 4+	0	1+	Nephrotic syndrome; "wire loops"
gm. both; smooth	50	2+	3+	3+	2+	1+	0	1+	
uced in size; oarsely granular	25	2+	3+	2+	2+	2+	0	2+	Osteomyelitis; amyloid in liver
gm. both; smooth, ale, yellow	5	0 to 2+	0 to 2+	1+	2+	1+	0	0	Nephrotic syndrome
ge, 450 gm. both; ightly granular	<2	2+	2+	2+	0 to 4+	0 to 4+	0	1+	"Wire loops"
ge, 340 gm. both; ale; hemorrhages	0	2+	2+	0	1+	0	0	4+	
y large, 360 gm. both; ellowish, slightly anular	0	3+	1+	0	0	0	0	4+	
ge, 430 gm. both; mooth	0	2+	1+	0	0	0	0	4+	
ge, edematous	0	1+	1+	0	1+	0	0	3+	
ge, 575 gm. both; mooth, pale; emorrhages	0	1+	1+	0	2+	0	0	4+	
gm. both; smooth	5	1+	1+	0	1+	0	0	4+	
ge, 480 gm. both; inely granular	2	2+	2+	0	0	0	0	3+	

Key to abbreviations: Obs. glom. = Obsolete glomeruli. Memb. trans. = Membranous transformation. Epith. cresc. = Epithelial crescents. N.D. = No data. ± to 4+ = Degree of change: ±, minimum; 4+, maximum.

in location (20 years); those with extracapillary lesions were next, with an average of 32 years; and those with membranous alterations were older still (48 years). The average duration of the disease was shortest in the patients with extracapillary lesions (5 months) and longest in those with the membranous type of process (18 months). Those with the intercapillary type fell between with an average duration of 13 months (11 months for those with hyaline deposits and 18 months for those without such deposits). These points are generally in

TABLE II

Summary of Alterations in Patients with Subacute Glomerulonephritis, Membranous and Mixed Types

Case no.	Sex	Age (yrs.)	Period of illness (mos.)	Blood pressure	Edema	Urine			Blood urea nitrogen (mg.)	Cholesterol (mg.)	Albumin/globulin ratio	Cause of death	Kidney
						Specif. gravity	Albumin	Red blood cells					
20	M	23	36+	190/100	3+	N.D.	3+	1+	110–134	N.D.	3.9/2.1	Paratyphoid fever	m. both; p llowish, slig anular
21	F	48	9	155/100	4+	1028	4+	0	22	500	2.2/2.0	Pulmonary embo nephrosis	e, 440 gm. ooth
22	M	50	12	200/110	3+	1025	4+	0	16	530	2.3/1.8	Convulsions; cerebral edema	e, 320 gm.
23	M	53	18	210/110	1+	1014	4+	+	20–42	280	1.4/3.3	Uremia	e, pale, yel
24	F	68	?	160/110	3+	1021	3+	1+	131	N.D.	2.4/2.4	Uremia	m. both; y htly granu
25	F	2	5	150/120	4+	1030	3+	1+	10–15	1280	1.0/2.7	Generalized edema	large, smo llowish
26	F	22	3	134/80	3+	1012	3+	3+	23–60	170	2.2/2.5	Sepsis; staphyloco	e, smooth
27	M	58	3?	154/90	0	1014	3+	3+	110–160	N.D.	N.D.	Uremia; pneumoni	m. both; s le; hemorr
28	F	67	3?	150/90	1+	1010	1+	2+	51–110	N.D.	N.D.	Uremia	m. both; s anular

Numbers 20 to 24 (5 patients) represent membranous type. Numbers 25 to 28 (4 patients) represent mixed type.

Key
formatio
±, mini

agreement with the observations of Bell.[8] As expected in the subacute stage of glomerulonephritis, most patients had marked albuminuria and edema. Three plus or more albuminuria was found in 23 patients, and 3+ edema in 13 patients. The fully developed nephrotic syndrome was present in 10. In 5 patients intercapillary lesions with fiber splitting and "wire-loop" hyaline deposits in the capillary walls underlay the syndrome (ages 4, 10, 11, 15 and 35 years). In the other 5 patients (ages 2, 23, 48, 50 and 68 years) membranous lesions prevailed. Thus, among the 7 patients with membranous lesions, the nephrotic syndrome was manifest in 5, confirming the association noted by Bell. Membranous lesions were most pronounced in patients with the nephrotic syndrome of long standing. This was even more strikingly the case in patients who had had the nephrotic syndrome in the past but no longer exhibited the characteristic symptoms.

COMMENT

The structure of the intercapillary space of the glomerulus and the nature of its cells and fibers in health and disease have been discussed elsewhere.[1,9] The cells are believed by various authors to be either of

TABLE II (continued)

Kidney	Intercapillary space: Obs. glom. (%)	Intercapillary space: Inflammation	Intercapillary space: Fibrosis	Intercapillary space: Hyalin	Capillary wall: Split	Capillary wall: Hyaline deposit	Capillary wall: Memb. trans.	Capillary wall: Epith. cresc.	Remarks
m. both; pale, llowish, slightly anular	30	0	0	0	0	0	4+	0	Nephrotic syndrome; renal vein thrombosis, recanalized
, 440 gm. both; ooth	0	0	0	0	0	0	3+	0	Nephrotic syndrome; bilateral renal vein thrombosis
e, 320 gm. both	2	1+	1+	0	1+	0	3+	1+	Nephrotic syndrome; thrombosis in small renal veins
e, pale, yellowish	5	1+	1+	1+	1+	0	3+	0	Operative specimen; patient died 6 mos. later
gm. both; yellowish, ightly granular	10	0	1+	0	0	0	3+	0	Nephrotic syndrome
large, smooth, pale, llowish	0	2+	0	0	0	0	1+	2+	Nephrotic syndrome
e, smooth	<2	2+	2+	2+	3+	3+	0	2+	"Wire loops"
gm. both; smooth, le; hemorrhages	20	1+	1+	1+	0	0	2+	2+	
gm. both; slightly anular	50	2+	2+	1+	0	0	0	3+	

Key to abbreviations: Obs. glom. = Obsolete glomeruli. Memb. trans. = Membranous transformation. Epith. cresc. = Epithelial crescents. N.D. = No data. ± to 4+ = Degree of change: ±, minimum; 4+, maximum.

connective tissue (histiocytic),[10,11] perithelial,[12] myoid,[13] or endothelial (endenchymal)[14,15] origin. The fibers are variously considered to be special connective tissue fibers (fibromucin),[16] "branches" of the basement membrane,[7] or "basement membrane like" material.[17]

Subacute glomerulonephritis of the intercapillary type is characterized by gradual replacement of the proliferated cells by fibers and the eventual formation of central lobular scars. Deposition of hyalin in the intercapillary space is a frequent but not invariable accompaniment of fibrosis. The hyalin is similar in its staining characteristics to that seen in arteriosclerosis. Presumably it is derived from the blood stream and deposited rather than formed locally, but at the present time nothing definite is known of its origin. The presence of hyalin is associated with a more rapid and more severe clinical course, the majority of the patients dying in uremia.

The fibers in the epithelial crescents differ from those in the intercapillary space. They arise from the basement membrane of Bowman's capsule, and their appearance in thin sections is consistent with the assumption that they arise as "branches" of the basement membrane.[9] At first they stain as do basement membranes, but later they acquire

the staining properties of collagen. It is not known whether they possess the characteristic electron microscopic periodicity of collagen.

Alteration of the capillary wall in glomerulonephritis received scant attention before Bell's observations in membranous glomerulonephritis.[8] We prefer the term "membranous transformation" because evidence of inflammation is often lacking. Bell described thickening of the capillary wall and indicated its frequent association with the nephrotic syndrome. The alteration has been shown by Jones[16] and by ourselves[9] to have a very characteristic structure. Jones suggested that the silver-positive bands or spikes were part of the basement membrane. It was our impression that they were related in some way to the trabeculae and foot processes of the epithelial cells. The hyaline material between the spikes stains differently from that found in the intercapillary space, in that it reacts weakly with the PAS stain.

Membranous transformation of the capillary wall occurs in subacute and chronic glomerulonephritis but is often unaccompanied by evidence of glomerular inflammation. Furthermore, it has been observed by us in association with other diseases such as lupus erythematosus and amyloidosis when these are accompanied by the nephrotic syndrome. Of special interest is the fact that the most severe forms of membranous transformation occur in patients who have had the nephrotic syndrome, but who no longer exhibit any of its clinical manifestations. These facts suggest that membranous transformation is neither a form of glomerulonephritis nor the cause of the nephrotic syndrome, but rather a result of the syndrome and the severe proteinuria which accompanies it. These changes may very well be caused by the trapping of protein between the basement membrane and the epithelial cells (podocytes), or in the outer layer of the basement membrane.

In none of our cases of membranous transformation was there much evidence of inflammation in the glomeruli, and in cases 20 and 21 such evidence was lacking completely. One may doubt, with good reason, the desirability of classifying these two instances as glomerulonephritis. It should be mentioned at this point that in selecting cases for this study we have omitted all examples of the nephrotic syndrome in which there were no obvious changes in the glomeruli as determined by light microscopy, or those which merely showed vacuolation of the glomerular endothelium. These cases will be reported in a later communication. On the other hand, inclusion of two examples of membranous transformation from other hospitals serves to exaggerate the frequency of this alteration in subacute glomerulonephritis.

Among our examples of membranous transformation there were 3

instances associated with renal vein thrombosis. It is well known that the latter may lead to the nephrotic syndrome[18] and possibly to membranous transformation. However, in none of our cases was there any evidence of venous thrombosis elsewhere in the body. In particular, there was no thrombosis of the inferior vena cava. The possibility must be considered that isolated thrombosis of renal veins is not always the cause of the nephrotic syndrome but rather may be its consequence.

Thickening of the capillary wall in subacute glomerulonephritis is most frequently the result of splitting of the wall into two layers. It is possible that such thickening may interfere with glomerular filtration. If hyalin accumulates between the split layers, the wall assumes the appearance of "wire loops." There has been some tendency in the literature to equate all thickening of the capillary wall with membranous transformation.[19] However, differences in the distribution and particularly in the structure of the various types of thickening militate against such generalization. We prefer to apply the term "membranous transformation" only to the lesion originally described by Bell, and to designate the other types of thickening as "splitting of the capillary wall" and "wire loop alteration" respectively.

The "wire loop" lesions of glomerulonephritis appear with less regularity and are less conspicuous than those in systemic lupus erythematosus and are also invariably associated with inflammation and hyaline deposits in the intercapillary space. It is our impression that the "wire loops" in lupus precede inflammation in the glomeruli or occur independently of it, while in glomerulonephritis they are secondary to the inflammation.

Summary and Conclusions

Twenty-eight examples of subacute glomerulonephritis were studied by means of thin (0.5 μ) sections.

The chief alterations observed in the glomeruli were: intercapillary inflammation and fibrosis, frequently accompanied by hyaline deposits; epithelial and fibrous crescents; thickening of the capillary wall caused either by splitting or reduplication, deposition of hyalin, or by "membranous transformation."

Each type of alteration is described and discussed in detail. Though most of the patients showed a predominance of one type of alteration, the great variety of possible combinations tended to impart an almost individual pattern to each case.

The nephrotic syndrome was present in 10 patients. In the younger age groups this was usually associated with intercapillary inflammation

and with splitting and hyaline deposits in the capillary wall. In the older age group it was more often accompanied by "membranous transformation" of the capillary wall.

"Membranous transformation" may be a feature in the lesion of subacute glomerulonephritis. It is suggested, however, that it is neither a part of the inflammatory process, nor the cause of the nephrotic syndrome, but rather a consequence of the latter.

REFERENCES

1. Grishman, E., and Churg, J. Acute glomerulonephritis. A histopathologic study by means of thin sections. *Am. J. Path.*, 1957, **33**, 993–1007.
2. McManus, J. F. A. Histological demonstration of mucin after periodic acid. (Letter to the editor.) *Nature, London*, 1946, **158**, 202.
3. Churg, J., and Prado, A. A rapid Mallory trichrome stain (chromotrope-aniline blue). *A. M. A. Arch. Path.*, 1956, **62**, 505–506.
4. Jones, D. B. Glomerulonephritis. *Am. J. Path.*, 1953, **29**, 33–51.
5. Ritter, H. B., and Oleson, J. J. Combined histochemical staining of acid polysaccharides and 1, 2 glycol groupings in paraffin sections of rat tissues. *Am. J. Path.*, 1950, **26**, 639–645.
6. Churg, J., and Grishman, E. Phase microscope studies of renal glomeruli. Glomerular deposits of "hyaline" substance. *Am. J. Path.*, 1953, **29**, 199–215.
7. Hall, C. V. Studies of Normal Glomerular Structure by Electron Microscopy. In: Proceedings of the Fifth Annual Conference on the Nephrotic Syndrome. Philadelphia, November 5–7, 1953. The National Nephrosis Foundation, Inc., New York, 1954, pp. 1–39.
8. Bell, E. T. Renal Diseases. Lea & Febiger, Philadelphia, 1950, ed. 2, 448 pp.
9. Churg, J., and Grishman, E. Application of thin sections to the problems of renal pathology. *J. Mt. Sinai Hosp.*, 1957, **24**, 736–744.
10. Zimmermann, K. W. Über den bau des Glomerulus der Säugerniere, Weitere Mitteilungen. *Ztschr. f. mikr.-anat. Forsch.*, 1933, **32**, 176–278.
11. Jones, D. B. Inflammation and repair of the glomerulus. *Am. J. Path.*, 1951, **27**, 991–1009.
12. Goormaghtigh, N. Le mesangium du floculus glomérulaire; ses reactions dans la glomérulonephrite aiguë et les nephrites hypertensives. *J. Urol., Paris*, 1951, **57**, 569–585.
13. Yamada, E. The fine structure of the renal glomerulus of the mouse. *J. Biophys. & Biochem. Cytol.*, 1955, **1**, 551–566.
14. Elias, A. H. The renal glomerulus by light and electron microscopy. In: Research in the Service of Medicine. G. D. Searle & Co., Chicago, 1956, **46**, 1–29.
15. Elias, A. H. De structura glomeruli renalis. *Anat. Anzeig.*, 1957, **104**, 26–36.
16. Jones, D. B. Nephrotic glomerulonephritis. *Am. J. Path.*, 1957, **33**, 313–329.
17. Farquhar, M. G.; Vernier, R. L., and Good, R. A. Studies on familial nephrosis. II. Glomerular changes observed with the electron microscope. *Am. J. Path.*, 1957, **33**, 791–817.
18. Pollak, V. E.; Kark, R. M.; Pirani, C. L.; Shafter, H. A., and Muehrcke, R. C. Renal vein thrombosis and the nephrotic syndrome. *Am. J. Med.*, 1956, **21**, 496–520.
19. Allen, A. C. The clinicopathologic meaning of the nephrotic syndrome. *Am. J. Med.*, 1955, **18**, 277–314.

[*Illustrations follow*]

LEGENDS FOR FIGURES

Standard sections were cut at 5 μ, stained with hematoxylin and eosin, and photographed at a magnification $\times$ 600. Thin sections were cut at 0.5 μ, stained with the periodic acid-Schiff reagent (PAS) or with periodic acid-silver methenamine (PA-SM) method, and photographed at magnification $\times$ 1,500.

FIG. 1. Case 8. Glomerular lobule, showing mononuclear cells and fibers in the intercapillary space. The capillary wall is thin and delicate, though some splitting is seen in the lower portion of the lobule. Thin section, PAS stain.

FIG. 2. Case 8. Lobule of another glomerulus, showing cells, fibers, and clumps of hyalin in the intercapillary space, and hyalin in the capillary walls. Thin section, PAS stain.

FIGS. 3 and 4. Case 25. Minimal thickening of the capillary walls is caused by early membranous transformation (arrows). Fig. 3. Standard section. Fig. 4. Thin section, PA-SM stain.

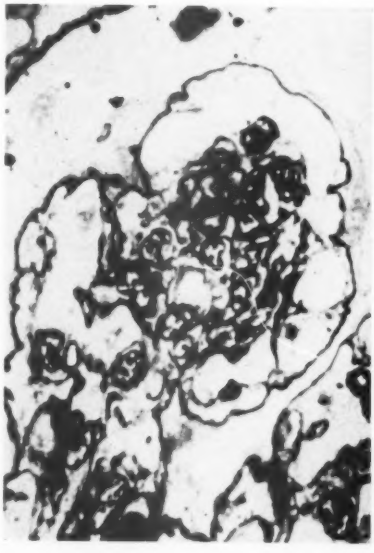

1

2

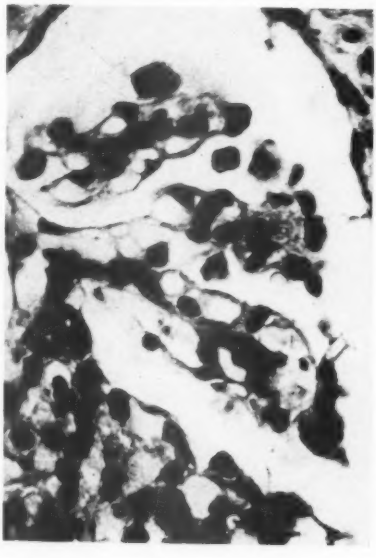

3

4

FIGS. 5 and 6. Case 20. Marked thickening of the capillary walls caused by advanced membranous transformation. Fig. 5. Standard section. Fig. 6. Thin section, PAS stain.

FIGS. 7 and 8. Case 4. Thickening of the capillary walls caused by splitting of the basement membranes. Cells can be seen between the split layers. Fig. 7. Standard section. Fig. 8. Thin section, PAS stain.

5

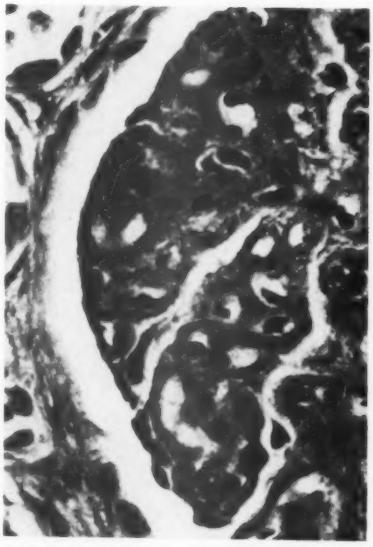

6

7

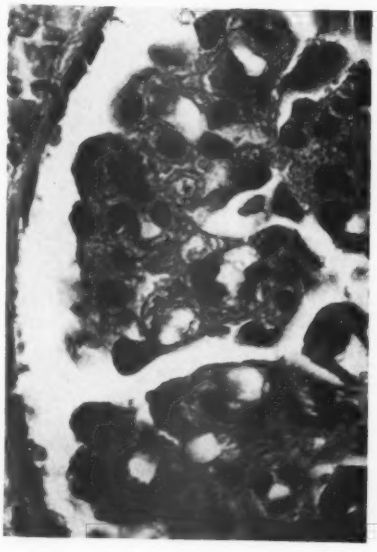

8

FIGS. 9 and 10. Case 12. "Wire-loop" thickening of the capillary walls is caused by deposition of hyalin between the split layers of basement membranes. In Figure 10 the "wire loops" can be seen along the periphery of the lobule (arrows); the widened intercapillary space in the center of the lobule also contains hyalin. Fig. 9. Standard section. Fig. 10. Thin section, PAS stain.

FIGS. 11 and 12. Case 26. In Figure 11 (section stained with PAS) capillary walls appear thick and homogeneous; in Figure 12 (stained with PA-SM) there is a thick deposit of weakly stained material, apparently between the basement membrane and the endothelium. Both figures, thin sections.

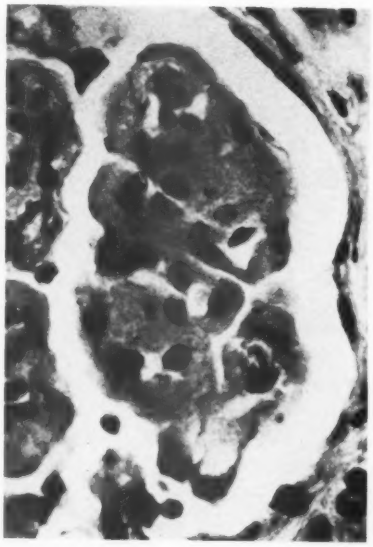

9

10

11

12

FIG. 13. Case 8. Hyaline droplets in visceral epithelial cells of the glomerulus (podocytes). Thin section, PAS stain.

FIG. 14. Case 16. Part of an epithelial crescent with pseudo-tubules, showing origin of "fibers" from the inner layer of Bowman's capsule (top). Capillary loops are in the right lower corner. Thin section, PAS stain.

FIG. 15. Case 11. Thickening and splitting of tubule basement membranes. Thin section, PAS stain.

FIG. 16. Case 8. Arteriole showing subintimal and medial deposits of hyalin. Thin section, PAS stain.

13

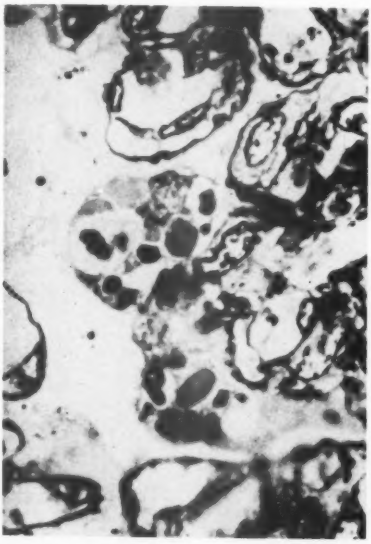

14

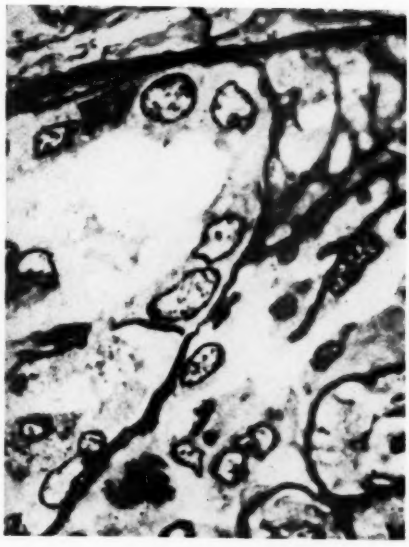

15

16

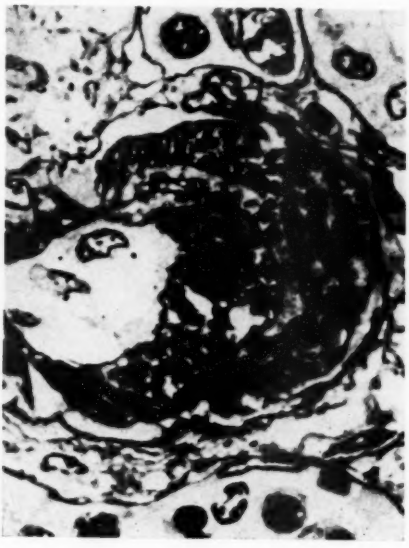

THE STRUCTURAL BASIS OF PROTEINURIA IN MAN *

Electron Microscopic Studies of Renal Biopsy Specimens from Patients with Lipid Nephrosis, Amyloidosis, and Subacute and Chronic Glomerulonephritis

David Spiro, M.D., Ph.D.

From the Department of Pathology, Harvard Medical School and the Edwin S. Webster Memorial Laboratories of the Department of Pathology of the Massachusetts General Hospital, Boston, Mass.

The fine structure of the normal mammalian renal glomerulus has been the subject of a number of recent electron microscopic studies.[1-12] These have led to several detailed investigations of changes in the glomerulus in various types of human renal disease.[13-15] Studies of the structure of the normal kidney suggest that the ultimate diffusion barrier in the glomerular capillary bed is the capillary basement membrane, since the endothelial and epithelial cellular layers are interrupted. Abnormal glomeruli have revealed only one structural variation, which is found consistently in conditions associated with proteinuria—a transformation of the normal foot processes of the epithelial cells into rather broad sheets of cytoplasm that invest the external surfaces of the glomerular capillary loops in a more or less continuous manner.[13,14] This alteration fails to explain the hyperpermeability to proteins in pathologic glomerular capillaries, and it is not surprising that several investigators have suggested that this phenomenon is probably secondary to some as yet unobserved abnormality in the basement membrane.[13,14] It is interesting to recollect that Allen[16] and many other pathologists have related proteinuria and the nephrotic syndrome to alterations in the basement membrane.

We have examined renal biopsy specimens from patients with various conditions associated with proteinuria, using higher resolution techniques than those utilized by previous investigators. The present publication deals with the observations in 3 patients with the nephrotic syndrome (one instance of juvenile "pure" lipid nephrosis, and two cases of amyloidosis) and in two patients with subacute and chronic glomerulonephritis accompanied by proteinuria. The observations thus far indicate that the structural common denominator of proteinuria is the existence of defects in the basement membrane of the glomerular capillary loops.

* Aided by a grant from the National Heart Institute of the National Institutes of Health, United States Public Health Service. [H-1834 (C_3)]

Presented at the Forty-seventh Annual meeting of the International Academy of Pathology, Cleveland, Ohio, April 23, 1958.

Received for publication, June 13, 1958.

Material and Methods

Percutaneous renal biopsy specimens procured from the patients studied were divided immediately, and portions were used for conventional histologic studies, the remainder being prepared for electron microscopy.[17] In most instances, tissues were stained with phosphotungstic acid to enhance contrast. Thin sections were cut with a Rotary Cantilever microtome,[18] and were examined in an RCA EMU 3B electron microscope. In addition to examining stained paraffin sections of the renal tissue under the light microscope, sections of all glomeruli "thin sectioned" (1 to 2 μ) for electron microscopy were examined under the phase microscope for supplementary diagnostic confirmation.

Three kidneys were procured from children at nephrectomy and served as a source of normal glomeruli. Two kidneys removed surgically during arachnoid-ureterostomy from infants 1 and 4 months old were also used for control studies.

Results

Normal Glomerulus

A number of investigators agree that of the 3 components of the capillary wall, the epithelial and endothelial cellular layers are discontinuous, whereas the basement membrane is continuous.[2,7-9,12] The endothelial cells exhibit characteristic interruptions or pores, and the epithelial cells (podocytes) form numerous branches eventuating in discrete foot processes (pedicels) that are applied to the external surfaces of the basement membrane (Figs. 1 to 3). Fine connections are often observed between the epithelial pedicels (Fig. 3). The basement membrane is defined in this study as the relatively dense layer, about 1,000 Å units in thickness, that separates endothelium from epithelium. In suitable preparations it appears to be composed of fine filaments which extend from the epithelial to the endothelial cells (Figs. 2 and 3). These features have been observed by one or the other of the previously cited authors.

An additional feature is the existence of fine (approximately 75 Å units in thickness) filaments in the cytoplasm of the epithelium (Fig. 2). In many instances, filamentous material within the foot processes of the epithelium appear to be continuous with the filaments forming the basement membrane (Figs. 2 and 3), suggesting that the epithelial cells may play an important role in maintaining the integrity of the basement membrane or in its synthesis. We occasionally observed ordered structure in the basement membrane that may best be described as a series of cross-linked, regularly arrayed filaments, the interfilamentous distance being somewhat less than 100 Å. It is prob-

able that what the light microscopist observes as "the basement membrane" actually consists of endothelium, basement membrane, and portions of the epithelial processes. Nothing resembling a mesangium has been found in the glomerulus. Preparations including the hilar vessels revealed fusion of what were probably the external and internal arteriolar elastic lamellas to form a layer continuous with the capillary basement membrane, as well as with the basement membrane of Bowman's capsule.[19] Occasional cells in the media of the entering arteriole disclosed structureless electron-dense bodies measuring 1 to 2 μ corresponding to the juxtaglomerular granules.[19]

The Neonatal Glomerulus

Up to the age of at least 4 months, immature glomeruli in the nephrogenic zone revealed a striking difference in the structure of the epithelium. In these glomeruli (Fig. 4), many of the capillaries were invested by broad sheets of dense epithelial cytoplasm instead of by discrete foot processes. The endothelial layer and basement membrane, however, exhibited characteristics similar to those of the normal, fully developed glomerulus.

Lipid Nephrosis

The most striking abnormality seen in lipid nephrosis occurred in the basement membrane. This structure exhibited irregular foci of thickening due to peripheral strand-like projections (Figs. 5 to 11). There were also regions in which the basement membrane was markedly attenuated (Figs. 6 to 9). As a result, the external surface of the basement membrane assumed a scalloped appearance. As noted by others,[13,14] the podocyte processes were replaced by broad sheets of protoplasm derived from the same cells. Sheets of epithelial cytoplasm, which were frequently quite dense, invested the external surface of the capillary, filling the interstices formed by the irregular basement membrane. In more tangential sections, a mosaic pattern due to alternating segments of basement membrane and epithelial cytoplasm were noted (Figs. 5 and 10). The most significant lesion was characterized by actual breaks or defects in the basement membrane, several hundred to 1,000 Å units in extent (Figs. 10 and 11). At the sites of these interruptions, epithelial and endothelial cells were in direct contact. The dense appearance of the epithelial cytoplasm adjacent to the basement membrane appeared to be due to the existence of numerous filaments, which were often continuous with the basement membrane (Figs. 7, 8 and 10).

The epithelium contained numerous cystic spaces filled with a substance of an electron density similar to that of intracapillary plasma.

In addition, large granules, possibly colloid droplets, were often seen in intimate relation to the podocyte vesicles (Figs. 5 and 6). These cysts and dense droplets occur in other diseases characterized by increased glomerular filtration of protein. They may be related to protein passage through the epithelial cytoplasm, although the exact relationship is obscure at present.

The endothelium frequently appeared to be hyperplastic, contained cytoplasmic vacuoles, and formed villus-like projections.

The glomeruli studied in this case were all of normal appearance when examined with the light microscope. This is not surprising, since the combined overall thickness of the endothelium, basement membrane and epithelial foot process layers was approximately normal despite the alterations observed with the electron microscope. The light microscopist probably visualizes these 3 layers of the capillary wall as "the basement membrane," and any changes occurring within this integrated structure, such as those seen in lipid nephrosis, would not be resolvable by conventional histologic techniques.

Amyloidosis

The earliest glomerular deposits of amyloid were seen beneath the endothelium (Fig. 12), and were surrounded peripherally by a normal basement membrane and a layer of podocytes. In the more extensive lesion, amyloid substance penetrated and replaced the portion of the basement membrane contiguous to the epithelium (Figs. 12 and 13). Under these circumstances, the podocytes exhibited the previously described alteration which consisted of replacement of foot processes by extensive sheets of cytoplasm (Figs. 12 to 14). Frequently, masses of amyloid were noted, external to what appeared to be an intact or thickened basement membrane (Fig. 14), indicating that actual basement membrane destruction was limited to relatively few foci, even in the presence of extensive amyloid deposition. The amyloid substance was composed of a very loose, irregular meshwork of thin (approximately 100 Å units) filaments that showed some evidence of beading or periodic structure (Figs. 14 to 16). The distance between the filaments was of the order of several hundred Å units. The epithelial cells contained vacuoles similar to those encountered in lipid nephrosis. Occasionally one observed cellular organelles embedded in a matrix of amyloid in the early lesions, suggesting that the material was synthesized by the endothelial cells. More advanced amyloidosis was characterized by sheets of amyloid substance and also numerous collagen fibers. In these instances the overall glomerular architecture was distinguished with extreme difficulty.

Subacute and Chronic Glomerulonephritis

This condition was characterized primarily by thickening of the basement membrane. Frequently, endothelial elements were found embedded in broad sheets of basement membrane (Fig. 17).

The epithelium exhibited a varying degree of loss of the normal foot process pattern, and its cytoplasm contained vacuoles. Some degree of endothelial cell hyperplasia was present. There were occasional defects in the thickened basement membrane (Fig. 18) which were similar to those described in lipid nephrosis. They were, however, not nearly as numerous. Here also there was apposition of epithelium and endothelium. Further progression of the lesion was characterized by the production of collagen fibers and the loss of recognizable glomerular structure.

Discussion

These electron microscopic studies on a limited number of renal biopsy specimens demonstrated the existence of a constant abnormality associated with proteinuria in several types of renal disorder. The abnormality consisted of a loss of continuity of the normally continuous basement membrane in the glomerular capillary wall. In lipid nephrosis and subacute and chronic glomerulonephritis, the basement membrane discontinuities actually consisted of gaps or pores, through which endothelial and epithelial cells were in intimate contact. In amyloid disease, the discontinuities were due to replacement of the basement membrane by amyloid substance with far looser structure. The defects in the basement membrane may constitute the structural basis of proteinuria. They were of appropriate size to permit relatively free diffusion of protein while excluding the cellular elements of the blood. The lesions described by others,[13,14] consisting of a transformation of the normal epithelial foot processes were also observed. These had been considered to represent the characteristic alteration in the lesion of nephrosis. It appears, however, that this represents a change which is secondary to the underlying alteration in the basement membrane.

The fact that a similar epithelial pattern was observed in the immature glomerulus suggests that this type of alteration is not necessarily present in glomeruli that are hyperpermeable to proteins. However, one should be cautious in considerations of the function of the neonatal glomerulus since there is some evidence that increased filtration of protein occurs in the newborn.[20] The reason for the confluence of foot processes in association with basement membrane lesions is not clear. It may well be due to an attempt by the epithelium to repair the filtration mechanism. This mechanism has been suggested by Farquhar and her colleagues.[13,14] On the other hand, the epithelium itself may be

intimately associated with the synthesis of the basement membrane. In renal disease there is thickening of the basement membrane as well as destruction of it, indicating that synthesis of this structure may occur at an increased rate. The apposition of broad sheets of epithelial cytoplasm to the external surfaces of the capillaries might thus reflect an increased rate of formation of the basement membrane. It is possible that both factors are involved: namely, the plugging of pores in the basement membrane, and an increased rate of membrane synthesis. The characteristic appearance of the infantile glomerulus might be explained on the basis of the second supposition.

The observations in the pathologic glomerulus support the thesis that the basement membrane is the ultimate diffusion barrier, at least in respect to protein. The filtration mechanism in the abnormal glomerulus is still rather obscure. It apparently is necessary for the plasma filtrate to pass through the cytoplasm of the altered epithelial cells. Whether this passage is by way of the endoplasmic reticulum or via other structures cannot be stated. The cystic alteration in the epithelium in patients with proteinuria may bear some relationship to such preformed intracellular channels.

It is believed that the failure of other investigators to have observed defects in the basement membrane in lipid nephrosis and glomerulonephritis is due to differences in techniques—mainly, the failure to improve contrast by means of phosphotungstic acid staining. It is interesting to point out, however, that Farquhar and co-workers[13,14] described the thickened basement membrane in glomerulonephritis and lipid nephrosis to be "moth eaten."

The localization of the earliest amyloid deposits in the subendothelial area is in accordance with Teilum's observations, which suggest its synthesis by endothelial cells.[21] However, whether the amyloid complex is actually synthesized by the endothelium or represents a deposit of material derived from the plasma,[22] cannot be ascertained definitely at present. The former hypothesis seems to be more likely. The present studies are in accordance with those of Cohen, Weiss and Calkins.[23] These authors demonstrated the subendothelial localization as well as the fibrous nature of the amyloid substance in the rabbit spleen in experimental amyloidosis.

We have not as yet examined by electron microscopy other forms of renal abnormality associated with proteinuria. However, on the basis of rather limited observations, the underlying structural alteration associated with increased glomerular capillary permeability to protein appears to consist of interruptions in the basement membrane.

Summary

The structure of the normal and neonatal glomerulus has been reviewed.

Electron microscopic investigation in examples of lipid nephrosis, amyloidosis and subacute and chronic glomerulonephritis with proteinuria have shown interruptions in the basement membrane as a constant structural alteration. These have been accompanied by alterations in glomerular epithelium previously described by others.

The significance of the abnormalities has been discussed in terms of normal and abnormal glomerular filtration. Increased protein filtration in lipid nephrosis and glomerulonephritis is probably the result, at least in part, of defects in the basement membrane. In amyloid disease, proteinuria is probably caused by the replacement of the basement membrane by the structurally looser amyloid substance, which permits increased diffusion of protein. The earliest deposits of glomerular amyloid were found in the subendothelial region of the capillary loops.

REFERENCES

1. Rinehart, J. F.; Farquhar, M. G.; Jung, H. C., and Abul-Haj, S. K. The normal glomerulus and its basic reactions in disease. *Am. J. Path.*, 1953, **29**, 21–31.
2. Hall, C. V. Studies of normal glomerular structure by electron microscopy. In: Proceedings of the Fifth Annual Conference on the Nephrotic Syndrome. Philadelphia, November 5–7, 1953. The National Nephrosis Foundation, Inc., New York, 1953, pp. 1–39.
3. Reid, R. T. W. Observations on the structure of the renal glomerulus of the mouse revealed by the electron microscope. *Australian J. Exper. Biol. & M. Sc.*, 1954, **32**, 235–239.
4. Mueller, C. B.; Mason, A. D., Jr., and Stout, D. G. Anatomy of the glomerulus. *Am. J. Med.*, 1955, **18**, 267–276.
5. Bargmann, W.; Knoop, A., and Schiebler, T. H. Histologische, cytochemische und elektronen-mikroskopische Untersuchungen am Nephron, mit Berücksichtigung der Mitochondrien. *Ztschr. Zellforsch.*, 1955, **42**, 386–422.
6. Policard, A.; Collet, A., and Giltaire-Ralyte, L. Recherches au microscope électronique sur la structure du glomérule rénal des mammifères. *Arch. anat. Micr.*, 1955, **44**, 1–19.
7. Pease, D. C. Electron microscopy of the vascular bed of the kidney cortex. *Anat. Rec.*, 1955, **121**, 701–721.
8. Rhodin, J. Electron microscopy of the glomerular capillary wall. *Exper. Cell Res.*, 1955, **8**, 572–574.
9. Yamada, E. The fine structure of the renal glomerulus of the mouse. *J. Biophys. & Biochem. Cytol.*, 1955, **1**, 551–566 .
10. Sakaguchi, H. Fine structure of the renal glomerulus. *Keijo J. Med.*, 1955, **4**, 103–118.
11. Rinehart, J. F. Fine structure of renal glomerulus as revealed by electron microscopy. *A. M. A. Arch. Path.*, 1955, **59**, 439–448.

12. Bergstrand, A. Electron microscopic investigations of the renal glomeruli. *Lab. Invest.*, 1957, **6**, 191–204.

13. Farquhar, M. G.; Vernier, R. L., and Good, R. A. Studies on familial nephrosis. II. Glomerular changes observed with the electron microscope. *Am. J. Path.*, 1957, **33**, 791–817.

14. Farquhar, M. G.; Vernier, R. L., and Good, R. A. An electron microscope study of the glomerulus in nephrosis, glomerulonephritis and lupus erythematosus. *J. Exper. Med.*, 1957, **106**, 649–660.

15. Bergstrand, A., and Bucht, H. Electron microscopic investigations on the glomerular lesions in diabetes mellitus (diabetic glomerulosclerosis). *Lab. Invest.*, 1957, **6**, 293–300.

16. Allen, A. C. The Kidney. Medical and Surgical Diseases. Grune & Stratton, New York, 1951, p. 158.

17. Hodge, A. J.; Huxley, H. E., and Spiro, D. Electron microscope studies on ultrathin sections of muscle. *J. Exper. Med.*, 1954, **99**, 201–206.

18. Hodge, A. J.; Huxley, H. E., and Spiro, D. A simple new microtome for ultrathin sectioning. *J. Histochem.*, 1954, **2**, 54–61.

19. Spiro, D. Unpublished observations.

20. Nelson, W. E. (ed.). Textbook of Pediatrics. W. B. Saunders Co., Philadelphia, 1954, p. 1049.

21. Teilum, G. Periodic acid-Schiff-positive reticulo-endothelial cells producing glycoprotein. *Am. J. Path.*, 1956, **32**, 945–959.

22. Miller, F., and Bohle, A. Vergleichende Licht- und elektronenmikroskopische Untersuchungen an der Basalmembran der Glomerulumcapillaren der Maus bei experimentellem Nierenamyloid. *Klin. Wchnschr.*, 1956, **34**, 1204–1210.

23. Cohen, A. S.; Weiss, L., and Calkins, E. A study of the fine structure of the spleen in experimental amyloidosis of the rabbit. (Abstract.) *Clin. Res.*, 1958, **6**, 237.

The author would like to express appreciation to Dr. Benjamin Castleman for his constant interest and encouragement. Grateful acknowledgment is made to the following: Dr. Lot B. Page of the Department of Medicine and Dr. John D. Crawford of the Children's Medical Service, Massachusetts General Hospital, who in addition to performing the renal biopsy procedures aided this study in many of its facets. Dr. John Craig of the Children's Medical Center, Boston, kindly provided the normal and neonatal tissue. Dr. Evan Calkins of the Department of Medicine was instrumental in providing the biopsy tissue in amyloid disease, and, with Dr. Alan Cohen of the Department of Medicine, generously contributed time and the product of their vast experience in the problem of amyloidosis. Miss Cadence H. Allison and Mrs. Victor Bayer gave invaluable technical assistance.

[*Illustrations follow*]

LEGENDS FOR FIGURES

Key to abbreviations in electron micrographs:

En = Endothelium	Dr = "Colloid droplet"
Nuc = Endothelial nucleus	BS = Bowman's space
BM = Basement membrane	RBC = Red blood cell
Ep = Epithelium	Am = Amyloid substance
Vac = Vacuole	

FIG. 1. Survey photograph of normal glomerulus. The 3 elements forming the glomerular capillary wall are seen: endothelium, basement membrane and epithelium. The endothelium exhibits the characteristic pores which in one area (arrow) are sectioned tangentially. Portions of epithelial cells and their foot processes are evident. The basement membrane is the dense layer between epithelium and endothelium. × 11,000.

FIG. 2. Normal glomerulus. Epithelial cytoplasm contains fine filaments. Basement membrane appears fibrous. In some areas there appears to be continuity between filamentous material in the epithelial foot processes and the basement membrane proper (arrow). Pores in the endothelium are seen in both radial and tangential orientations. × 28,100.

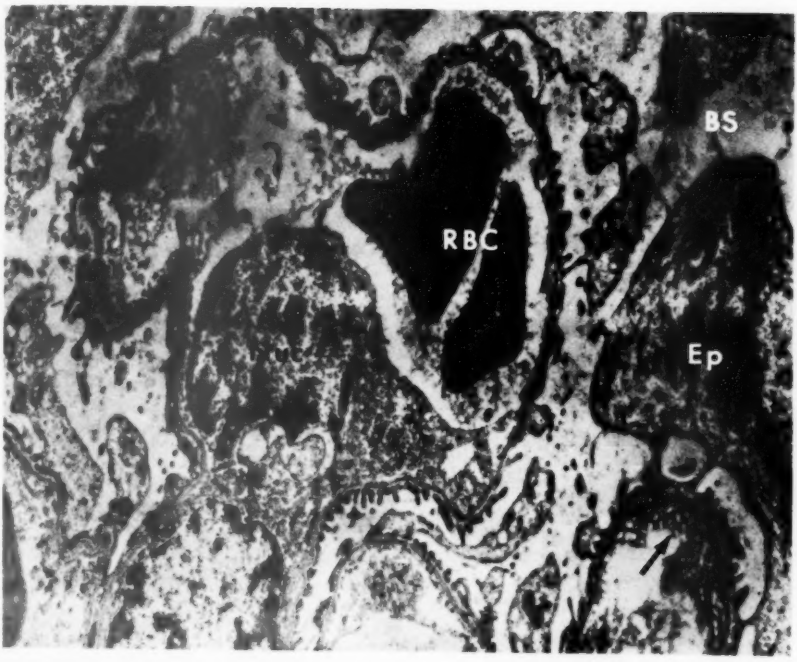

1

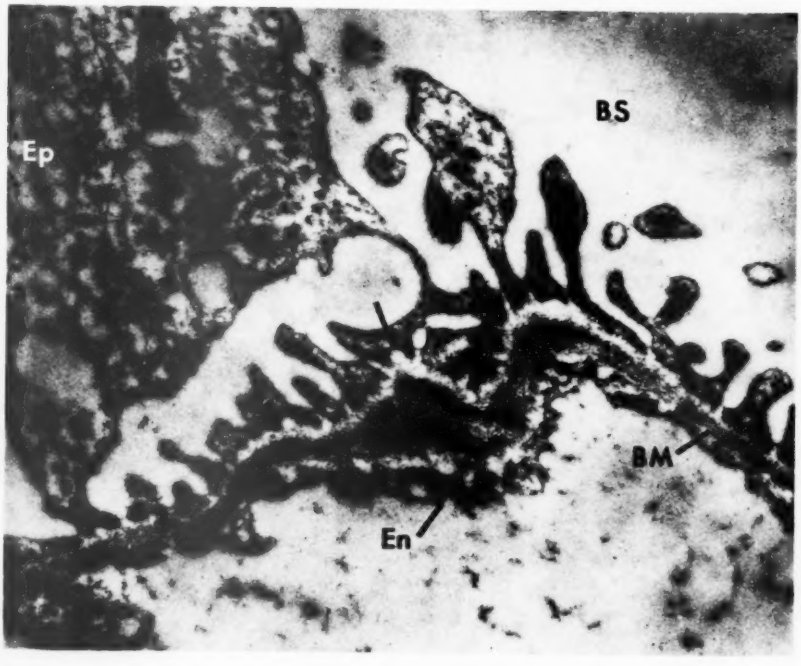

2

FIG. 3. Normal glomerulus. The fibrous nature of the basement membrane is evident. Continuity between epithelial filaments and the basement membrane can be seen (arrows). There are also lateral connections between epithelial pedicels. × 42,600.

FIG. 4. Neonatal glomerulus from nephrogenic zone. Differentiation of discrete foot processes in the epithelium is not present. The external aspect of the basement membrane is invested by broad sheets of epithelial cytoplasm. × 23,000.

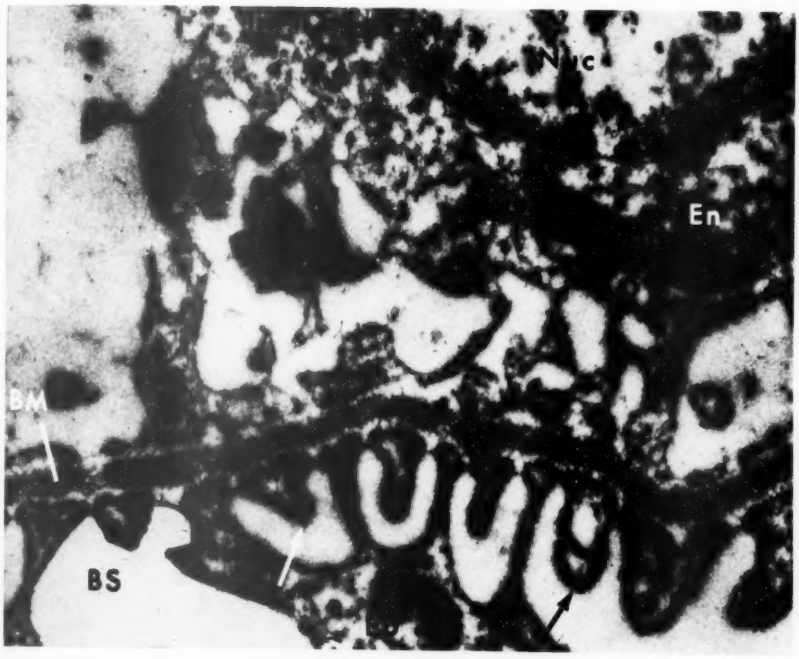

3

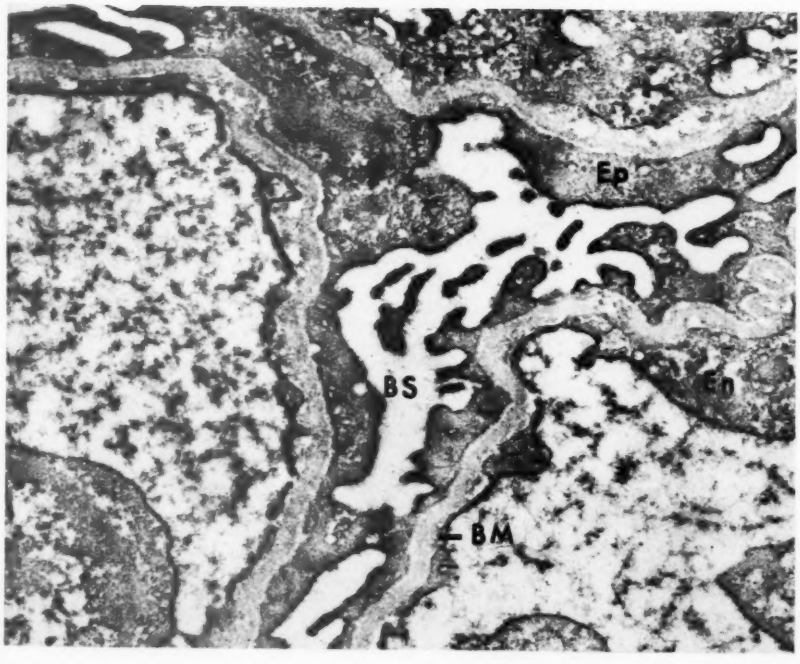

4

FIG. 5. Lipid nephrosis. The basement membrane is irregular and varies in thickness. The normal foot process pattern of the epithelium is replaced by confluent sheets of cytoplasm. The epithelial cells contain vacuoles which are frequently associated with "colloid droplets." Endothelium is hyperplastic. × 35,000.

FIG. 6. Lipid nephrosis. An irregular basement membrane which is markedly narrowed in one area (arrow) is seen. The epithelium consists of confluent masses of cytoplasm which contain vacuoles and droplets. The endothelium is slightly thickened. × 29,600.

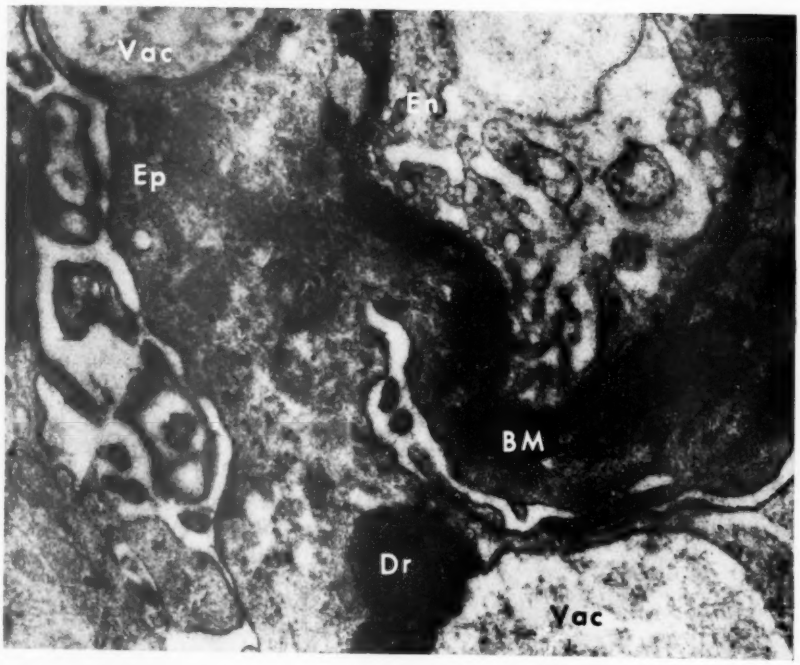

5

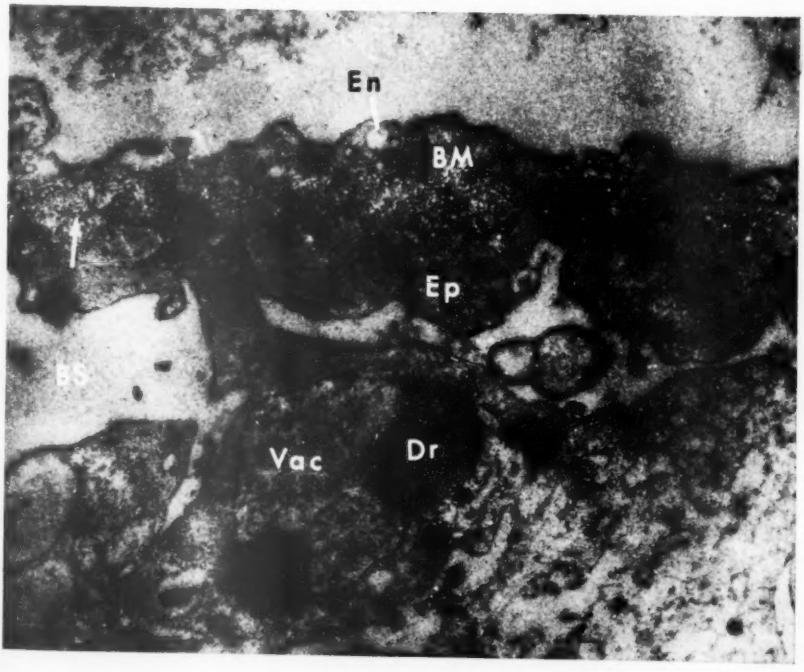

6

FIG. 7. Lipid nephrosis. Several areas of marked narrowing of the basement membrane are seen (arrows). The dense appearance of the juxta-basement membrane portions of the epithelium is apparently due to the presence of numerous cytoplasm filaments which continue into the basement membrane proper. × 37,100.

FIG. 8. Lipid nephrosis. In one region the basement membrane is markedly attenuated (arrow). At other points there are peripheral strand-like overgrowths of basement membrane. Epithelium again reveals the presence of fine filaments. Endothelium is thickened and contains vacuoles. × 49,100.

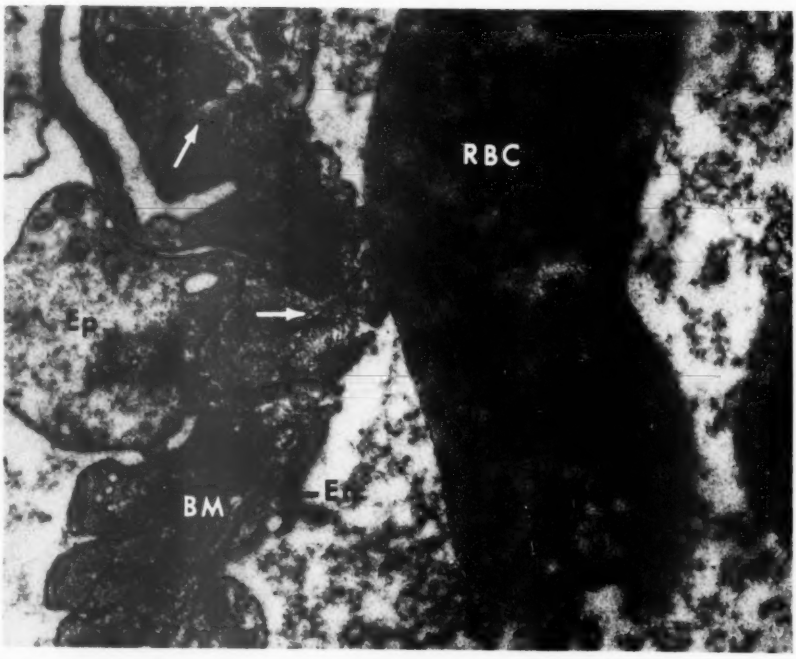

7

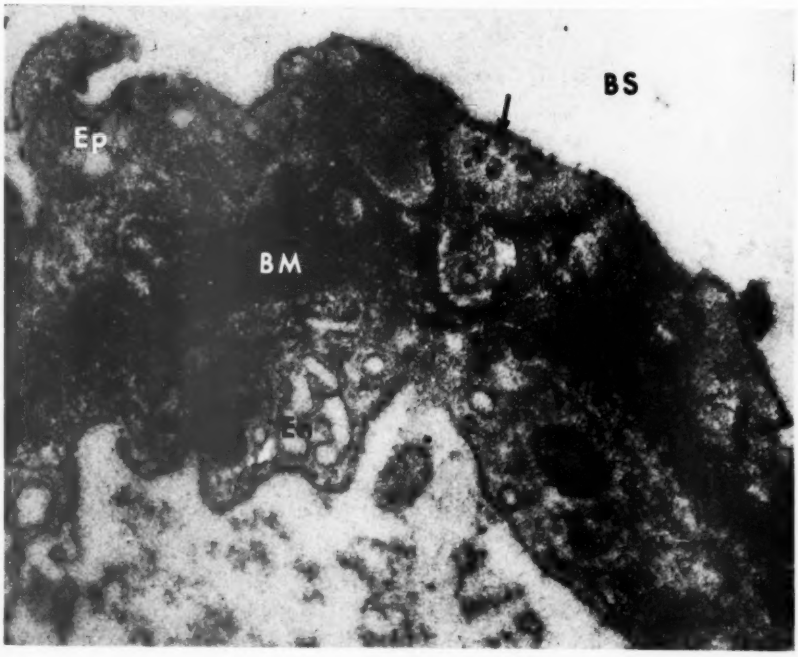

8

FIG. 9. Lipid nephrosis. Similar to preceding page. Alternating zones of thickening and attenuation of the basement membrane are evident. × 51,500.

FIG. 10. Lipid nephrosis. An obvious defect in the basement membrane is visible (arrow). In this region there is contact between epithelial and endothelial cytoplasm. × 44,800.

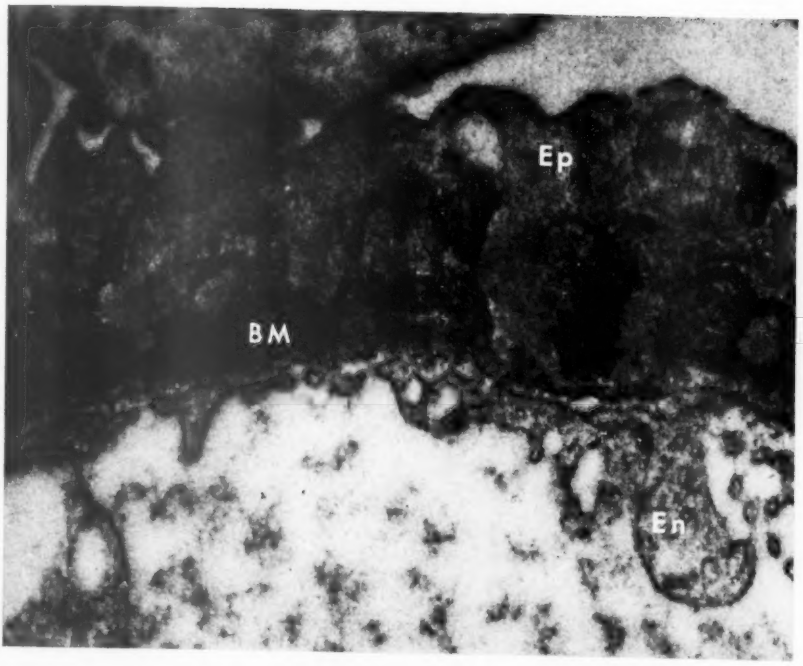

9

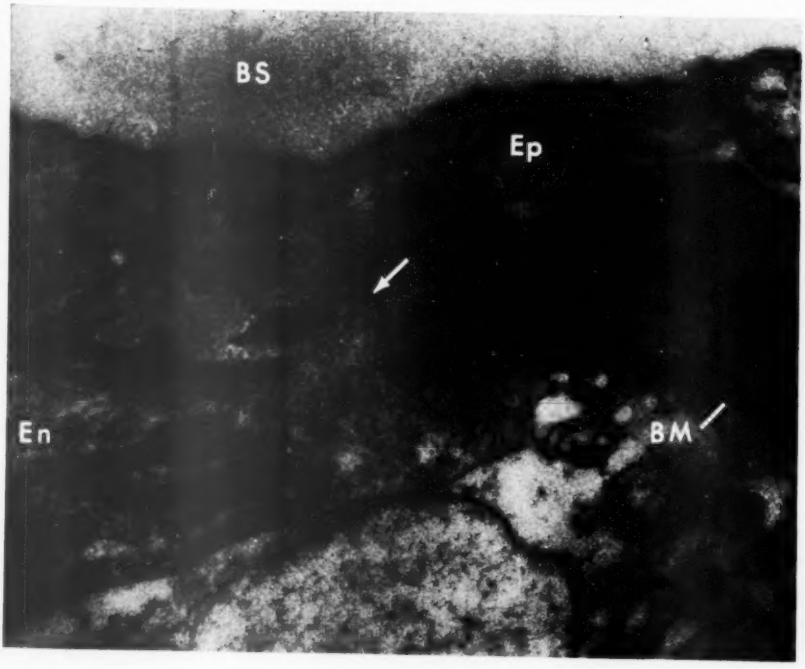

10

FIG. 11. Lipid nephrosis. A defect in the basement membrane (arrow) as well as areas of basement membrane overgrowth are apparent. × 41,900.

FIG. 12. Amyloidosis. At the upper left a subendothelial deposit of amyloid substance is present, internal to an intact basement membrane. On the right another nodule of amyloid is present which has penetrated and replaced the basement membrane. In this region the epithelium reveals confluence of its foot processes into a broad cytoplasmic sheet. The portion of the capillary wall intervening between the amyloid deposits is essentially normal. × 12,700.

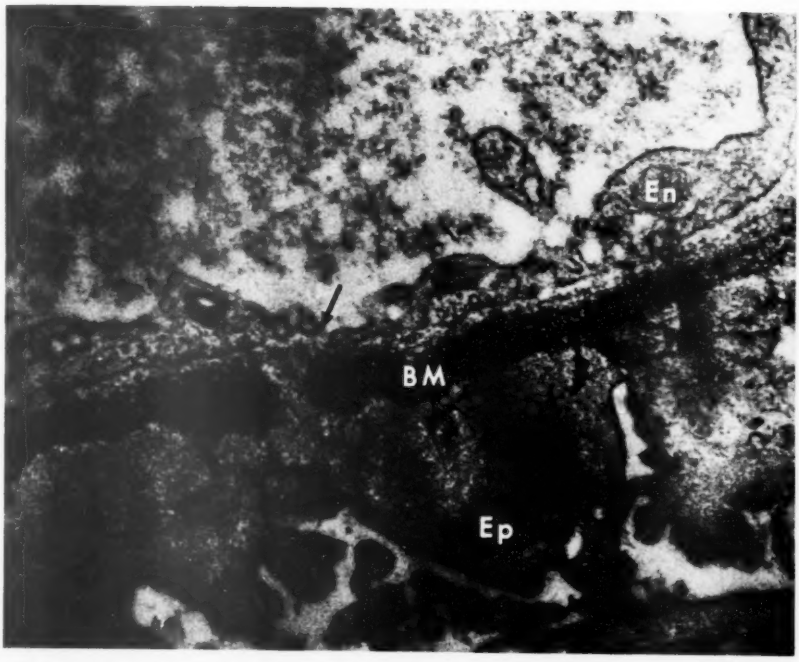

11

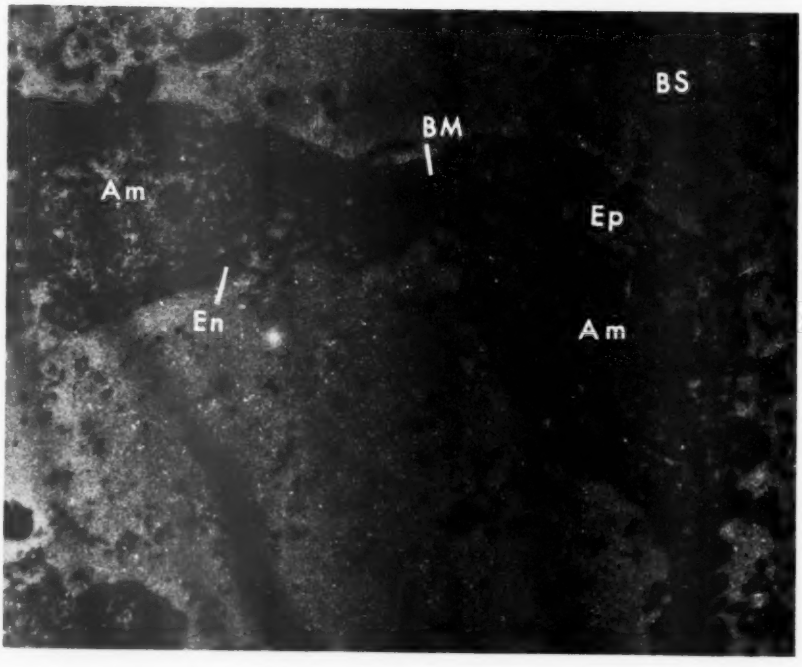

12

FIG. 13. Amyloidosis. A localized mass of amyloid has replaced the basement membrane and extends from the endothelial cell layer to the epithelial layer. × 24,600.

FIG. 14. Amyloidosis. The capillary wall is markedly thickened as the result of amyloid deposit. The amyloid substance consists of a loose meshwork of fine filaments. Remnants of basement membrane are present. Epithelium is organized in a continuous sheet of cytoplasm. × 36,000.

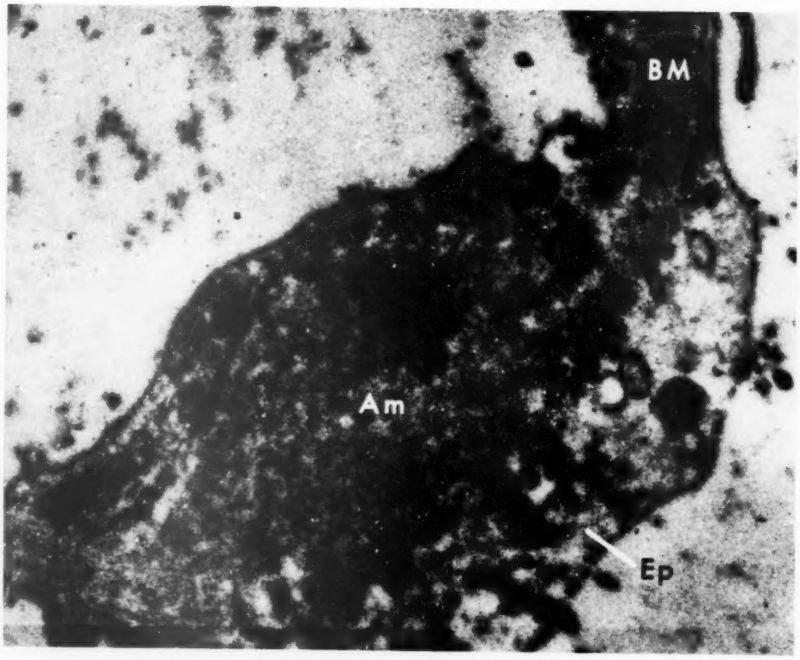

13

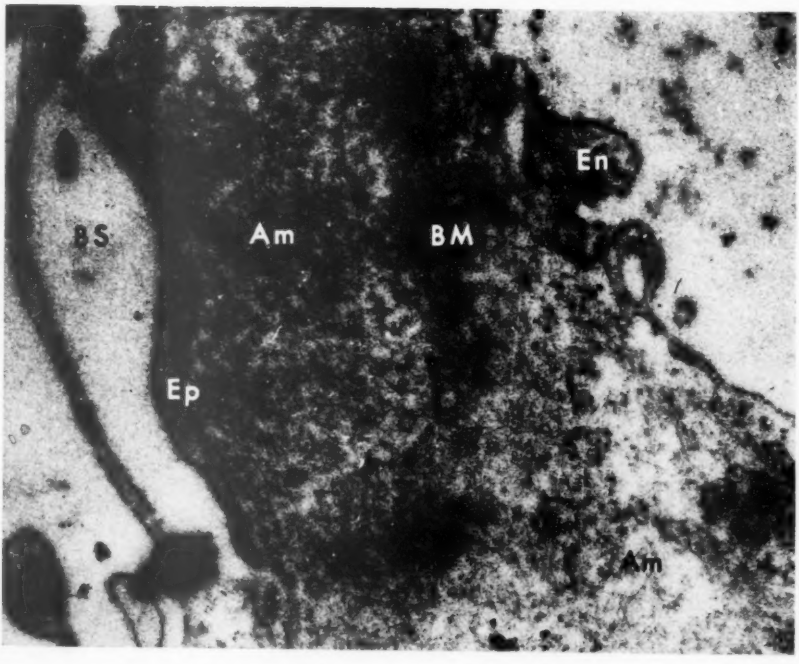

14

FIG. 15. Amyloidosis. The loose fibrous nature of the amyloid is apparent. × 16,800.

FIG. 16. Amyloidosis. A mass of glomerular amyloid exhibits a fibrous nature. × 25,800.

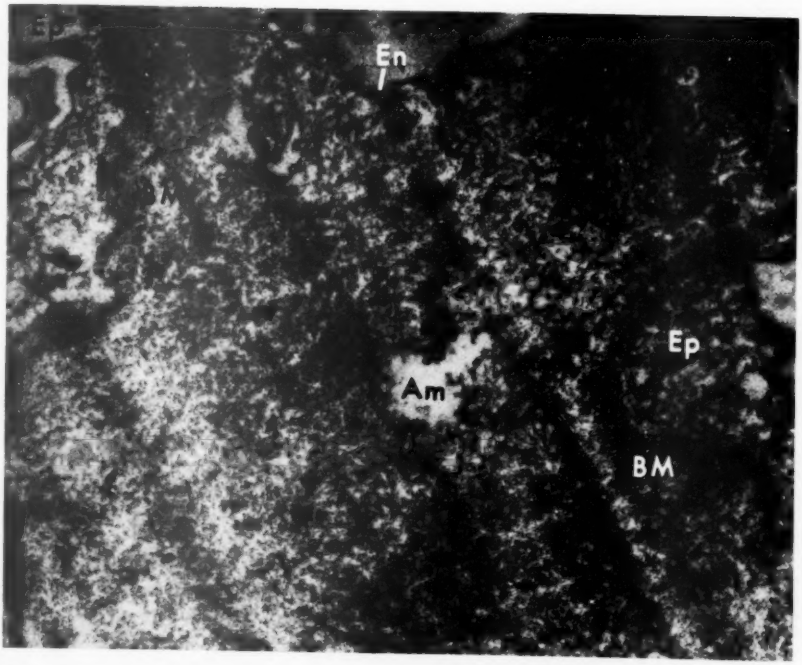

15

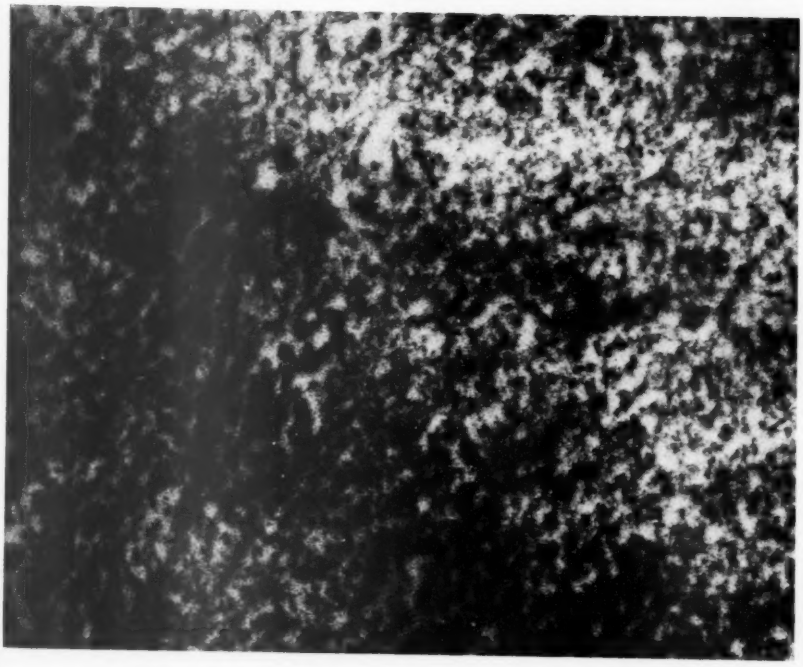

16

FIG. 17. Subacute and chronic glomerulonephritis. Broad sheets of thickened basement membrane contain embedded endothelial cells. × 13,500.

FIG. 18. Subacute and chronic glomerulonephritis. At the lower right the capillary wall is relatively normal except for a thickened basement membrane. Toward the center and top of the photograph the basement membrane is defective (arrow), permitting apposition of the endothelial and epithelial cell layers. In this region the epithelium appears as a confluent sheet of cytoplasm. × 22,400.

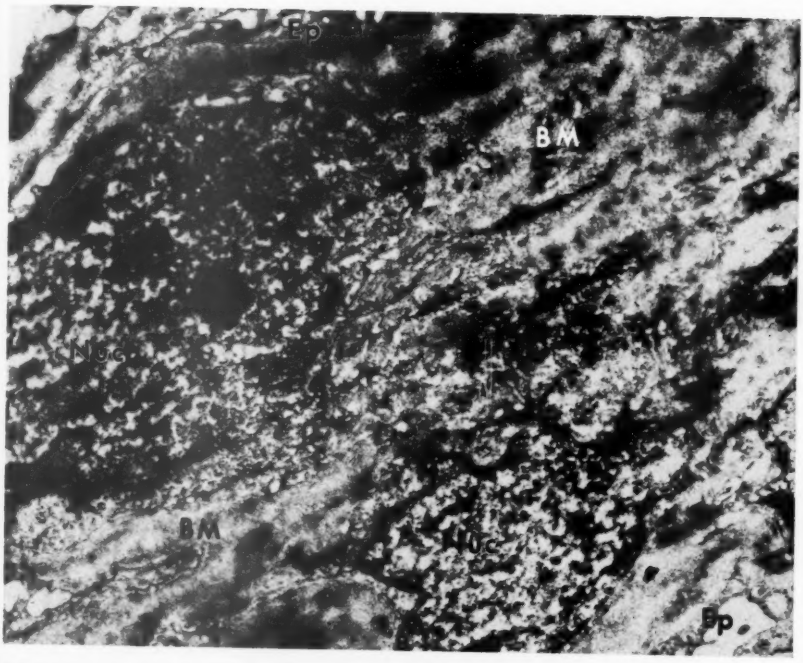

17

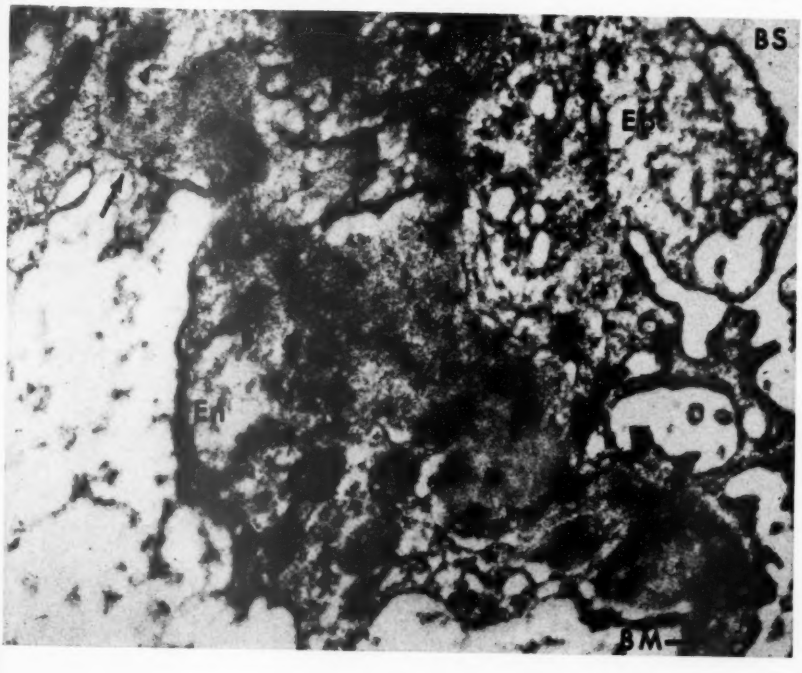

18

LOCALIZATION OF COLLOIDAL SUBSTANCES IN VASCULAR ENDOTHELIUM. A MECHANISM OF TISSUE DAMAGE

I. Factors Causing the Pathologic Deposition of Colloidal Carbon *

Baruj Benacerraf, M.D.; Robert T. McCluskey, M.D., and Dorothy Patras, M.D.
From the Department of Pathology, New York University College of Medicine, New York, N.Y.

The classical description by Aschoff[1] defined a group of cells, designated as the reticuloendothelial system (R.E.S.), which are characterized by their highly phagocytic behavior toward colloidal particles and dyes. He included in this system the Kupffer cells, the cells lining the sinuses of the spleen, lymph nodes and bone marrow, and the endothelial cells in the adrenal and anterior pituitary. These cells are normally concerned with the removal of particulate matter from the blood. The phagocytic capacity of endothelium in other locations has been a subject of controversy.[2] Foot[3] has reported phagocytosis of India ink in pulmonary vessels. Domagk and Neuhaus,[4] as well as Klostermeyer,[5] claimed that the endothelial cells of pulmonary capillaries and to a lesser extent of glomeruli were phagocytic for bacteria. This was denied by Pratt[6] who considered the bacteria in the lungs to be within macrophages rather than in capillary endothelium.

The arrest of colloids in sites other than the R.E.S. can be explained on the basis of two distinct mechanisms. First, it may be caused by the coagulation or flocculation of the suspension investigated in the circulation and its consequent arrest in capillaries, and secondly, it may be the result of alteration of the endothelium itself whereby it becomes phagocytic or sticky for the circulating colloid.

The work of Halpern, Benacerraf and Biozzi[7] emphasized the importance of using tracer colloidal suspensions which remain well dispersed in the blood in a wide range of concentration and which are devoid of toxicity. They demonstrated that the abnormal localization of India ink observed in lung capillaries was caused by a process of intravascular coagulation of fibrin brought about by the shellac in the preparation.

However, even if a preparation is used that is stable in the circulation and does not cause intravascular clotting, the endothelium of blood vessels can still be shown to accumulate carbon under certain circum-

* This study was aided by grants from the Nephrosis Foundation and the American Heart Association.
Received for publication, June 26, 1958.

stances.[8] The endothelial cells of capillaries and venules in the skin have been found to take up carbon or dyes at the site of injection of inflammatory agents such as histamine.[8,9] Jancso[8] suggested that histamine "activates" endothelium to become phagocytic. Whatever the exact mechanism, the occurrence of stickiness of endothelium for circulating colloids as well as platelets and leukocytes is a well known feature of the inflammatory reaction.

The purpose of this study is to investigate the deposition of colloidal particles in other sites than the R.E.S. under the influence of: dosage of colloid employed; blockade of the R.E.S.; the systemic effects of vasoactive amines and soluble antigen-antibody complexes in antigen excess.

It is generally accepted that the phagocytosis of particulate matter by the macrophage system is beneficial to the organism. However, the significance of the arrest of potentially harmful or toxic colloidal materials or bacteria in other sites by the mechanisms investigated in the present study has not been sufficiently emphasized as a mechanism of tissue damage.

Material and Methods

Use was made of a nontoxic stable suspension of carbon C11-1431a from the firm Günther, Wagner, of Hanover, Germany. This preparation, made of particles about 250 Å in size, contains approximately 100 mg. of carbon per ml. in a solution of partially hydrolyzed gelatin and phenol. For most of the experiments this preparation was diluted with a solution of gelatin, as previously described,[10] to further guarantee the stability of the suspension. When large doses were to be administered, the preparation was dialyzed against water to remove the phenol. This carbon suspension has been used to explore the phagocytic function of the R.E.S.[11] The clearance of these efficiently phagocytized carbon particles follows an exponential function of time, $C = C_0 10^{-KT}$ where C = concentration of carbon at time T. The constant K expresses the rate of phagocytosis and varies inversely with injected dose. $K \times D$ = constant, which illustrates the saturating effect of phagocytized carbon on the R.E.S. All experiments were performed on adult white male Swiss Webster mice. The animals were sacrificed by decapitation, and sections were prepared of heart, lung, liver, spleen, kidney, stomach, skin, and, in some cases, aorta and brain.

Antigen-antibody complexes were prepared from rabbit antiserums against 3 times recrystallized hen ovalbumin or bovine serum albumin (BSA). The serums were analyzed for antibody by the quantitative precipitin technique.[12]

The antiovalbumin serum contained 1.44 mg. per ml. of antibody

protein. Ten ml. of this serum were precipitated at the equivalence point by antigen. After several washings in saline and centrifugation, the precipitate was redissolved in 150 mg. ovalbumin in 4 ml. of saline. Five ml. of anti-BSA containing 2.3 mg. of antibody protein per ml. were precipitated with BSA at its equivalence point and subsequently redissolved with 25 mg. of BSA in 1 ml. of saline. The soluble complexes were injected as described below.

Experiments

The Effect of Dosage on the Distribution of Carbon Particles

It has been established that when 16 mg. of carbon per 100 gm. of body weight are injected intravenously into mice, the carbon particles are cleared within an hour by the R.E.S. About 90 per cent of the injected carbon is found in the liver and spleen. No carbon is found in the endothelium of kidney, lung, heart, or skin.[11,13] The same results were observed in the present study (Fig. 1).

It was found that the repeated daily injection of 16 mg. of carbon per 100 gm. for 5 days in a group of 10 mice did not result in deposition of carbon in sites outside the R.E.S. In order to investigate the effect of overloading the R.E.S. on the distribution of injected carbon, 4 doses of 70 mg. of carbon per 100 gm. were injected into 12 mice in 48 hours. Another group of 12 mice received the same dose once a day for 6 days. This severe overloading of the R.E.S. resulted in death of 7 of the 24 mice in spite of the nontoxic properties of the carbon suspension, presumably because of increased susceptibility to infection. Despite a marked increase in capacity of the R.E.S. as evidenced by the enlargement of the liver and spleen to twice their normal combined weights, the distribution of the carbon particles under these conditions was quite different from what was seen with the smaller dose. The endothelial cells of arteries, veins and capillaries in many locations were heavily laden with carbon particles. In the liver itself, carbon was seen not only in markedly enlarged Kupffer cells, but also within the endothelium of sinuses, hepatic and portal veins, and to a lesser extent in the hepatic cells themselves, where it had a finely granular appearance (Fig. 2). In the spleen there was marked hyperplasia and increased phagocytosis in the red pulp. In the lung, carbon was present in macrophages within alveoli and in the endothelial cells of pulmonary arteries and capillaries (Fig. 3). The kidney showed a striking accumulation of particles within glomeruli (Fig. 4) and also within endothelium of blood vessels of all sizes. In the heart, granules of carbon were seen within the endothelium lining the chambers and covering the heart valves (Fig. 5) and within the endothelium of coronary arteries. The

larger arteries such as the aorta showed phagocytosis by endothelial cells (Fig. 6).

Thus it can be seen that with prolonged and excessive administration of colloidal particles, phagocytosis by endothelium can be demonstrated in regions where it is not normally observed. The phagocytic properties of the cells of the R.E.S. can therefore be considered as an especially active function of endothelium in general. The accumulation of carbon in areas other than the R.E.S. varied in intensity and was most marked in glomeruli, small vessels of the heart, pulmonary arteries, and most small veins. As will be shown, these are in general the areas in which the endothelium can be most easily activated.

The Effect of Previous R.E.S. Blockade on the Distribution of Carbon Particles

In the experiments described above, the overloading of the R.E.S. caused by the repeated injections of carbon may have been an important determining factor in the altered distribution observed. To investigate this further, a group of 5 mice received injections of 3 doses of thorotrast, 1 ml. per 100 gm., every 48 hours. Such a course of treatment with thorotrast has been shown to cause effective saturation of the phagocytic activity of the R.E.S.[14] Twenty-four hours after the last dose, the mice received 16 mg. of carbon per 100 gm.

In these mice, the amount of carbon in the R.E.S. was less than that usually seen (Fig. 7), and carbon particles were found in endothelium in other locations, particularly in renal glomeruli (Fig. 8). All the cells of the R.E.S. were markedly swollen and contained pale pink or yellow granules, representing phagocytized thorium dioxide. In the spleen there were numerous nodular accumulations of swollen macrophages in the form of granulomatous lesions (Fig. 9). The glomerular cells were markedly swollen and contained pale pink or yellow material, representing thorotrast, as well as carbon (Fig. 8).

The Effects of Vasoactive Amines on the Distribution of Carbon Particles

The work of Jancso[8] and Biozzi, Mene and Ovary[9] has emphasized the role of histamine in producing activation of the endothelium of blood vessels of the skin to phagocytize colloidal carbon. These effects have been studied locally and are associated with increased capillary permeability, which is also a feature of the inflammatory reaction. Experiments were performed to ascertain whether the systemic administration of histamine, serotonin or adrenalin would cause deposition

of carbon in the vascular endothelium of various organs, when 16 mg. of carbon per 100 gm. were injected, a dose which is normally removed exclusively by the R.E.S. Serotonin was injected intravenously in doses of 0.25, 0.5, and 1.5 mg. Histamine dihydrochloride was given in doses of 5 mg. intravenously or intraperitoneally; the mouse is notably resistant to the lethal effect of histamine. Adrenalin was administered intraperitoneally in doses of 0.05 and 0.1 mg. Combinations of these substances were also used in some instances, employing the same doses. Within a few minutes after the injection of these agents, the carbon suspension was injected slowly and the animals sacrificed one to two hours later.

The experiments were performed several times on groups of at least 4 mice for each substance or combination of substances tested. Since in some mice given adrenalin or serotonin, thrombi were observed, similar investigations were also carried out using animals given 100 to 200 U.S.P. units of heparin (Organon) intravenously, 15 minutes before the experiments.

In all of the experiments most of the carbon was phagocytized by the R.E.S. in the usual fashion, but the agents studied caused deposition in various other sites as will be described below.

Histamine. Abnormal deposition of carbon in histamine-treated animals was seen as follows: Fine granules of carbon were found in endothelial cells of glomeruli but not elsewhere in the kidneys. The capillaries and venules of the heart and the serosa of the stomach also contained carbon in endothelial cells. No more than traces of carbon were found in the vessels of the skin or lung. Pretreatment with heparin did not alter these effects of histamine.

Adrenalin. The changes observed with adrenalin were striking. There was marked accumulation of carbon in the venules and capillaries in the renal medulla (Fig. 10) and a small amount in glomeruli. The venules and capillaries in the gastric mucosa seemed to have their lining coated with carbon (Fig. 11). In the lung and to a lesser extent in the kidney, carbon was present in the form of large intravascular clumps, suggesting thrombus formation. Pretreatment with heparin reduced considerably the accumulation of carbon in the form of clumps, but did not reduce the amount of carbon in renal glomeruli or in the gastric mucosa.

Serotonin. Serotonin caused relatively slight abnormal deposition of carbon. As in the case of adrenalin, carbon was found in the vessels of the renal medulla and in the form of clumps in the lung. In the latter location, this was largely prevented by pretreatment with heparin.

The combination of serotonin and adrenalin increased the severity of adrenalin effects, and in this situation also the formation of thrombi in the lung and kidney was largely prevented by heparin.

The Effect of Soluble Antigen-Antibody Complexes on the Distribution of Carbon

Histamine and serotonin are released from mast cells as a result of antigen-antibody interaction. Germuth[15] has shown that soluble antigen-antibody complexes, when injected intravenously into guinea pigs, caused anaphylactic reactions due to liberation of agents such as histamine. In order to investigate the effects of release of endogenous histamine and related substances on the distribution of carbon, 6 mice received injections of soluble antigen-antibody complexes. Three mice were given 3.5 mg. of anti-BSA in the form of soluble complexes with BSA, and 3 other mice received 2.5 mg. of antiovalbumin in the form of soluble complexes with ovalbumin. Five minutes later 16 mg. of carbon per 100 gm. were slowly injected intravenously, and the animals were sacrificed about two hours later.

The changes observed in carbon distribution were more striking than with any of the pharmacologic agents investigated. In the kidney there were many fine granules in glomerular endothelial cells (Fig. 12). In the heart, carbon was seen in the endocardium, including the heart valves (Fig. 13), in coronary arteries and in the small blood vessels, especially in the epicardial fat (Fig. 14). There was considerable accumulation of carbon in the venules and capillaries throughout the wall of the stomach (Fig. 15). In the skin and subcutaneous tissues there was marked accumulation of carbon in the endothelium of small blood vessels (Fig. 16). In the lung there was virtually no carbon, indicating that there had been no intravascular clotting.

Discussion

Repeated injections of colloidal materials leading to prolonged elevation of blood levels resulted in phagocytosis by endothelial cells in sites other than the R.E.S. The histologic findings clearly demonstrated the presence of colloidal carbon within vascular endothelial cells. Although this occurred in virtually all endothelial cells, storage of carbon was more prominent in certain regions than in others; venules and renal glomeruli showed the most striking accumulation.

The data provide evidence for the phagocytic properties of endothelium outside of the R.E.S., a problem which has been discussed frequently.[2] Under normal circumstances the great avidity of the R.E.S. for colloidal particles and its great capacity do not allow the

demonstration of these properties. These findings are in agreement with the recent observation of Buck who found accumulation of thorium dioxide within endothelial cells of large arteries in rabbits following the administration of large doses of thorotrast.[16]

Aside from circumstances where there is overloading of the R.E.S., phagocytosis by vascular endothelium is known to occur at sites of inflammation and after local injections of histamine.[8,9] The present study was not concerned with the mechanism by which this was brought about. The activation of endothelium may be the result of altered function of the cells, or a consequence of a change in the endothelial surface which renders it sticky for a variety of materials and which may represent the first step in phagocytosis. Whatever the mechanism, this phenomenon may be of importance in the pathogenesis of disease states which depend upon the localization of injurious colloidal or particulate material, in such sites as heart valves, renal glomeruli or arteries.[17]

The systemic administration of serotonin, adrenalin, or histamine causes localization of carbon in the vessels of the heart, kidney, and stomach. The effects of serotonin or adrenalin may be determined in part by the occurrence of intravascular clotting or by changes in hemodynamics. Infusion of adrenalin has been shown to accelerate blood clotting *in vivo*.[18] The systemic administration of histamine appears to result in abnormal localization attributable to changes in the endothelium itself, especially in renal glomeruli and small vessels of the heart.

The most interesting results were seen after the administration of soluble antigen-antibody complexes which are known to cause liberation of endogenous histamine, serotonin, and possibly other substances from mast cells.[15] There was striking accumulation of carbon in glomerular endothelium and the small blood vessels of the heart, similar to what occurred after the administration of histamine, but in addition there was marked deposition of carbon in small blood vessels in the skin and in and around the stomach. It is reasonable to relate the findings with the large number of mast cells in these areas. The phenomena described may have some bearing on the pathogenesis of lesions of experimental serum sickness, since antigen-antibody complexes, which are handled as unstable colloids by the R.E.S.[19] circulate during the period when lesions appear and are localized at the sites of tissue damage.[17,20]

Summary

Phagocytosis of colloidal carbon by vascular endothelium of blood vessels, glomeruli and heart valves was demonstrated after injection of amounts of carbon which overloaded the reticuloendothelial system.

Blockade of the R.E.S. by thorotrast resulted in deposition of carbon in the glomeruli, and in endothelium in other locations, following injection of carbon in amounts normally cleared by the R.E.S.

Systemic administration of histamine caused abnormal localization of carbon particles in vascular endothelium, especially in glomeruli and small blood vessels of the heart. Treatment with serotonin or adrenalin also brought about abnormal localization of carbon, which was partly prevented by prior administration of heparin.

Soluble antigen-antibody complexes caused marked abnormal deposition of injected carbon in glomeruli, heart valves, and small blood vessels in the skin and stomach.

The significance of these observations with respect to the production of tissue damage is discussed.

REFERENCES

1. Aschoff, L. Morphologie des Retikuloendothelialen Systems. In: Handbuch der Krankheiten des Blutes und der Blutbildenden Organe. Enzyklopaedie der Klinischen Medizin. Spezieller Teil. Schittenhelm, A. (ed.). Springer, Berlin, 1925, Vol. 2, pp. 473–491.
2. Altschul, R. Endothelium. Its Development, Morphology, Function and Pathology. Macmillan Co., New York, 1954, 157 pp.
3. Foot, N. C. Studies on endothelial reactions. VII. Changes in the distribution of colloidal carbon noted in the lungs of rabbits following splenectomy. *J. Exper. Med.*, 1923, **37**, 139–151.
4. Domagk, G., and Neuhaus, C. Die experimentelle Glomerulonephritis. *Virchows Arch. path. Anat.*, 1927, **264**, 522–540.
5. Klostermeyer, W. Über Phagocytose in Capillarendothelien. *Virchows Arch. path. Anat.*, 1933, **288**, 703–716.
6. Pratt, D. W. Experimentelle Untersuchungen über die Kapillarwände der Leber, die Beziehungen der Kupffer'schen Sternzellen zu ihnen, nebst Beobactungen über die Tätigkeit der Kapillarendothelien in verschiedenen Kapillargebieten. *Beitr. path. Anat.*, 1927, **78**, 544–550.
7. Halpern, B. N.; Benacerraf, B., and Biozzi, G. Quantitative study of the granulopectic activity of the reticulo-endothelial system. I. The effect of the ingredients present in India ink and of substances affecting blood clotting *in vivo* on the fate of carbon particles administered intravenously in rats, mice and rabbits. *Brit. J. Exper. Path.*, 1953, **34**, 426–440.
8. Jancso, N. Speicherung; Stoffanreicherung im Retikuloendothel und in der Niere. Akademiai Kiado, Budapest, 1955, 468 pp.
9. Biozzi, G.; Mene, G., and Ovary, Z. L'histamine et la granulopexie de l'endothélium vasculaire. *Rev. Immunol.*, 1948, **12**, 320–334.
10. Biozzi, G.; Benacerraf, B., and Halpern, B. N. Quantitative study of the granulopectic activity of the reticulo-endothelial system. II. A study of the kinetics of the granulopectic activity of the R.E.S. in relation to the dose of carbon injected. Relationship between the weight of the organs and their activity. *Brit. J. Exper. Path.*, 1953, **34**, 441–457.

11. Benacerraf, B.; Biozzi, G.; Halpern, B. N., and Stiffel, C. Physiopathology of the Reticulo-endothelial System. A Symposium. Established under the joint auspices of UNESCO and WHO. Halpern, B. N.; Benacerraf, B., and Delafresnaye, J. F. (eds.). Blackwell Scientific Publications, Ltd., Oxford, and Charles C Thomas, Springfield, Ill., 1957, 317 pp.

12. Kabat, E. A., and Mayer, M. M. Experimental Immunochemistry. Charles C Thomas, Springfield, Ill., 1948, 567 pp.

13. Biozzi, G.; Benacerraf, B.; Stiffel, C., and Halpern, B. N. Étude quantitative de l'activité granulopexique du système réticulo-endothélial chez la Souris. *Compt. red. Soc. de biol.*, 1954, **148**, 431–435.

14. Benacerraf, B., and Sebestyen, M. Unpublished data.

15. Germuth, F. G., Jr., and McKinnon, G. E. Studies on the biological properties of antigen-antibody complexes. I. Anaphylactic shock induced by soluble antigen-antibody complexes in unsensitized normal guinea pigs. *Bull. Johns Hopkins Hosp.*, 1957, **101**, 13–42.

16. Buck, R. C. The fine structure of endothelium of large arteries. *J. Biophys. & Biochem. Cytol.*, 1958, **4**, 187–190.

17. McCluskey, R. T., and Benacerraf, B. Localization of colloidal substances in vascular endothelium. A mechanism of tissue damage. II. Experimental serum sickness with acute glomerulonephritis induced passively in mice by antigen-antibody complexes in antigen excess. *Am. J. Path.*, 1959 (to be published).

18. Forwell, G. D., and Ingram, G. I. C. The effect of adrenaline infusion on human blood coagulation. *J. Physiol.*, 1957, **135**, 371–383.

19. Benacerraf, B.; Sebestyen, M., and Cooper, N. S. The clearance of antigen-antibody complexes from the blood by the reticulo-endothelial system. *J. Immunol.* (in press).

20. Dixon, F. S.; Vasquez, T. T.; Weigle, W. O., and Cochrane, G. G. Pathogenesis of serum sickness. *A. M. A. Arch. Path.*, 1958, **66**, 18–28.

[*Illustrations follow*]

LEGENDS FOR FIGURES

All sections were stained with hematoxylin and eosin.

FIG. 1. Liver from a mouse given 16 mg. of carbon per 100 gm. and sacrificed one hour later. The Kupffer cells are loaded with carbon. × 175.

FIG. 2. Liver from mouse given 4 injections of 70 mg. of carbon per 100 gm. in 48 hours. The Kupffer cells are markedly swollen and loaded with carbon. Carbon is also present within endothelium in portal vein and hepatic cells. × 200.

FIG. 3. Pulmonary artery from mouse shown in Figure 2. Carbon particles are found within endothelial cells. × 300.

FIG. 4. Kidney from mouse given 70 mg. of carbon per 100 gm. daily for 6 days. The glomeruli show marked accumulation of carbon. × 300.

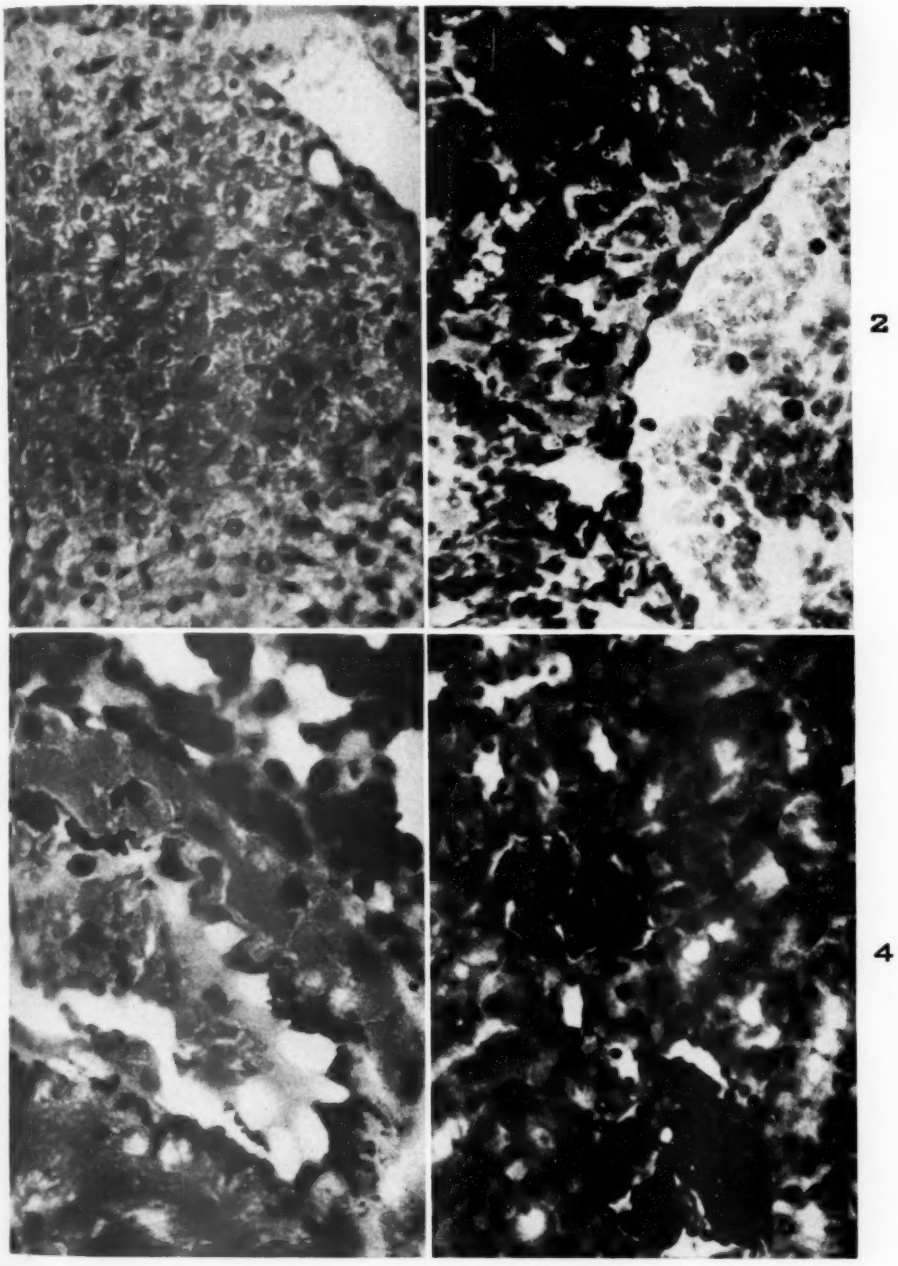
1
2
3
4

FIG. 5. Mitral valve from mouse given 70 mg. of carbon per 100 gm. for 6 days. There is marked irregular deposition of carbon within the valve leaflet. × 385.

FIG. 6. Aorta from mouse given 4 injections of 70 mg. of carbon per 100 gm. in 48 hours. Fine particles of carbon are present in endothelial cells. × 650.

FIG. 7. Liver from mouse given 3 injections of thorotrast every 48 hours, followed by 16 gm. of carbon per 100 gm. The mouse was sacrificed 4 hours after the carbon injection. The Kupffer cells are swollen and contain yellow or pink granules (thorotrast) and only a small amount of carbon. × 175.

FIG. 8. Kidney from mouse shown in Figure 7. The glomerular cells are swollen and contain yellowish pink granules (thorotrast) and some carbon particles. × 650.

5

6

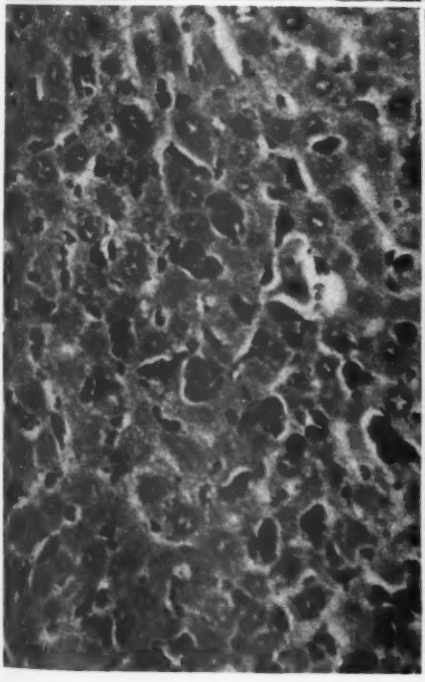

7

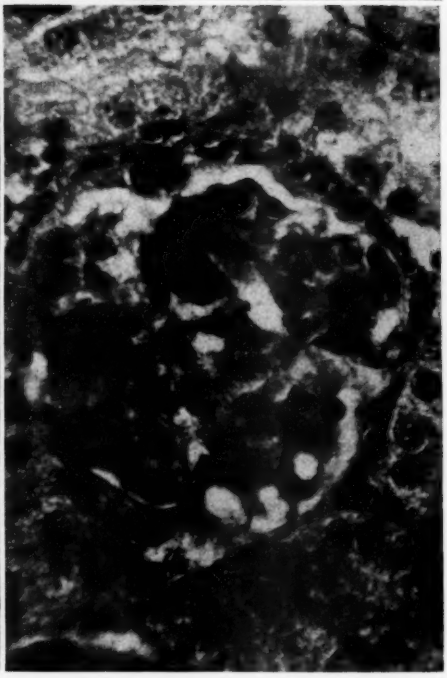

8

FIG. 9. Spleen from mouse given 3 injections of thorotrast every 48 hours followed by 16 mg. of carbon per 100 gm. There are nodular aggregates of mononuclear cells containing thorotrast. Only a small amount of carbon is present. × 175.

FIG. 10. Renal medulla from mouse given 0.1 mg. of adrenalin followed by carbon, 16 mg. per 100 gm. The mouse was sacrificed one hour later. The lining of the blood vessel in the center is covered with carbon. × 450.

FIG. 11. Gastric mucosa from mouse shown in Figure 10. There is carbon lining the endothelial surface of the small blood vessels. × 175.

FIG. 12. Kidney from mouse given soluble antigen-antibody complexes (BSA-anti-BSA) followed by carbon, 16 mg. per 100 gm. The mouse was sacrificed two hours later. The glomerular cells are swollen and contain fine particles of carbon. × 450.

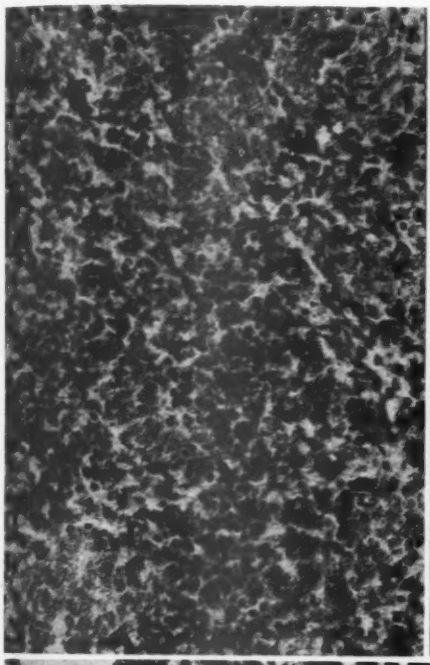

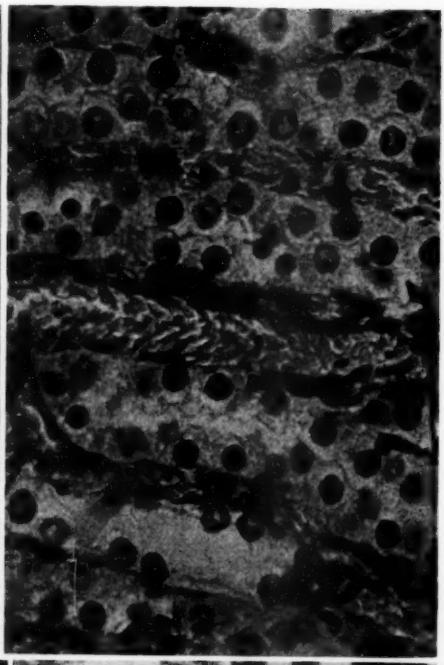

10

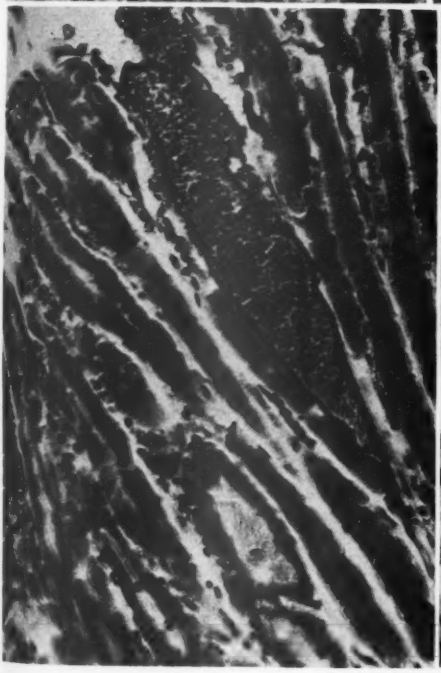

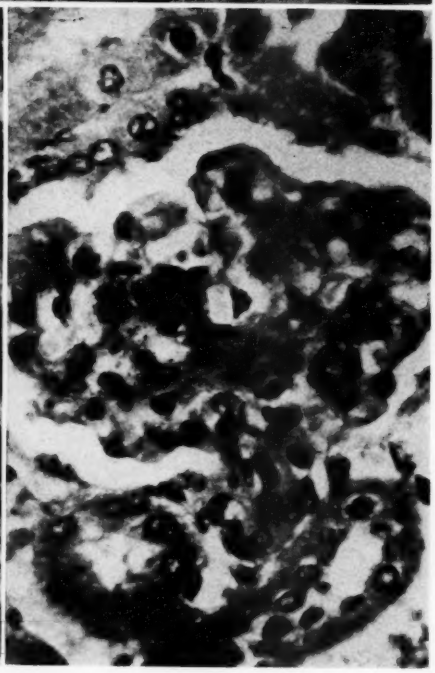

12

FIG. 13. Mitral valve from mouse given soluble antigen-antibody complexes (ovalbumin-antiovalbumin) followed by 16 mg. of carbon. The mouse was sacrificed two hours later. Some of the endothelial cells of the valve contain carbon particles. × 650.

FIG. 14. Heart from mouse shown in Figure 13. The small vessels in the pericardial adipose tissue contain carbon in their endothelial cells. × 300.

FIG. 15. Stomach wall from mouse given soluble antigen-antibody complexes (BSA-anti-BSA) followed by carbon, 16 mg. per 100 gm. The mouse was sacrificed two hours later. The small vessels in the muscular wall contain carbon in their endothelial cells. × 140.

FIG. 16. Skin from mouse shown in Figure 15. The venules show accumulation of carbon within endothelial cells. × 300.

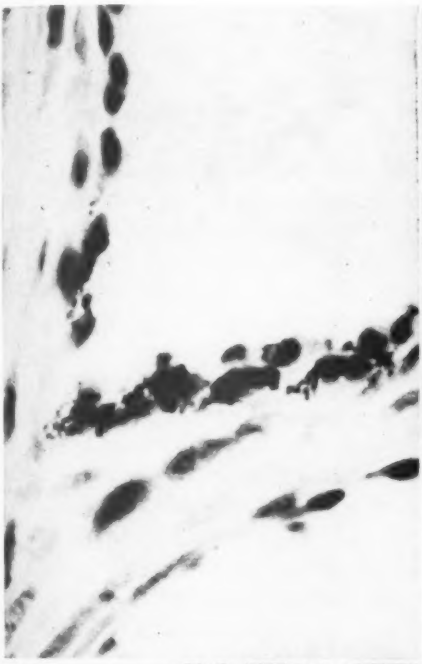

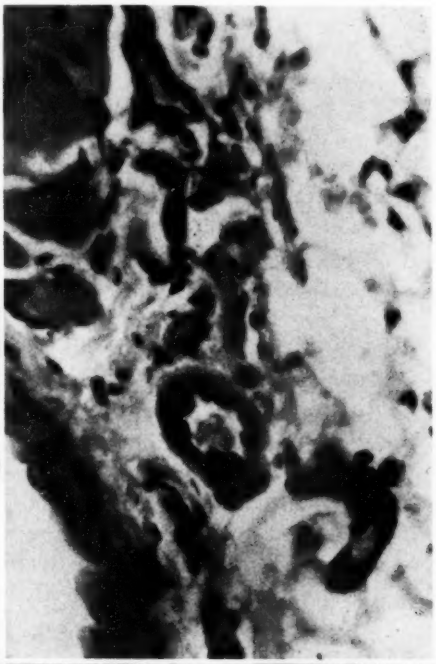

14

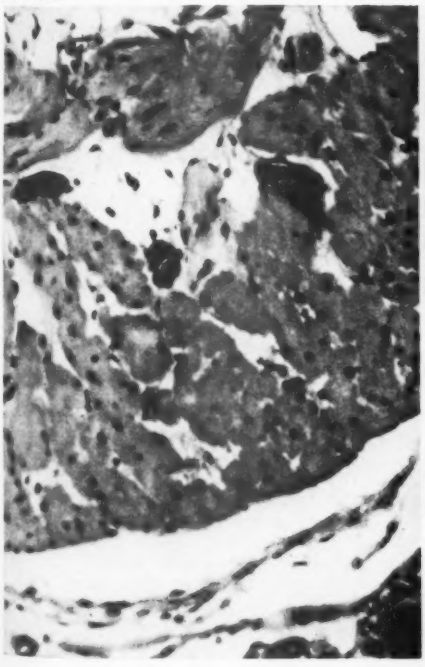

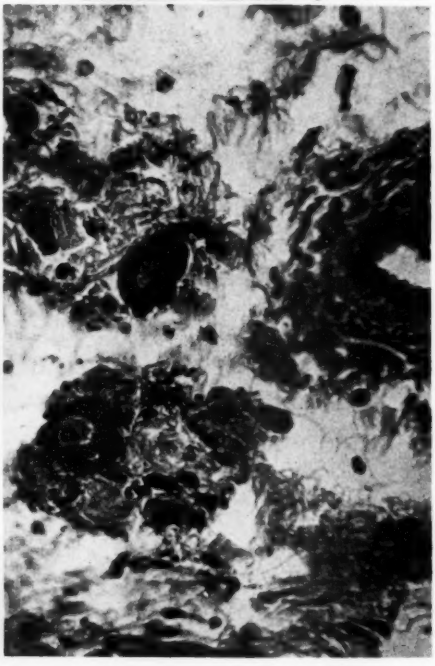

16

THE MORPHOLOGIC ELEMENTS IN THE EARLY LESIONS OF ARTERIOSCLEROSIS *

HENRY Z. MOVAT, M.D., Ph.D.;† M. DARIA HAUST, M.D., and ROBERT H. MORE, M.D.
From the Department of Pathology of Queen's University and the Kingston General Hospital, Kingston, Ont., Canada

Although some of the early focal intimal thickenings of the aorta commence as minute accumulations of lipids, other early lesions develop by a different mechanism. It was found that not all develop as lipid-rich lesions, nor do they all progress to a stage of atheroma. More advanced and even old lesions, although quite prominent, can be almost completely devoid of lipid. Therefore, the term "arteriosclerosis" instead of "atherosclerosis" is preferred.

The material for this study was selected on the basis of gross appearance. The lesions considered to be early appeared grossly as (1) circumscribed and diffuse glassy translucent elevations; (2) white opaque elevations (plaques); (3) small red mural thrombi; or (4) yellow dots and streaks. In addition, one group of lesions was included even though they were so small that they represented a chance observation. These were not visible grossly and were discovered accidentally on microscopic examination; they were also considered to represent early alterations.

The staining and other technical procedures were carried out as described in another publication.[1] From a total of 148 aortas, 470 sections were examined: 56 represented fatty dots and streaks; 129 were gelatinous elevations; 5 were small, just visible thrombi; and 13 were small, grossly invisible thrombi. The white opaque elevations (plaques) will be dealt with in a subsequent publication.

RESULTS

Gelatinous Elevations

The basic change, whether circumscribed or diffuse, consisted of an edematous swelling of the intima. This was caused by "insudation" of serum or plasma into the intima. In the swollen intima the 2 to 3 layered pattern described previously[2] was frequently distorted or no longer discernible. The various components of connective tissue, such as collagen, elastic fibers, and ground substance, and cellular elements,

* Supported by grants-in-aid from Public Health Research Grants of Canada and the Bickell Foundation of Toronto, Canada.
Received for publication, March 24, 1958.
† Present address: Department of Pathology, University of Toronto, Banting Institute, Toronto, Ont., Canada.

as well, had undergone lysis. In sections stained with toluidine blue, the metachromasia normally present in the intima was diminished and at times absent, indicating a diminution, "dilution," or perhaps depolymerization of acid mucopolysaccharides (AMP). In sections in which the AMP were stained with Alcian blue, such as pentachrome I or II[3] or Alcian blue-PAS-orange G, a decrease of Alcian blue-positive substance was noted. In milder lesions the elastic and collagen fibers were separated by the swollen ground substance (Fig. 1). Occasionally this change was confined only to the connective tissue layer of the intima (Fig. 2). In more pronounced lesions the 2 or 3 layered pattern described in the normal intima[2] was often completely wiped out (Fig. 3). Although some fibrin could often be demonstrated in milder lesions, insuded threads of fibrin constituted an almost constant finding in more advanced lesions. The fibrin was present in the form of threads and stellate structures (Fig. 4), sometimes conglomerating to form clumps, and at times a meshwork, in which entrapped red cells were frequently noted (Fig. 5). Occasionally the serofibrinous insudate caused not only separation, but also swelling of collagen fibers (Fig. 6). Lipids could be demonstrated in the insudate at times. Whether the lipid had been present at the site of the lesion before the insudation had taken place, or whether it was a component of the insudate, could not be determined. The fat was present extracellularly in dispersed or finely granular form, or as intracellular lipid (Fig. 7).

Fatty Dots and Streaks

Microscopically, the small yellow dots were found to be comprised of accumulations of foam cells, located either beneath the endothelium (Fig. 8) or somewhat deeper in the intima (Fig. 9). Larger accumulations of foam cells corresponded to typical grossly visible yellow streaks. The largest streaks were formed by confluence of numerous foam cells (Fig. 10). Despite the marked accumulation of lipids seen in some lesions (Fig. 11), there was neither increase of connective tissue nor reactive fibrosis in response to the deposition of lipids. If such fatty lesions were covered by a fibrous cap, the origin of the latter could always be traced to recent or old mural thrombi.[4-8]

Grossly Invisible Fibrin Thrombi

This group of early alterations was discovered accidentally, no lesion being visible in the gross. While in large mural thrombi, described elsewhere,[5,6] most of the blood constituents could be demonstrated, these small lesions proved to be recent mural thrombi composed of fibrin and platelets (Fig. 12). The fibrinous nature could be well dem-

onstrated with the phosphotungstic acid hematoxylin stain, in which a meshwork of fibrin was manifest in the less dense parts. Despite extension of some thrombi over relatively large areas (Fig. 13), the underlying intima showed no morphologic alterations. Some small mural thrombi, however, covered an intima which was the seat of insudation and swelling as described above (Fig. 14). When such thrombi had been present for some time, the fibrinous material appeared as acidophilic bands. Endothelium usually covered the thrombi, incorporating them into the wall of the aorta. The fate of mural thrombi will be discussed in a subsequent paper.[6]

Small Fibrin Thrombi, Barely Visible Grossly

This last group of early lesions revealed a composition similar to the one just described; i.e., they consisted of fibrin and platelets. At times, however, some other constituents of the blood, such as red blood cells, could also be demonstrated.

Discussion

Insudative lesions in the intima of the aorta were first described by Ribbert in 1904.[9] Despite a clear demonstration, these observations were neglected. In 1942 Bredt,[10] stimulated by Klinge's studies in rheumatic aortitis,[11] examined the lesions in pulmonary arteries and described swelling of the intima as the earliest visible change in arteriosclerosis of that vessel. Similar alterations were found in the aorta by Holle.[12] Meyer[13] was the first to describe fibrinous insudation occurring predominantly in the distal parts of plaques. This was believed to cause further progression of the plaques. Meyer used the term "insudation" in the belief that he was dealing with an inflammatory exudate in the sense of Virchow, who referred to arteriosclerosis as "*endarteritis chronica deformans*."

We have adopted the term "insudate"[14] as proposed by Meyer in order to emphasize the fact that the protein-rich material is deposited *into* the substance of the intima. Whether this represents an inflammatory process is presently undetermined. If we accept Rössle's[15] concept of serous inflammation, during the course of which lysis of connective tissue elements may be encountered, in contradistinction to noninflammatory edema, then the lesion in the aortic intima is of inflammatory nature. Whether the lipid material found in these lesions has been deposited into the intima along with serum or plasma, or whether it had been there previously, could not be determined in our studies.

An interesting aspect of the early lesions in which the lipids were a

predominant feature was the lack of a reactive fibrosis. It is generally believed that the fibrosis occurring in arteriosclerosis represents a reaction to the lipid pool. We could find no evidence for this hypothesis in our studies. If there was any fibrosis present, its origin from fibrinous material was always evident. These fibrin or fibrin-platelet thrombi, usually found on the surface of an intima, showed some degree of alteration such as serous or serofibrinous insudation or deposition of lipids. In some cases, however, the intima was unaltered. Submicroscopic changes of the intima may have preceded the deposition of mural thrombi. We are thus in partial agreement with Rokitansky,[16] Clark, Graef and Chasis,[17] and contemporary British investigators,[18-21] that arteriosclerosis may develop as a result of thrombotic encrustation. However, this is only one way in which this complex lesion has its inception. The other two demonstrable mechanisms are serous or serofibrinous insudation and deposition of lipids.

Summary

The structure of lesions which appeared to represent the earliest alteration in the development of arteriosclerosis has been described and the gross and microscopic features correlated.

Corresponding to the gelatinous translucent elevations, a swelling of the intima and insudation of serum and fibrin with or without lipids were noted. The microscopic counterpart of the yellow dots and streaks was an intracellular accumulation of lipid material. A remarkable observation was the absence of reactive fibrosis in fatty lesions. An incidental feature was the existence of small mural fibrin thrombi deposits, not only on altered but also on morphologically unaltered intima.

These observations clearly indicate that the early focal lesions of arteriosclerosis in the aortic intima have at least 3 distinct patterns in their structural and chemical composition. It is not possible from these observations to determine whether further evolution of the 3 lesions may lead to a common end stage.

REFERENCES

1. Movat, H. Z., and More, R. H. The nature and origin of fibrinoid. *Am. J. Clin. Path.*, 1957, **28**, 331–353.
2. Movat, H. Z.; More, R. H., and Haust, M. D. The diffuse intimal thickening of the human aorta with aging. *Am. J. Path.*, 1958, **34**, 1023–1031.
3. Movat, H. Z. Demonstration of all connective tissue elements in a single section. *A. M. A. Arch. Path.*, 1955, **60**, 289–295.
4. Haust, M. D.; Movat, H. Z., and More, R. H. The role of fibrin thrombi in the genesis of the common white plaque in arteriosclerosis. (Abstract.) *Circulation*, 1956, **14**, 483.

5. Haust, M. D., and More, R. H. Morphologic evidence and significance of permeation in the genesis of arteriosclerosis. (Abstract.) *Circulation,* 1957, **16,** 496.
6. Haust, M. D.; More, R. H., and Movat, H. Z. The mechanism of fibrosis in arteriosclerosis. *Am. J. Path.,* 1959 (to be published).
7. More, R. H.; Movat, H. Z., and Haust, M. D. Role of mural fibrin thrombi of the aorta in genesis of arteriosclerotic plaques. Report of two cases. *A. M. A. Arch. Path.,* 1957, **63,** 612–620.
8. More, R. H., and Haust, M. D. Encrustation and permeation of blood proteins in the genesis of arteriosclerosis. (Abstract.) *Am. J. Path.,* 1957, **33,** 593.
9. Ribbert, H. Ueber die Genese der arteriosklerosen Veränderungen der Intima. *Verh. Deut. Path. Ges.,* 1904, **8,** 168–177 (quoted by Meyer, W. W.[13]).
10. Bredt, H. Entzundung und Sklerose der Lungenschlagader. *Virchows Arch. path. Anat.,* 1942, **308,** 60–152.
11. Klinge, F. Der Rheumatismus; pathologisch-anatomische und experimentell-pathologische Tatsachen und ihre Auswertung für das ärtzliche Rheumaproblem. *Erg. Path. u. path. Anat.,* 1933, **27,** 1–351.
12. Holle, G. Über Lipoidose, Atheromatose und Sklerose der Aorta und deren Beziehungen zur Endaortitis. *Virchows Arch. path. Anat.,* 1943, **310,** 160–256.
13. Meyer, W. W. Die Bedeutung der Eiweissablagerungen in der Histogenese arteriosklerotischer Intimaveränderungen der Aorta. *Virchows Arch. path. Anat.,* 1949, **316,** 268–316.
14. Movat, H. Z., and More, R. H. Morphologic and histochemical studies on the development and progression of arteriosclerosis. (Abstract.) *Circulation,* 1955, **12,** 484.
15. Rössle, R. Über die serösen Entzündungen der Organe. *Virchows Arch. path. Anat.,* 1944, **311,** 252–284.
16. Rokitansky, C. A Manual of Pathological Anatomy. Day, G. E. (trans.). The Sydenham Society, London, 1852, Vol. 4, p. 272 (quoted by Duguid[20]).
17. Clark, E.; Graef, I., and Chasis, H. Thrombosis of the aorta and coronary arteries, with special reference to the "fibrinoid" lesions. *Arch. Path.,* 1936, **22,** 183–212.
18. Crawford, T., and Levene, C. I. The incorporation of fibrin in the aortic intima. *J. Path. & Bact.,* 1952, **64,** 523–528.
19. Duguid, J. B. Thrombosis as a factor in the pathogenesis of aortic atherosclerosis. *J. Path. & Bact.,* 1948, **60,** 57–61.
20. Duguid, J. B. Pathogenesis of arteriosclerosis. *Lancet,* 1949, **2,** 925–927.
21. Duguid, J. B. The arterial lining. *Lancet,* 1952, **2,** 207–208.

[*Illustrations follow*]

LEGENDS FOR FIGURES

FIG. 1. Edematous swelling of the ground substance with separation of the formed connective tissue elements of the intima. Trichrome stain. × 110.

FIG. 2. Edematous swelling of the connective tissue layer of the intima, due to insudation of serum, causing "lysis" of acid mucopolysaccharide (AMP) and cells. Pentachrome I stain. × 100.

FIG. 3. Marked intimal swelling associated with decreased staining of AMP and lysis of formed connective tissue elements and cells. The normal 3 layered pattern, which was present in the adjacent normal intima, has been eradicated. Pentachrome I stain. × 30.

FIG. 4. Serofibrinous insudate of intima. The serous fluid seen as homogeneous gray material (light bluish-pink in sections) and the fibrin as black (intensely red in sections) threads, stellate structures, and clumps. Heidenhain's azan stain. × 200.

FIG. 5. Dense meshwork of fibrin with entrapped red cells in a serofibrinous insudate. Phosphotungstic acid hematein stain. × 450.

FIG. 6. Argentophilia of collagen fibers in a gelatinous plaque of the intima. The serous fluid between the fibers is seen as a homogeneous gray material. Gomori's silver impregnation. × 200.

FIG. 7. Intracellular lipid seen as varying-sized black clumps and extracellular lipid in the form of granular material deposited along the elastic fibers. Carbowax section; Fettrot and hematoxylin stains. × 250.

FIG. 8. Accumulation of foam cells below the endothelium. Hemalum, phloxine, and saffron stains. × 100.

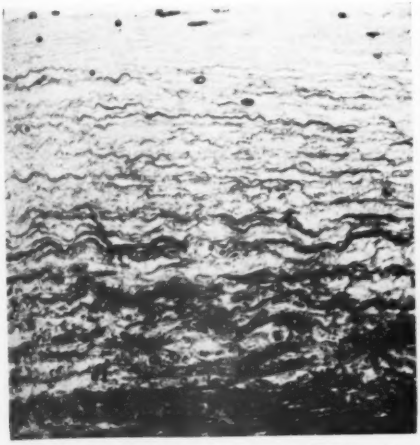

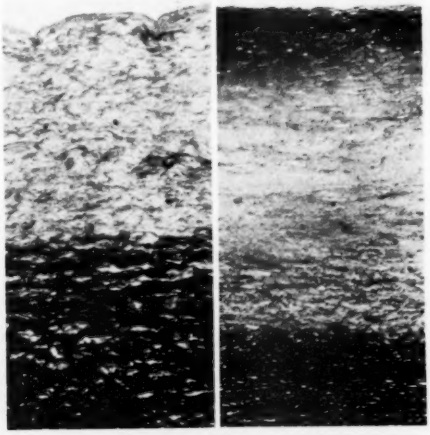

2, 3

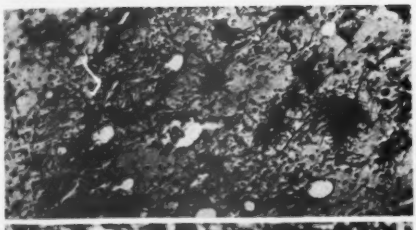

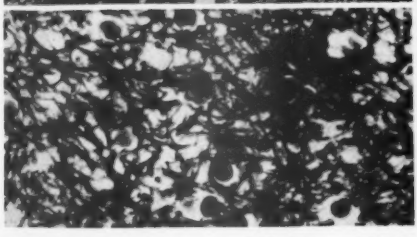

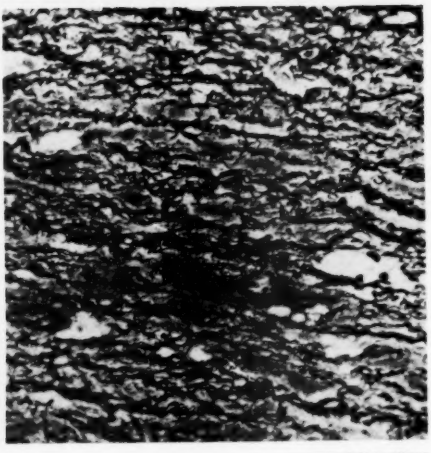

6

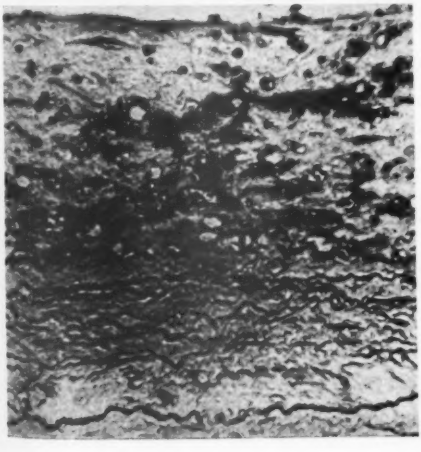

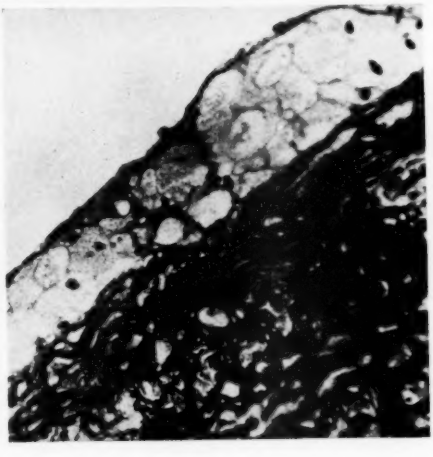

8

FIG. 9. A row of foam cells in the intima representing a small dot in the gross. Pentachrome II stain (elastica omitted). × 250.

FIG. 10. Numerous lipophages forming a fatty streak. Note slight bulging of the intima. Carbowax section; Fettrot and hematoxylin stains. × 250.

FIG. 11. Numerous lipophages in the upper part of the intima and extracellular lipids forming an early atheroma at the base of the intima. Carbowax section; oil red O, Alcian blue, and hematoxylin stains. × 250.

FIG. 12. Small mural platelet-fibrin thrombus on the surface of unaltered intima. Trichrome stain. × 250.

FIG. 13. Small mural thrombus covering the intima over a large area. Intima shows no morphologic alteration. Phosphotungstic acid hematoxylin stain. × 150.

FIG. 14. Mural thrombus seen as a black streak on top of an intima showing insudative changes. Endothelium partly covers the thrombus, representing the first step in its incorporation into the vessel wall. Phosphotungstic acid hematoxylin stain. × 250.

9

10

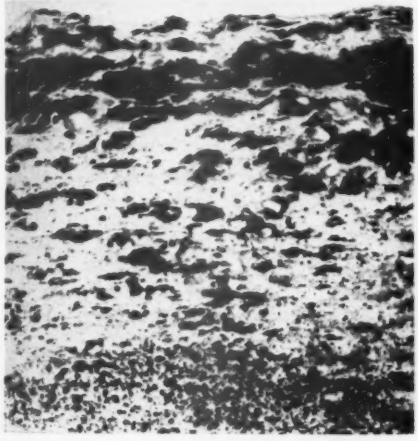

11

12

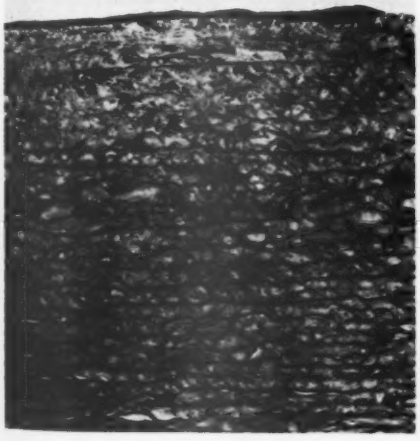

13

14

PHAGOCYTOSIS OF MAST CELL GRANULE BY THE EOSINOPHILIC LEUKOCYTE IN THE RAT*

RONALD A. WELSH, M.D., and JACK C. GEER, M.D.
From the Department of Pathology, Louisiana State University, School of Medicine, New Orleans, La.

During the course of an electron microscope study of mast cell degranulation in the rat peritoneal cavity, following administration of compound 48/80, eosinophilic leukocytes were discovered containing large ovoid bodies in their cytoplasm, identical in structure to liberated mast cell granules. The present report concerns the identification of these ovoid bodies in the eosinophils as mast cell granules which have undergone phagocytosis, and includes a discussion of the possible implications of this phenomenon.

MATERIALS AND METHODS

An inbred strain of crossed Sprague-Dawley and Rose-Illinois adult rats was used for study. One milliliter of Tyrode's solution containing 0.1 mg. of compound 48/80 was injected intraperitoneally into each of 12 rats. Compound 48/80, a condensation of p-methoxyphenethylmethylamine with formaldehyde, was graciously supplied by Burroughs Wellcome and Company, Inc., Tuckahoe, New York. At intervals of 5, 10, and 15 minutes, the peritoneal cavity was opened under ether anesthesia and the fluid aspirated gently with a pipette. Twelve control rats were treated in a like manner with Tyrode's solution injected into the peritoneal cavity. A portion of the aspirated fluid was fixed in buffered 1 per cent osmic acid[1] with added sucrose[2] for 30 minutes, and each specimen was then centrifuged at 2,000 r.p.m. for 2 minutes, dehydrated in graded alcohols, and embedded in methacrylate. Ultrathin sections were prepared and examined in an RCA EMU-3c electron microscope. Fresh smears of the aspirated fluid were made on glass slides. These were allowed to dry in air, and were stained with Wright stain.

RESULTS

Electron Microscopy

The changes in the mast cells were similar to those described in previous work by Bloom, Larsson and Smith,[3] and Smith and Lewis,[4] and will not be elaborated in detail. Figure 1 depicts a normal mast

* Supported in part by grants from the American Heart Association and the National Institutes of Health (H-2549).
Received for publication, July 2, 1958.

cell as observed in our study and Figure 2, a mast cell undergoing degranulation following the administration of compound 48/80.

Extracellular mast cell granules were noted at all time intervals following the injection of compound 48/80. The extracellular granules were similar to those within the mast cells; however, the majority of liberated granules were covered by a thin irregular coating of granular amorphous material (Fig. 3).

Eosinophilic leukocytes were identified by their smaller, often elliptical granules containing a typical dense band or bar. In some cases the central bar in the eosinophilic granule appeared less dense than the remainder of the granule. This change was observed in the control rats with the same frequency as in the cells of animals to which compound 48/80 had been administered. No granules resembling mast cell granules were seen in the cytoplasm of the eosinophilic leukocytes of the controls.

At all time periods following the injection of compound 48/80, occasional eosinophils contained varying numbers of small ovoid bodies in their cytoplasm, lying in a clear space surrounded by a single membrane. The ovoid bodies were identical in size and shape with mast cell granules and often had small bits of granular amorphous material adherent to their surfaces (Fig. 3).

In the controls a rare histiocyte or mesothelial cell was found containing ingested ovoid granules morphologically identical to mast cell granules. Since mesothelial cells may act as phagocytes under certain conditions, exact differentiation from histiocytes was not attempted, and the noncommittal term "phagocyte" was used for the two cells when ingested material was found in their cytoplasm. Phagocytes containing similar ovoid bodies surrounded by a membrane were noted frequently at all time intervals after injection of compound 48/80.

Light Microscopy

Wright-stained, air-dried smears from the control rats showed no evidence of blue granules in over 500 eosinophils examined; however, in smears at all time intervals following the injection of compound 48/80, varying numbers of large blue stained granules were found in an average of 20 per cent of the eosinophilic leukocytes. There were usually 2 or 3 blue granules per cell, but occasional eosinophils contained 12 or more. These granules were similar to those in mast cells and to the large numbers of extracellular mast cell granules encountered. Mast cell granules were seen in the cytoplasm of other phagocytes and eosinophilic leukocytes with approximately the same frequency.

Discussion

The peritoneal cavity of the rat is an ideal locale for this type of study since a rich harvest of mast cells, eosinophils, histiocytes, lymphocytes, and mesothelial cells can be obtained normally from this region. The differential counts of the peritoneal fluid vary somewhat, but mast cells range between 5 and 15 per cent, and eosinophils from 20 to 30 per cent of all cells. Compound 48/80 is one of the least toxic histamine liberators available and appears to show cytologic effect only upon mast cells, producing a rapid discharge of granules to the extracellular environment. Previous reports of mast cell changes seen by electron microscopy following the administration of compound 48/80 and other agents that produce mast cell degranulation, e.g. stilbamidine, protamine, toluidine blue, and x-radiation, have not specifically indicated alterations of eosinophilic leukocytes.[3,4] The mastocytoma of the dog was studied by electron microscopy, but no granules resembling those of the mast cell were described in the cytoplasm of eosinophils.[5]

Several possibilities should be considered to account for the presence of mast cell granules in eosinophils: (1) artifacts of manipulation prior to fixation or during centrifugation; (2) specific alteration of granules in the eosinophilic leukocytes; and (3) phagocytosis of mast cell granules by eosinophils.

The first possibility does not appear to be likely since control specimens did not show similar bodies in the cytoplasm of eosinophils when examined either by electron or light microscopy. It is unlikely that granules could be forced into the fixed cytoplasm of a cell without definite evidence in the electron photomicrographs of mechanical rupture of the cell membrane, and such a rupture has not been found. The possibility that the cytoplasmic bodies in eosinophils were altered eosinophilic granules is feasible if one were to postulate that the rat eosinophil contains granules which possess the properties of mast cell granules. Study of the eosinophils in the controls failed to reveal any granules exhibiting this capacity, and there was no indication that the eosinophil granule underwent any morphologic change following the injection of compound 48/80.

The third possibility, that these are ingested mast cell granules, seems most likely in view of the known phagocytic activity of the eosinophil.[6,7] The ovoid bodies observed are the same size and shape as mast cell granules; they have a coating or rim of granular material attached to their outer surfaces similar to that noted on granules liberated from mast cells, and are surrrounded by a limiting membrane identical to that of mast cell granules ingested by other phagocytes. A

question that immediately comes to mind is why these bodies have not been identified previously in eosinophils with the light microscope under these conditions. One probable answer to this lies in the fact that following administration of compound 48/80, the mast cell granule loses its metachromatic property,[8] thus making it difficult if not impossible to identify it with any degree of certainty. In smears procured after the administration of compound 48/80 and stained with Wright stain, bluish bodies similar to mast cell granules can be identified easily in eosinophils. In this case, however, the possibility of superimposition of extracellular granules on the eosinophils must be considered. Electron microscopy proves that granules identical to those in mast cells are incorporated within the cytoplasm of eosinophils.

To our knowledge, this is the first report of phagocytosis of mast cell granules by the eosinophilic leukocyte. It is possible that this represents a nonspecific action, but other experimental work on these two cells points to interrelationships that lend more significance to the phenomenon. Mast cell granules are known to be a potent source of histamine,[9] and histamine alone produces an increased number of eosinophils in the circulating blood.[10] A chemical substance with antihistaminic properties has been obtained from eosinophils,[11] and it has been postulated that the eosinophilic leukocyte acts as an inactivator of histamine and histamine-like substances.[12] The eosinophil has also been shown to be capable of transporting specific antigen.[13] The fact that this cell engulfs mast cell granules may indicate a common line of defense. Thus, in the event of marked histamine release, the eosinophil could serve as a means of rapid isolation and neutralization of the histamine-laden particles. In the lesion of urticaria pigmentosa, for example, characterized as it is by a dense infiltration of tissue by mast cells and a rich histamine content, stroking of the lesion causes disruption of the mast cells, edema, and an influx of eosinophils.[14] In the mastocytoma of the dog, a tumor of mast cells, eosinophils form a prominent component and are scattered diffusely throughout the lesion.[8] This tumor also contains a high concentration of histamine.[15]

"Basophilic bodies" have been described in the cytoplasm of human eosinophilic leukocytes.[16,17] The exact nature of these has not been determined, although Di Mayorca, Lanzavecchia and Le Coultre[17] have suggested that they are mast cell granules. They differ from those seen in the rat eosinophil in the absence of a surrounding clear space with outer limiting membrane. It is not known whether or not mast cell granules engulfed by rat eosinophils assume a similar appearance after a period of several days; further studies are needed to determine this possibility. Based on the observations in our study, we believe that

the "basophilic bodies" in circulating eosinophils in man should be seriously suspected as representing phagocytosis of mast cell granules.

Summary

Phagocytosis of mast cell granules by eosinophilic leukocytes is described in the rat following intraperitoneal injection of compound 48/80. The possible significance of this phenomenon is discussed in relation to histamine release and allergic inflammation. It is suggested that the phagocytosis of mast cell granules may be the basis for the "basophilic bodies" seen in circulating eosinophils in human subjects.

REFERENCES

1. Palade, G. E. A study of fixation for electron microscopy. *J. Exper. Med.*, 1952, **95**, 285–298.
2. Caulfield, J. B. Effects of varying the vehicle for OsO_4 in tissue fixation. *J. Biophys. & Biochem. Cytol.*, 1957, **3**, 827–830.
3. Bloom, G.; Larsson, B., and Smith, D. The reaction of peritoneal mast cells in the rat to various activators. *Acta path. et microbiol. scandinav.*, 1957, **40**, 309–314.
4. Smith, D. E., and Lewis, Y. S. Electron microscopy of the tissue mast cell. *J. Biophys. & Biochem. Cytol.*, 1957, **3**, 9–14.
5. Bloom, G.; Friberg, U., and Larsson, B. Some observations on the fine structure of mast cell tumors (masto-cytoma). *Nord. Vet. Med.*, 1956, **8**, 43–55.
6. Weinberg, M., and Séguin, P. Recherches biologiques sur l'éosinophile. Deuxième partie. Propriétés phagocytaires et absorption de produits vermineux. *Ann. Inst. Pasteur*, 1915, **29**, 323–346.
7. Ingraham, E., and Wartman, W. B. Chemotropism of human eosinophilic polymorphonuclear leukocytes. *Arch. Path.*, 1939, **28**, 318–322.
8. Padawer, J., and Gordon, A. S. Mammalian mast cells and histamine liberators. (Abstract.) *Anat. Rec.*, 1955, **121**, 411.
9. Riley, J. F. Pharmacology and functions of the mast cells. *Pharmacol. Rev.*, 1955, **7**, 267–277.
10. Vaughn, J. The stimulation of the eosinophil leucocyte. *J. Path. & Bact.*, 1952, **64**, 91–102.
11. Vercauteren, R., and Peeters, G. On the presence of an antihistaminicum in isolated eosinophilic granulocytes. *Arch. internat. pharmacodyn.*, 1952, **89**, 10–14.
12. Vaughn, J. The function of the eosinophile leukocyte. *Blood*, 1953, **8**, 1–15.
13. Godlowski, Z. Z. Transportation of anaphylactogenic property by eosinophil. *Brit. J. Exper. Path.*, 1948, **29**, 511–524.
14. Lever, W. F. Histopathology of the Skin. J. B. Lippincott, Philadelphia, 1954, ed. 2, p. 57.
15. Cass, R.; Riley, J. F.; West, G. B.; Head, K. W., and Stroud, S. W. Heparin and histamine in mast-cell tumours from dogs. *Nature, London*, 1954, **174**, 318–319.

16. Low, F. N., and Freeman, J. A. Electron Microscopic Atlas of Normal and Leukemic Human Blood. The Blakiston Division, McGraw-Hill Book Co., New York, 1958, p. 11.

17. Di Mayorca, G.; Lanzavecchia, G., and Le Coultre, A. Studio sulla morphologia dei leucociti umani normale e leucemici col metodo della sezione solttili al microscopio elettronico. *Rendic. Ist. lombardo sc.*, 1956, 90, 559–572.

We wish to acknowledge the technical assistance of Miss Yvonne Stich.

LEGENDS FOR FIGURES

FIG. 1. Normal mast cell from peritoneal cavity of control rat. × 8,350.

FIG. 2. Mast cell five minutes after administration of compound 48/80. The granules lie in a clear space and can be seen escaping extracellularly. Note the granular amorphous material that surrounds the granules. × 8,350.

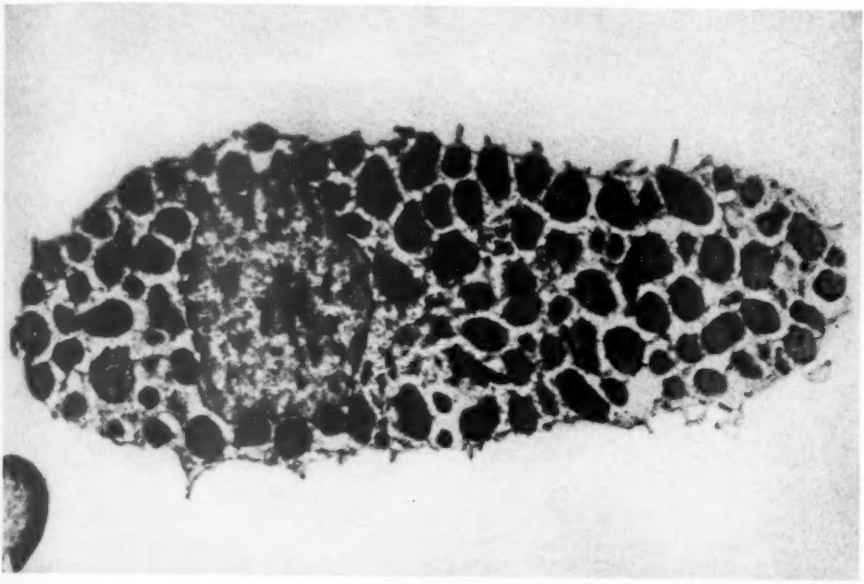

1

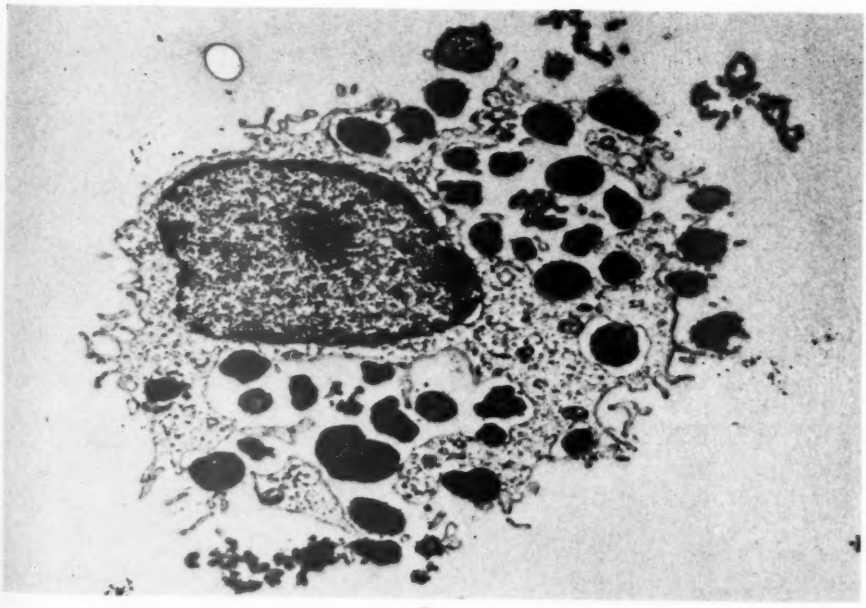

2

FIG. 3. Upper. Two eosinophilic leukocytes are present. The lower one contains a mast cell granule in its cytoplasm. In the upper right corner are several extracellular mast cell granules. × 13,440.
Insert, bottom left. Higher magnification of mast cell granule seen in an eosinophil. × 31,275. Insert, bottom right. Higher magnification of extracellular mast cell granule. × 31,275.

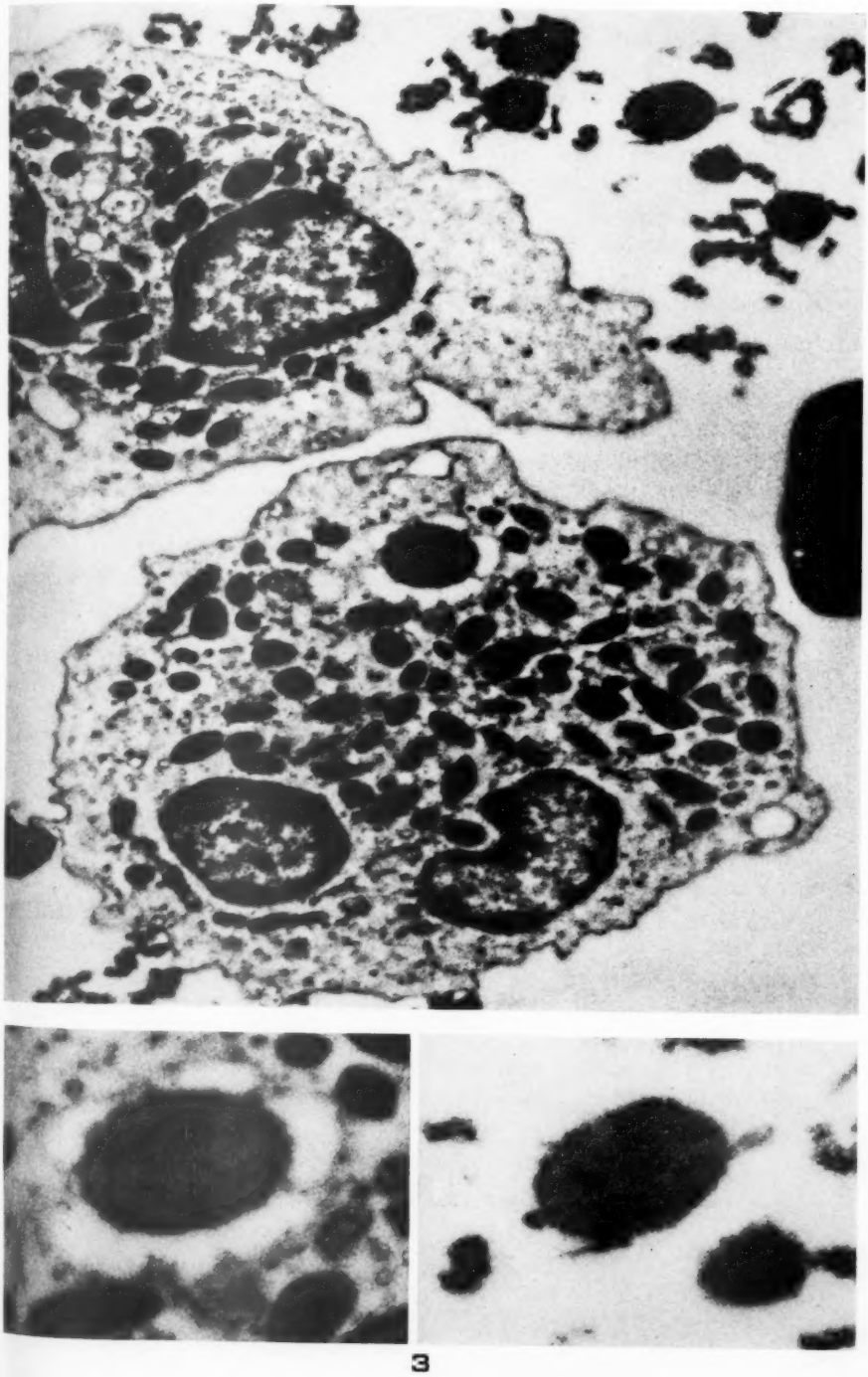

3

A HISTOCHEMICAL STUDY OF FIVE OXIDATIVE ENZYMES IN CARCINOMA OF THE LARGE INTESTINE IN MAN *

LEE W. WATTENBERG, M.D.†
From the Department of Pathology, University of Minnesota Medical School, Minneapolis, Minn.

In the present report, the results of a histochemical study of 5 oxidative enzymes in normal colonic mucosa, benign proliferative lesions, and in carcinoma of the large intestine are presented. This investigation was undertaken as an effort to demonstrate a histochemical reaction pattern in cells of carcinoma of the colon which would be distinctive from those occurring in either normal mucosa or benign proliferative lesions in this region.

In recent years, advances in histochemistry have made it possible to study a number of important oxidative enzymes in histologic sections. The advances have been due largely to the development of procedures utilizing tetrazolium salts. The oxidation-reduction potential of tetrazolium salts is such that they can serve as hydrogen acceptors in a number of oxidative enzymatic reactions. They are water soluble and almost colorless in the oxidized form but upon reduction form highly insoluble and intensely colored formazans. They therefore have the prerequisite properties of histochemical reagents for demonstrating oxidative enzymes and accordingly have been put to this use.[1-5]

In the present investigation, techniques employing tetrazolium salt reduction have been utilized for the demonstration of 5 oxidative enzymes: diphosphopyridine nucleotide (DPN) diaphorase, triphosphopyridine nucleotide (TPN) diaphorase, succinic dehydrogenase, α-glycerophosphate dehydrogenase, and monoamine oxidase. DPN diaphorase and TPN diaphorase catalyze the oxidation of reduced diphosphopyridine nucleotide (DPNH), and reduced triphosphopyridine nucleotide (TPNH), respectively.[6] Succinic dehydrogenase is a component of the citric acid cycle and thus is one of a group of enzymes which catalyze the oxidation of pyruvate. The α-glycerophosphate dehydrogenase catalyzes the reversible oxidation of L-α-glycerophosphate and is of importance in neutral fat and phospholipid metabolism.[7] Monoamine oxidase is believed to be primarily a detoxifying enzyme.[8] The 5 enzymes have been studied in normal and hyperplastic mucosa, adenomatous polyps, and carcinoma of the large

* This investigation was aided by a grant from the American Cancer Society.
Received for publication, June 16, 1958.
† This study was performed during the author's tenure as a Lederle Medical Faculty Awardee.

intestine in man. As will be described, a distinctive reaction pattern, consisting of high DPN diaphorase and TPN diaphorase activities and low succinic dehydrogenase, α-glycerophosphate dehydrogenase and monoamine oxidase activities, has been observed in carcinomas. This pattern differs from those found in cells of the normal mucosa and benign proliferative lesions.

Material and Methods

The study is based upon observations made in surgically resected specimens. Included were 35 samples of large intestine resected for infiltrating carcinoma: rectum, 17; descending colon, 10; transverse colon, 4; ascending colon, 2; and cecum, 2. There were also 7 specimens of colon resected for mucosal polyps and two specimens for diverticulitis. An additional 28 adenomatous polyps of the large bowel mucosa were examined. Of the latter, 18 were incidental lesions in specimens resected for infiltrating carcinoma and 10 were from specimens resected solely for the polyps. Twenty areas of focal hyperplasia were studied. All of these were located in the mucosa close to infiltrating carcinoma. There were, in addition, a number of biopsy specimens: rectal fragments removed during proctoscopy of 5 patients with carcinoma of the rectum, and mucosa excised in 8 instances from transverse colostomy sites.

Within 15 minutes after excision of tissue, blocks were cut, placed on block holders, and frozen by thrusting into pulverized dry ice. Blocks were cut from several portions of the neoplasm in specimens resected for carcinoma. Particular emphasis was placed on obtaining tissue from the periphery of lesions, and whenever possible, adjacent mucosa was included in the same block. Additional specimens of mucosa were taken from sites at various distances from the lesions.

All sections employed in this study were frozen sections cut in a cryostat by a technique previously described.[9] Sections 16 μ in thickness were used in the two diaphorase procedures, and sections 10 μ in thickness in the procedures demonstrating succinic dehydrogenase, α-glycerophosphate dehydrogenase, and monoamine oxidase. One or two sections were placed on a cover slip which was then quickly brought to room temperature to allow thawing. The sections were dried for 5 minutes at room temperature and then stored in a refrigerator at 4° C. until used within 3 hours. Storage did not result in demonstrable loss of activity in any of the procedures employed. The sections were washed in salt solution (*vide infra*) for 5 minutes at 4° C. and then again for 5 minutes at room temperature. Since all of the reaction mixtures used required expensive chemicals, a technique

employing small volumes was utilized. The incubations were carried out in a water bath which had a sheet of glass at its surface. Small squares of glass cut from conventional slides were positioned at regular intervals along the glass sheet, and the cover slips were placed on top of these. Three tenths of a ml. of the reaction mixture preheated to 37° C. was placed over the section or sections on each cover slip. The cover slip and its glass support were then covered with a Coplin jar cover to prevent evaporation. Following completion of the reaction, the cover slips were washed 5 minutes in salt solution, fixed for 30 minutes in 10 per cent formalin and mounted in glycerin or glycerogel.

Reagents

DPNH, TPNH and tryptamine•HCl were obtained from the California Foundation for Biochemical Research; nicotinamide, sodium succinate and sodium glycerophosphate•$5H_2O$ (25 per cent alpha) were procured from the Matheson Company, Inc.; neotetrazolium chloride and Nitro-BT [2,2′-di-p-nitrophenyl-5,5′-diphenyl-3,3′-(3,3′-dimethoxy-4,4′-biphenylene)-ditetrazolium chloride] from the Dajac Laboratories; and inorganic salts (reagent) from Merck and Company.

All reaction mixtures and washes contained the following inorganic salts: NaCl, 0.11 M; KCl, 0.003 M; Mg_2SO_4, 0.001 M and Na_2HPO_4, 0.03 M, adjusted to pH 8.0. For demonstrating DPN diaphorase and TPN diaphorase, the reaction mixtures contained, respectively, DPNH, 1.5 mg. per ml., and TPNH, 1.5 mg. per ml. Neotetrazolium, 0.6 mg. per ml., was employed in both diaphorase procedures. For demonstrating succinic dehydrogenase, the reaction mixture contained sodium succinate, 0.05 M; for α-glycerophosphate dehydrogenase, sodium glycerophosphate (25 per cent alpha), 0.05 M; and for monoamine oxidase, tryptamine•HCl, 0.05 M. In these 3 procedures, Nitro-BT, 0.5 mg. per ml., was regularly employed.

Factors in the Selection of Incubation Period and Tetrazolium Salt

In the procedures for the demonstration of the two diaphorases, neotetrazolium was employed and the sections were incubated for 10 minutes at 37° C. The incubation period is of importance in determining the color contrast between cells of different degrees of reactivity. Both normal and pathologic mucosal epithelium go through the same sequence of color changes with progressively longer incubation periods, but the more reactive cells proceed more rapidly than the less reactive ones. The initial color was pink, and by increasing the incubation period, progressively deeper shades of red were obtained. Further increase in the incubation period resulted in the formation of a blue

precipitate; additional incubation induced progressively deeper shades of blue. The blue color is due to diformazan, the complete reduction product of neotetrazolium. The precise chemical composition of the red colored product is not certain.[10]

With the incubation period chosen for the demonstration of the two diaphorases, the less reactive cells stained some shade of red whereas the more reactive cells stained a predominantly blue color. The choice of a reaction time which yielded one color for more reactive cells and another for less reactive ones provided maximum contrast for microscopic study. The contrast was even further enhanced by extracting sections with 95 per cent ethanol for 5 minutes following incubation. The blue diformazan was largely insoluble under these conditions whereas the red product was soluble. This extraction was not used routinely because sufficient contrast existed without it and information obtained from the varied depth of red staining was lost.

Nitro-BT can be used in place of neotetrazolium in demonstrating the two diaphorases. With this substance, all cells giving a positive reaction stained blue, the less reactive cells appearing lighter blue. The contrasts obtained were, in general, not as good as with neotetrazolium.

In the procedures for demonstrating succinic dehydrogenase, α-glycerophosphate dehydrogenase and monoamine oxidase, Nitro-BT was employed; the sections were incubated for 15 minutes at 37° C. Neotetrazolium can be substituted, but much better preparations with sharper contrasts were obtained with Nitro-BT.

Results

Normal Mucosa

No difference was noted between the reactions of the mucosa of the large intestine from patients with carcinoma and of that from patients with benign polyps or diverticulitis. In general the DPN diaphorase procedure yielded red staining and the TPN diaphorase method light red staining in the normal mucosa (Figs. 1 to 3). With the DPN diaphorase procedure, the cells of the surface epithelium and in the bases of the crypts stained relatively intensely, being a moderately dark red color with some blue diformazan evident. In the demonstration of TPN diaphorase, the surface epithelium also stained relatively intensely; however, the cells in the bases of the crypts did not stain darker than other cells in the crypts (Table I). In some specimens there was uniform staining of surface and all crypt cells with both diaphorase methods, the color being more intense for DPN diaphorase than for TPN diaphorase.

Succinic dehydrogenase, α-glycerophosphate dehydrogenase and monoamine oxidase all resulted in moderately dark blue staining of the normal mucosa. The staining patterns obtained for succinic dehydrogenase and α-glycerophosphate dehydrogenase were virtually identical. The most intense staining was generally found in the cells at the bases of the crypts, which exhibited a deep blue color. The surface epithelium was a slightly lighter color, and the cells of the crypts, except those at the base, stained slightly lighter still (Fig. 6). The succinic dehydrogenase procedure resulted in a slightly darker staining of all cell types than that obtained with the α-glycerophosphate dehydrogenase method. The surface epithelium stained for monoamine oxidase with about the same intensity as for succinic dehydrogenase, and all of the cells in the crypts stained uniformly and lighter (Table I).

Some variation in intensity of staining for all 5 enzymes occurred in different specimens; the basis for this was not apparent.

Carcinoma of the Colon and Rectum

The carcinomas were predominantly well differentiated. However, in most of the lesions, poorly differentiated tumor cells were found at the invading margins and occasionally in other locations. A few of the neoplasms contained large numbers of poorly differentiated cells, but none was composed entirely of this type of epithelium. The poorly differentiated carcinoma appeared in a variety of forms such as isolated clumps, fingerlike cords, solid pegs, or highly atypical glands. All of these had similar reaction patterns.

With DPN diaphorase and TPN diaphorase, intense staining of both poorly and well differentiated cells was seen (Figs. 1 to 5 and 7 to 10). With the DPN diaphorase method, the amount of blue diformazan deposited was often sufficiently great to afford a dark blue color. The TPN diaphorase procedure generally produced a slightly lighter staining of neoplastic cells than the DPN diaphorase method (Table I). The deep staining for both enzymes did not occur in all tumor cells but was a selective phenomenon determined by at least 3 factors. The location of the cells within the tumor was one of these. The most intense staining was found in cells in areas with greatest proliferative activity, as at the invading margins of the neoplasms, the periphery of tumor cell aggregates, and in isolated cell groups (Fig. 7). In contrast, lighter staining was more likely in locations prone to undergo degeneration, as in the center of tumor masses and regions adjacent to ulceration or marked inflammatory reaction. The degree of cellular differentiation constituted a second factor. A considerably higher

proportion of poorly differentiated neoplastic cells exhibited intense staining (Figs. 8 and 9). Among glandular elements, the flat, non-secreting epithelium was particularly likely to have high diaphorase activities (Fig. 10). The third controlling factor was less well defined and appeared to be related to some general characteristic of the tumor itself. Some tumors were considerably more reactive than others despite cytologic similarity. Apparently cells with comparable structural characteristics may vary in staining intensity from tumor to tumor.

TABLE I

Typical Histochemical Reaction Patterns in Normal and Pathologic Mucosal Epithelium

Cell type	Formazan deposition				
	DPN diaphorase*	TPN diaphorase*	Succinic dehydrogenase†	α-Glycerophosphate dehydrogenase†	Monoamine oxidase†
Normal mucosa, surface epithelium	4+	3+	5+	4+	5+
Normal mucosa, crypt cells (not at base)	3+	2+	4+	3+	3+
Normal mucosa, base of crypts	4+	2+	6+	5+	3+
Hyperplasia, surface and crypt epithelium	3+	4+	1+	1+	1+
Polyp, mucus secreting epithelium	3+	2+	4+	3+	3+
Polyp, superficial cells of atypical glands	3+	2+	3+	2+	2+
Polyp, deeper cells of atypical glands	6+	2+	8+	7+	5+
Carcinoma, well differentiated	8+	6+	7+	6+	5+
Carcinoma, poorly or well differentiated‡	8+	6+	1+	1+	1+

* Neotetrazolium in reaction mixture: 8+ (maximum formazan deposition) very deep blue; 7+ to 6+, progressively lighter blue; 5+, purple (predominantly blue); 4+, purple (predominantly red); 3+, red; 2+, light red; 1+, pink.

† Nitro-BT in reaction mixture: 8+ (maximum formazan deposition), very deep blue; 7+ to 1+, progressively lighter blue.

‡ This reaction pattern is observed in a higher proportion of poorly differentiated than well differentiated carcinoma cells.

Both poorly and well differentiated carcinoma cells showed weak staining with the procedures demonstrating succinic dehydrogenase, α-glycerophosphate dehydrogenase and monoamine oxidase. In many instances the cells exhibited light blue staining, and in some specimens they were colorless (Fig. 6). While the decrease in activity was usually parallel in all 3 enzymes, in some instances monoamine oxidase was diminished to a comparatively greater extent than the other two.

On the other hand, although many well differentiated neoplastic cells stained lightly, among them were comparable elements whose staining intensities for all 3 enzymes equalled or surpassed those of the deepest staining cells in the normal mucosa from the same specimen (Fig. 11). Variations in staining intensity could be observed in segments of adjacent tumor acini (Figs. 11 and 12). In glands which stained deeply, the greatest intensity was often apparent in periluminal organelles. In regard to both staining intensity and intracellular formazan distribution, these carcinomatous elements closely resembled cells in the atypical glands of benign mucosal polyps, as described below.

Comparison of the Histochemical Reaction Patterns in Biopsy and Resected Specimens

In 3 patients it was possible to compare preoperative biopsy specimens containing both normal rectal mucosa and carcinoma with comparable tissues in the surgically resected specimens. No differences in the reactions were observed with any of the 5 histochemical procedures. Biopsy tissue from 8 transverse colostomy sites also exhibited reaction patterns within the range of those obtained in resected specimens. This was also the case in two biopsy specimens of inoperable carcinoma of the rectum.

Focal Mucosal Hyperplasia

Small focal areas of hyperplasia may be found in the mucosa of the large intestine in the vicinity of carcinomas.[11,12] These lesions appeared as small, round or oblong, mucosal elevations, ranging from a fraction of a millimeter to several millimeters in diameter. Twenty such lesions have been included in the present study. Microscopically, they contained elongated glands, many of which exhibited irregular cellular proliferation into the lumens. In longitudinal section the gland wall had a sawtooth appearance, and in cross section the lumen appeared stellate (Figs. 13 to 15). A similar irregular cellular proliferation also occurred in the surface epithelium.

Lesions of this nature were characterized by marked decrease in formazan deposition in the course of demonstrating succinic dehydrogenase, α-glycerophosphate dehydrogenase and monoamine oxidase (Figs. 16 and 20). The magnitude of the staining reduction was such that the surface and glandular epithelium, with the exception of the cells in the deep portion of the crypts, were almost colorless. The cells in the deep portion of the crypts generally stained more intensely (Fig. 16). The DPN diaphorase activity of the hyperplastic glands

was not significantly different from that of normal mucosa. The TPN diaphorase activity was either the same as in normal mucosa or increased in amount (Figs. 17 to 19).

Benign Adenomatous Polyps

Twenty-five benign adenomatous polyps are included in the present study. These were all relatively small lesions (maximum diameter, 1.5 cm.) which showed no evidence of malignancy. In no instance was there anaplasia, loss of nuclear polarity, or invasion of the stalk. Two types of glandular epithelium could be distinguished although there were transition forms between them. One type was a mucus producing epithelium characterized by large numbers of goblet cells (Fig. 25). This was virtually identical with the normal glandular epithelium of the large intestine. The second type of epithelium was atypical and formed glands of atypical character. Such glands, in their most characteristic form, contained few or no goblet cells (Figs. 21 and 25). The cells were generally columnar with elongated nuclei in basal position. Large numbers of mitotic figures were sometimes present. While a variable proportion of the total mass of glandular tissue in any polyp might consist of either of the two types of epithelium, in general the atypical epithelium was most prevalent in the superficial portion and the mucus secreting epithelium in the deeper portion. However, it was not unusual to find atypical glands penetrating the entire thickness of a polyp, or nests of similar cells immediately adjacent to the stalk.

The reaction patterns of the 5 oxidative enzymes were essentially the same in the mucus secreting epithelium of polyps as in normal glands (Table I). In contrast, the atypical epithelium exhibited a different pattern (Figs. 21 to 26). In straight glands the superficial portions often stained for succinic dehydrogenase, α-glycerophosphate dehydrogenase and monoamine oxidase in either the same manner or were lighter than the glands of the normal mucosa. The diaphorase activities were also comparable to those found in normal epithelium. In the deeper portions of the atypical glands, marked increases in staining for succinic dehydrogenase, α-glycerophosphate dehydrogenase and monoamine oxidase were often noted. In addition, there might also be an increased staining for DPN diaphorase. With the TPN diaphorase procedure, an increased formazan deposition was not observed (Table I).

In the cells which showed deep staining, the most intense coloration was often found in the cytoplasm bordering the lumen (Fig. 26). With the succinic dehydrogenase and α-glycerophosphate dehydrogenase procedures, which gave the most precise intracellular resolution of the

5 procedures employed, the intense staining could be seen to be a result of formazan deposition in periluminal organelles. In staining intensity and intracellular formazan distribution, these cells resembled those in differentiated carcinoma which stained relatively intensely for succinic dehydrogenase, α-glycerophosphate dehydrogenase, and monoamine oxidase.

Malignant Polyps

Three malignant polyps were available for study. Each was located in the sigmoid colon. Much of the epithelium was similar to the atypical epithelium in benign polyps, but piling up of epithelial cells was more pronounced (Fig. 31). Areas were found in which frankly carcinomatous glands existed. These were characterized by loss of orderly organization of the epithelium and of nuclear polarity. There was also marked irregularity of nuclear appearance, with large and bizarre forms (Fig. 30). The malignant zones appeared as narrow segments of the polyp extending from the surface to the base, as groups of glands at the surface, or as small focal areas within the polyp.

The noncarcinomatous atypical epithelium showed staining for DPN diaphorase and TPN diaphorase comparable to that found in benign polyps (Figs. 27 and 28). In areas of carcinoma, increased staining occurred with both procedures. This increase varied from slight to marked and approached that found in the more reactive cells in infiltrating carcinoma (Figs. 27 and 28). Increased DPN diaphorase reactivity was more widespread than that of TPN diaphorase. Glands with increased TPN diaphorase staining, with very occasional exceptions, also showed an increase in DPN diaphorase activity.

Most of the noncarcinomatous atypical epithelium stained intensely with the procedures for the demonstration of succinic dehydrogenase, α-glycerophosphate dehydrogenase and monoamine oxidase. The staining properties were often similar to those observed in the deeper portions of the atypical glands in benign polyps. In sharp contrast, the areas of the polyps containing malignant epithelium were almost colorless when stained for succinic dehydrogenase (Fig. 29) and α-glycerophosphate dehydrogenase. Reduced activity of these enzymes was more widespread than was the increased activity of the diaphorase. Staining for monoamine oxidase was less consistently decreased than in the case of succinic dehydrogenase and α-glycerophosphate dehydrogenase.

Discussion

In the present study, a characteristic histochemical reaction pattern distinct from those found in normal, hyperplastic, or benign neoplastic cells has been observed in certain cells of carcinoma of the large intes-

tine. The pattern was characterized by the histochemical demonstration of high DPN diaphorase and TPN diaphorase activity and low activity of succinic dehydrogenase, α-glycerophosphate dehydrogenase, and monoamine oxidase. The pattern was found in both poorly and well differentiated carcinoma cells, but the proportion of poorly differentiated elements manifesting the pattern was greater than that of well differentiated cells. The pattern was most consistently observed at the invading tumor margin, at the periphery of tumor cell aggregates, and in isolated cell groups. The cell predilection and the distribution of the reactions suggest that this pattern is a characteristic of the more malignant cells in this type of neoplasm.

The significance of the variations from the established reaction patterns has not been clarified. The pattern in which all 5 enzymes showed high degrees of reactivity was assumed to indicate a lesser degree of malignancy since it has only been found in well differentiated carcinoma cells. Of interest is the fact that high activity of succinic dehydrogenase, α-glycerophosphate dehydrogenase and monoamine oxidase and intense periluminal formazan deposition were observed in both well differentiated carcinoma and in atypical glands of adenomatous polyps. Another variation, the occurrence of relatively weak diaphorase activity, was frequently found in areas prone to undergo degeneration. It appeared to reflect the altered metabolism of degenerating or less active malignant cells.

The exact biochemical meaning of the histochemical observations made in the present study is not known. However, when considered in relationship to the large body of data pertaining to malignant neoplasms, they permit certain inferences in interpretation. Cancer cells have been shown repeatedly to possess a high glycolytic activity,[13,14] whereas the activities of cytochromes have been found to be low.[14,15] This circumstance would favor the accumulation of reduced pyridine nucleotide coenzymes since much of the reoxidation of the coenzymes occurs via the cytochrome electron transport system. However, quantitative studies of the ratio of DPN to DPNH and TPN to TPNH show no significant alteration in these ratios in malignant neoplastic tissues.[16,17] This suggests that reoxidation is occurring by an alternate pathway. Reoxidation of DPNH during the formation of lactate from pyruvate is one such pathway. On the other hand, this reaction has a potential limitation in that an excessive accumulation of lactate may occur in a rapidly glycolyzing cell which is unable to adequately rid itself of the lactate. DPN diaphorase represents another pathway by which DPNH could be reoxidized, in this instance without lactate

formation. Thus a high DPN diaphorase activity could facilitate rapid glycolysis without leading to lactate accumulation. Likewise, a high TPN diaphorase activity could have a parallel function in facilitating the oxidative reactions of the hexose monophosphate shunt by reoxidizing the TPNH formed during these reactions.[18]

The hydrogen acceptors in the histochemical procedures for demonstrating the diaphorases are the tetrazolium salts. The nature of the compound or compounds which accept hydrogen from these reduced flavoprotein diaphorases *in vivo* has not been established. One interesting possibility is that in the cells of carcinoma of the large intestine, the diaphorases catalyze reductive synthetic reactions. They would thus utilize the hydrogen from the reduced pyridine nucleotide coenzymes in reactions which might be of considerable importance to rapidly proliferating cells. That reductive synthetic reactions do occur has been well demonstrated in fatty acid synthesis where reduction of ethylene linkages of acyl derivatives of coenzyme A by reduced flavoproteins occurs as part of the reaction mechanism for increasing carbon chain length.[19,20] Information is lacking as to what type of compounds might be synthesized as a result of a similar type of reaction sequence in which the diaphorases take part.

The weak staining for succinic dehydrogenase observed in poorly differentiated and some well differentiated carcinoma cells is in accord with the low activities found by others in quantitative studies of this enzyme in some neoplasms.[15] The significance of these findings relates directly to the highly controversial issue of whether or not there is a diminished activity of the entire citric acid cycle in cancer cells. Two extremes of opinion exist. One is represented by the belief that a decrease in citric acid cycle activity occurs in malignant neoplasms, and that this may result in a shift of metabolic equilibriums in favor of synthetic reactions. At the other extreme is the opinion that definitive evidence of a significant functional defect in the citric acid cycle has not been proven to occur in intact tumor cells.[21]

The weak staining for α-glycerophosphate dehydrogenase can be interpreted to indicate the existence of a mechanism for diverting dihydroxyacetone phosphate from lipid metabolism into pathways more important to the tumor cells. Monoamine oxidase is a detoxifying enzyme which would be of little importance to tumor metabolism. A decrease in activity of this enzyme would not be unexpected since it is well established that a loss in activity of enzymes with specialized functions may occur in malignant cells.[22]

The histochemical features which have been postulated to represent

a highly developed malignant reaction pattern in carcinoma of the large intestine can be considered to have two general aspects. The first is the high degree of activity exhibited by the two diaphorases, which may facilitate glycolysis and the oxidative reactions of the hexose monophosphate shunt and may also be of importance in synthetic reactions. The second is the demonstration of the reduced activity of succinic dehydrogenase, α-glycerophosphate dehydrogenase and monoamine oxidase. It is possible that these enzymes are unimportant in the tumor cells, at least at the level of activity at which they occur in normal mucosa, or that the decrease in activity diverts metabolites into pathways more important for the neoplastic elements. The demonstration of high degrees of activity of the 3 enzymes observed in some well differentiated carcinomas may be interpreted as a manifestation of a malignant pattern of a lesser degree, occurring in cells of the type found in the deeper portion of atypical glands in benign adenomatous polyps.

Summary

A histochemical study of 5 oxidative enzymes, DPN diaphorase, TPN diaphorase, succinic dehydrogenase, α-glycerophosphate dehydrogenase, and monoamine oxidase, has been carried out in tissues of the large intestine: normal mucosa, hyperplastic mucosa, benign adenomatous polyps, and carcinoma.

A reaction pattern, distinct from those found in normal, hyperplastic, or benign neoplastic cells, has been observed in carcinoma. The pattern is characterized by high DPN and TPN diaphorase activity and low succinic dehydrogenase, α-glycerophosphate dehydrogenase, and monoamine oxidase activity.

This distinctive reaction pattern is not present in all components of these neoplasms. It is most consistently observed in the cells at the invading margin, at the periphery of tumor cell aggregates, and in isolated cell groups. It is least commonly encountered in regions which are the seat of degenerative alteration. The pattern occurs in a higher proportion of poorly differentiated than well differentiated carcinoma cells.

In hyperplasia there is low succinic dehydrogenase, α-glycerophosphate dehydrogenase and monoamine oxidase activity. Elevation of the TPN diaphorase activity may occur, but the DPN diaphorase activity is not increased.

Several types of reaction are found in benign adenomatous polyps. These do not, however, duplicate the distinctive findings which occur in carcinoma. A striking feature is the presence of high succinic dehy-

drogenase, α-glycerophosphate dehydrogenase and monoamine oxidase activity in the deeper portions of the atypical glands. In malignant polyps, carcinomatous elements react in a manner similar to that of invasive carcinoma.

REFERENCES

1. Rutenberg, A. M.; Wolman, M., and Seligman, A. M. Comparative distribution of succinic dehydrogenase in six mammals and modification in the histochemical technic. *J. Histochem.*, 1953, **1**, 66–81.
2. Farber, E.; Sternberg, W. H., and Dunlap, C. E. Histochemical localization of specific oxidative enzymes. I. Tetrazolium stains for diphosphopyridine nucleotide diaphorase and triphosphopyridine nucleotide diaphorase. *J. Histochem.*, 1956, **4**, 254–265.
3. Nachlas, M. M.; Tsou, K-C.; de Souza, E.; Cheng, C-S., and Seligman, A. M. Cytochemical demonstration of succinic dehydrogenase by the use of a new p-nitrophenyl substituted ditetrazole. *J. Histochem.*, 1957, **5**, 420–436.
4. Glenner, G. G.; Burtner, H. J., and Brown, G. W., Jr. The histochemical demonstration of monoamine oxidase activity by tetrazolium salts. *J. Histochem.*, 1957, **5**, 591–600.
5. Wattenberg, L. W. Studies on rickettsial toxins. III. Histochemical survey of selected tissue enzymes in mice receiving murine typhus toxin. *Am. J. Path.*, 1955, **31**, 875–881.
6. Adler, E.; von Euler, H., and Günther, G. Diaphorase I and II. *Nature, London*, 1939, **143**, 641–642.
7. Sumner, J. B., and Myrbäch, K. The Enzymes. Academic Press, Inc., New York, 1951, Vol. II, Part 1. pp. 302–303.
8. Sumner, J. B., and Myrbäch, K.[7] pp. 536–544.
9. Wattenberg, L. W. Microscopic histochemical demonstration of steroid-3β-ol dehydrogenase in tissue sections. *J. Histochem.*, 1958, **6**, 225–232.
10. Burtner, H. J.; Bahn, R. C., and Longley, J. B. Observations on the reduction and quantitation of neotetrazolium. *J. Histochem.*, 1957, **5**, 127–134.
11. Schmieden, V., and Westhues, H. Zur Klinik und Pathologie der Dickdarmpolypen und deren klinischen und pathologisch-anatomischen Beziehungen zum Dickdarmkarzinom. *Dtsch. Ztschr. f. Chirurg.*, 1927, **202**, 1–124.
12. Lockhart-Mummery, J. P., and Dukes, C. The precancerous changes in the rectum and colon. *Surg. Gynec. & Obst.*, 1928, **46**, 591–596.
13. Warburg, O. On the origin of cancer cells. *Science*, 1956, **123**, 309–314.
14. Greenstein, J. P. Some biochemical characteristics of morphologically separable cancers. *Cancer Res.*, 1956, **16**, 641–653.
15. Schneider, W. C., and Potter, V. T. Biocatalysts in cancer tissue. III. Succinic dehydrogenase and cytochrome oxidase. *Cancer Res.*, 1943, **3**, 353–357.
16. Glock, G. E., and McLean, P. Levels of oxidized and reduced diphosphopyridine nucleotide and triphosphopyridine nucleotide in tumors. *Biochem. J.*, 1957, **65**, 413–416.
17. Jedeikin, L. A., and Weinhouse, S. Metabolism of neoplastic tissue. VI. Assay of oxidized and reduced diphosphopyridine nucleotide in normal and neoplastic tissues. *J. Biol. Chem.*, 1955, **213**, 271–280.
18. Racker, E. Alternate pathways of glucose and fructose metabolism. In: Advances in Enzymology and Related Subjects of Biochemistry. Nord, F. F. (ed.). Interscience Publishers, Inc., New York, 1954, **15**, 141–182.

19. Lynen, F. Functional group of coenzyme A and its metabolic relations, especially in the fatty acid cycle. *Fed. Proc.*, 1953, **12**, 683–691.

20. Beinert, H., and Page, E. On the mechanism of dehydrogenation of fatty acyl derivatives of coenzyme A. V. Oxidation-reductions of the flavoproteins. *J. Biol. Chem.*, 1957, **225**, 479–497.

21. Weinhouse, S. Oxidative metabolism of neoplastic tissues. *Advances Cancer Res.*, 1955, **3**, 269–325.

22. Greenstein, J. P. Biochemistry of Cancer. Academic Press, Inc., New York, 1954, pp. 327–501.

LEGENDS FOR FIGURES

Formazan deposits appear as black or a darker gray than that of the background. All preparations are frozen sections.

FIG. 1. Carcinoma of the large intestine. Mucosa above, carcinoma in submucosa below. Hematoxylin and eosin stain. × 40.

FIG. 2. Section from same block as Figure 1. DPN diaphorase. × 40.

FIG. 3. Section from same block as Figure 1. TPN diaphorase. × 40.

FIG. 4. Carcinoma of the colon. Well differentiated tumor in the outer part of the muscularis (above); poorly differentiated tumor in the subserosa (below). DPN diaphorase. × 50.

FIG. 5. Section from the same block as Figure 4. TPN diaphorase. × 50.

FIG. 6. Section from same block as Figure 4. Succinic dehydrogenase. × 50. Insert in left lower corner, normal mucosa from same specimen included for comparison. Succinic dehydrogenase. × 50.

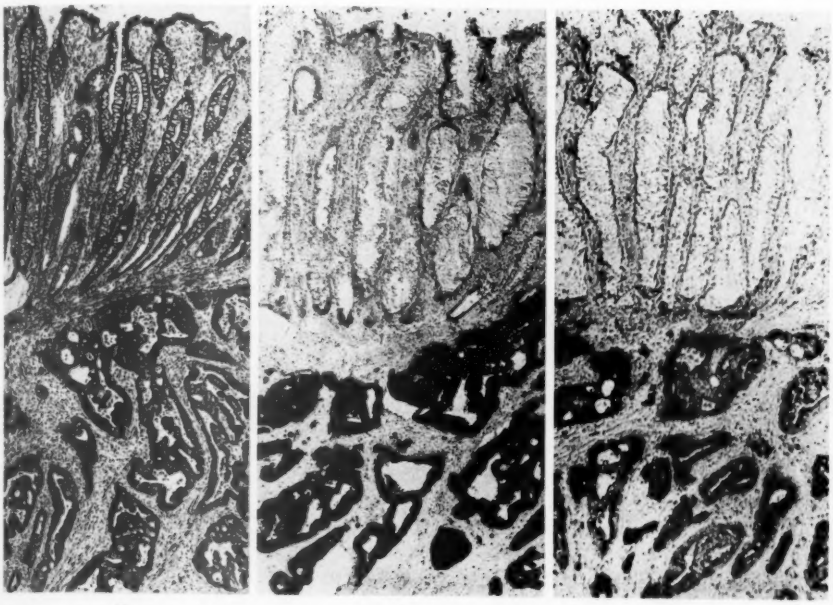

1 2 3

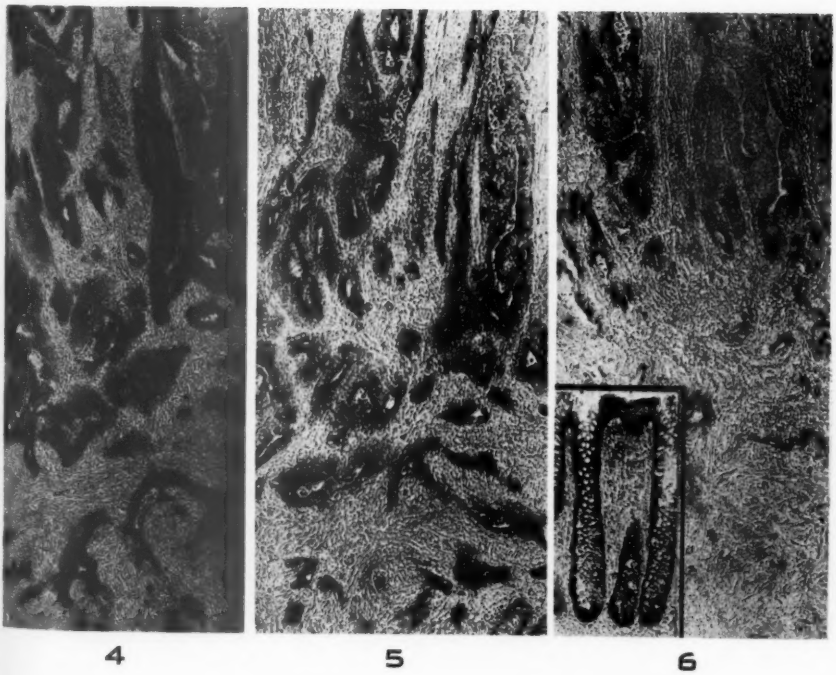

4 5 6

FIG. 7. Carcinoma. DPN diaphorase. Note variations in intensity of staining in different portions of the tumor with isolated tumor glands and the periphery of tumor aggregates showing more intense staining. × 30.

FIG. 8. Carcinoma. DPN diaphorase. Most of tumor is poorly differentiated and stains intensely. × 50.

FIG. 9. Carcinoma of the colon. DPN diaphorase. Margin of the tumor. Poorly differentiated tumor cells in lower portion of photograph. × 110.

FIG. 10. Carcinoma. DPN diaphorase. Note deep staining of tumor glands, some of which have relatively flat epithelium. × 140.

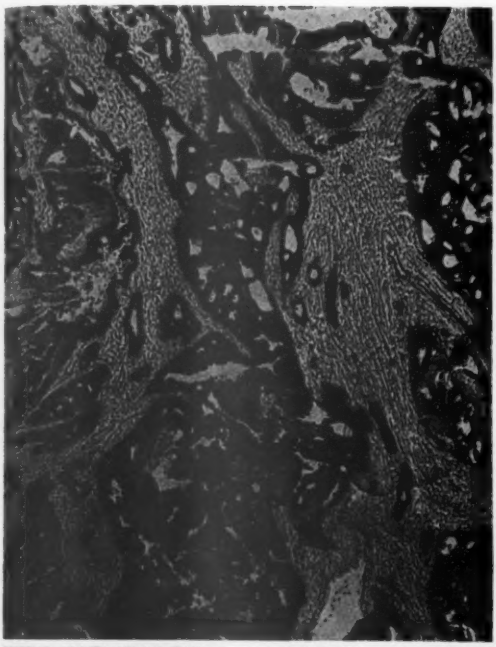

7

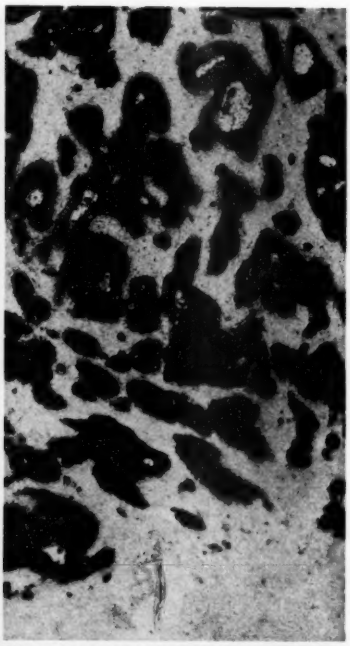

8

9

10

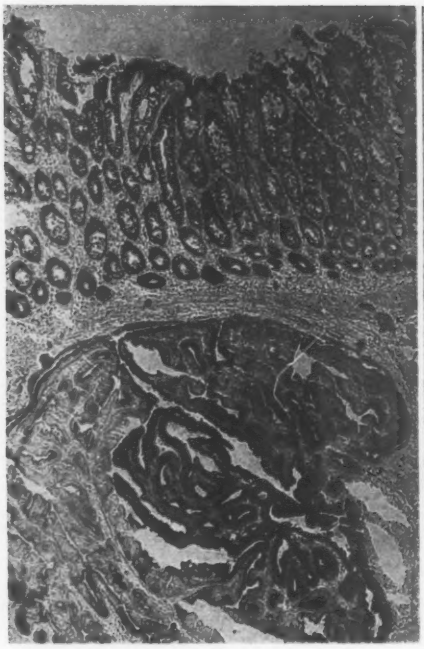

11

12

FIG. 11. Carcinoma. Succinic dehydrogenase. Mucosa above, tumor nodule in submucosa below. Note variation in intensity of staining in different portions of the neoplasm. × 35.

FIG. 12. Higher magnification of upper middle portion of tumor in Figure 11. Note relative intensity of periluminal staining. Succinic dehydrogenase. × 100.

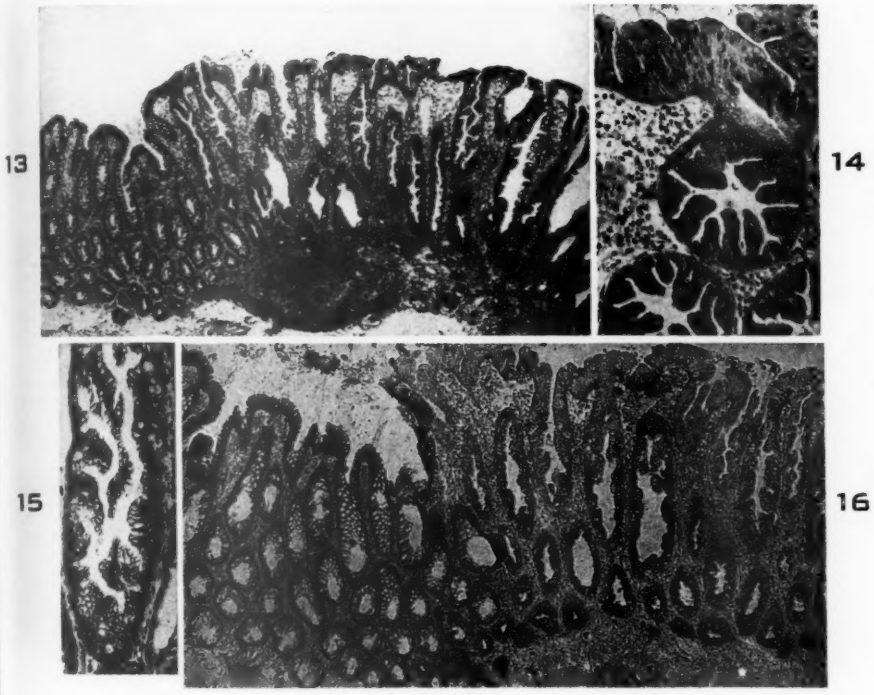

FIG. 13. Focal mucosal hyperplasia of the colon. Normal mucosal glands on the left, hyperplastic glands on the right. Hematoxylin and eosin stain. × 30.

FIG. 14. Hyperplastic glands in cross section. Note stellate appearance of lumens. Hematoxylin and eosin stain. × 150.

FIG. 15. Segment of hyperplastic gland in longitudinal section. Note irregular cellular proliferation into the lumen. Hematoxylin and eosin stain. × 100.

FIG. 16. Focal mucosal hyperplasia. Same block as Figure 13. Succinic dehydrogenase. × 45.

FIG. 17. Focal hyperplasia. Normal mucosal glands on the right, hyperplastic glands on the left. Hematoxylin and eosin stain. × 85.

FIG. 18. Section from same block as Figure 17. DPN diaphorase. × 85.

FIG. 19. Section from same block as Figure 17. TPN diaphorase. × 85.

FIG. 20. Section from same block as Figure 17. Succinic dehydrogenase. × 85.

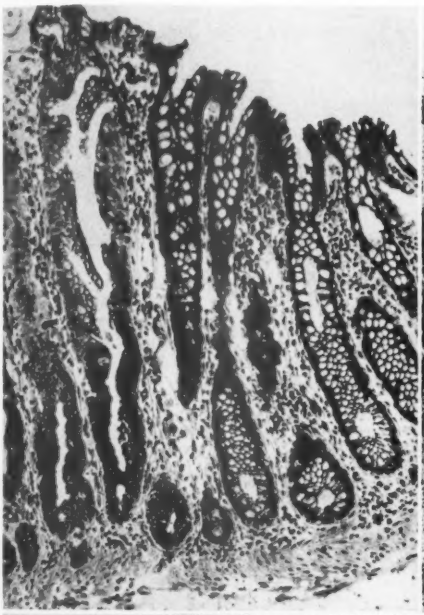

17

18

19

20

FIG. 21. Benign adenomatous polyp. Glands adjacent to lumen surface (above) are composed of atypical epithelium. Hematoxylin and eosin stain. × 30.

FIG. 22. Section from same block as Figure 21. DPN diaphorase. × 30.

FIG. 23. Section from same block as Figure 21. TPN diaphorase. × 30.

FIG. 24. Section from same block as Figure 21. Succinic dehydrogenase. × 30.

FIG. 25. Benign adenomatous polyp. Note mucus secreting epithelium with large numbers of goblet cells, lower portion of field, and darker staining atypical epithelium, upper portion of field. Hematoxylin and eosin stain. × 45.

FIG. 26. Section from same block as Figure 25. Succinic dehydrogenase. Atypical epithelium stains darkly. Note intensity of periluminal staining. × 45.

21

22

23

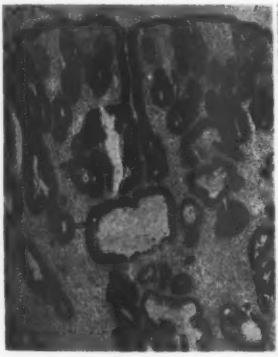

24

25

26

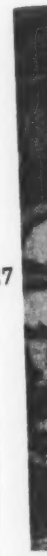

FIG. 27. Malignant mucosal polyp. Surface of polyp on the right. Central darker staining region shows characteristic "malignant" alterations in both histochemical and hematoxylin and eosin stained preparations. DPN diaphorase. × 40.

FIG. 28. Section from same block as Figure 27. TPN diaphorase. × 40.

FIG. 29. Section from same block as Figure 27. Succinic dehydrogenase. × 40.

FIG. 30. "Malignant" epithelium characteristic of central portion of Figures 27 to 29. Hematoxylin and eosin stain. × 600.

FIG. 31. Atypical epithelium characteristic of top and bottom borders of Figures 27 to 29. Hematoxylin and eosin stain. × 600.

27

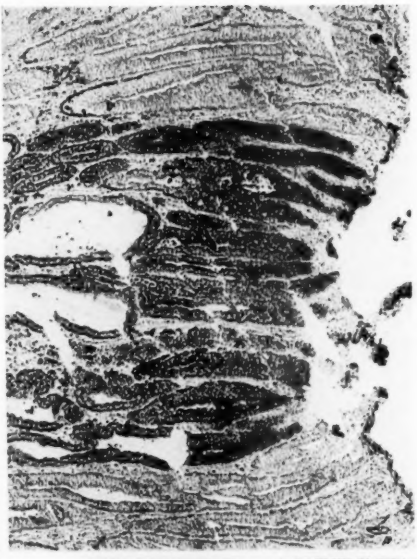

28

29

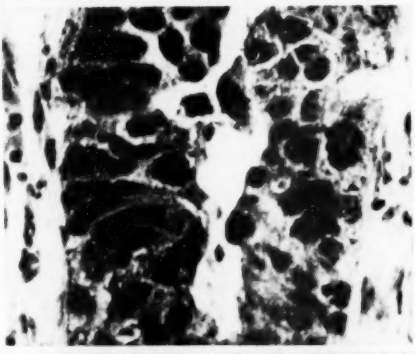

30

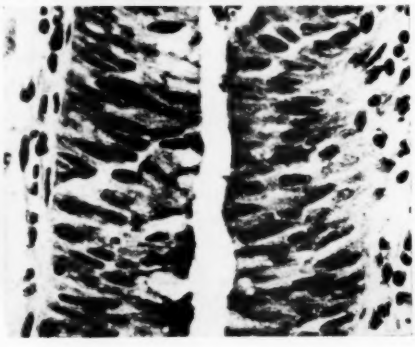

31

HISTOCHEMICAL CHANGES IN LIVER SUCCINIC DEHYDROGENASE DURING RAPID GROWTH FOLLOWING PARTIAL HEPATECTOMY *

BJARNE PEARSON, M.D.; FRED GROSE, B.S., and ROSA GREEN
From the Detroit Institute of Cancer Research and Department of Pathology, Wayne State University College of Medicine, Detroit, Mich.

Although succinic dehydrogenase activity has been detected in the livers of mice during rapid growth following partial hepatectomy by Tsuboi, Yokoyama, Stowell and Wilson,[1] no histochemical studies of this enzyme have been made. Seligman and Rutenburg[2] first demonstrated the enzyme in tissue sections by means of blue tetrazolium. However, this salt, as well as many others subsequently used, did not give precise enzyme localization. Improved results following the use of thin sections of 5 μ and a new salt, 2-(p-iodophenyl)-3-(p-nitrophenyl)-5-phenyl tetrazolium chloride (INT) was introduced by Pearson and Defendi in 1954.[3] The use of this salt was also found to provide quantitative data from single slide studies.[4]

One of the difficulties with the tetrazolium salts is the size and continued growth of formazan crystals following preparation. This has made the study of normal and, in particular, pathologic tissues extremely difficult. In 1956 Tsou, Cheng, Nachlas and Seligman[5] and in 1957-1958 Pearson[6,7] introduced two new tetrazolium salts in which the formazan was fine and particulate and crystallization did not progress with storage of slides. The new salts made it possible to study changes in succinic and other dehydrogenases in pathologic material with added confidence. A study of a number of dehydrogenases is now in progress.[8]

Even though the tetrazolium salt used for succinic dehydrogenase gave rise to extremely fine particulate formazan, the latter was slightly lipid soluble, which tended to obscure the precise localization of the enzyme in tissues containing an abundance of lipids. Inasmuch as lipids accumulate in the liver following partial hepatectomy, a method was sought to remove lipids without destroying the enzyme. In 1950, Morton[9] demonstrated that n-butanol extracted the succinic dehydrogenase in homogenized heart tissue without affecting the enzyme. Numerous attempts by us to use this procedure in the pretreatment

* This investigation was supported in part by research grant number C-2624 from the National Cancer Institute, United States Department of Health, Education and Welfare, and in part by Institutional Grants from the American Cancer Society, Inc., and the American Cancer Society, Southeastern Michigan Division.

Received for publication, May 14, 1958.

Presented at the Fifty-fifth Annual Meeting of the American Association of Pathologists and Bacteriologists, Cleveland, April 24, 1958.

of tissue sections met with partial success. It was found, however, that one of the main limiting factors was the need to use the lipid solvent in extreme cold. A large number of experiments were performed, and it was found that a mixture of n-butanol and ether (in a 1:1 ratio) at extremely low temperatures did not destroy the enzyme and permitted the preparation of tissue sections which, in addition, exhibited excellent structural preservation. Furthermore, this pretreatment resulted in an apparent dissociation of succinic dehydrogenase from other factors. It no longer reacted with tetrazolium salts, or did so only partially, and required the addition of phenazine methosulfate.[10,11]

The purpose of the present study is to show that the use of a new tetrazolium salt, 2,2′-diphenyl-5,5′-di-(*m*-nitrophenyl)-3,3′-(4,4′-biphenylene) ditetrazolium chloride, produces particulate formazan necessary for fine enzyme localization. When tissue is pretreated for the removal of lipids, succinic dehydrogenase may be studied histochemically during periods of rapid growth following partial hepatectomy. It is also desired to describe the changes in enzyme structure as occasioned by rapid changes in tissue growth and restitution.

Material and Methods

Small blocks of tissue (2 to 3 mm.) were taken from the livers of mice immediately following sacrifice. These were frozen at −70° C. in a bath of dry ice and alcohol, and placed in the Linderstrom-Lang cryostat to be sectioned at −20° C.[6,7] Sections were cut at 5 μ and stored at −25° C. for periods not exceeding 3 days. This length of storage did not affect the enzyme. From 15 to 18 slides were placed in a standard glass staining rack, inserted in a staining dish containing a mixture of 1:1 n-butanol and ether, precooled to −65° C. in Dewar flasks, one third filled with dry ice and ethanol. Slides containing tissues were pretreated in the n-butanol and ether mixture for 50 minutes. They were then washed in 3 changes of water for 1 to 2 minutes each, with agitation, and placed in Coplin jars containing the following incubating solution at 25° C. for 30 minutes:

0.1 M sodium succinate, 5 cc.
N,N-dimethylformamide, 5 cc.
0.1 M phosphate buffer (pH 7.6), 5 cc.
2,2′-diphenyl-5,5′-di-(*m*-nitrophenyl)-3,3′-(4,4′-biphenylene) ditetrazolium chloride,* 10 mg.
phenazine methosulfate (conc. 1 mg. per cc.), 1 cc.

The N,N-dimethylformamide was used as a solvent for the tetra-

* Supplied by Synthetical Laboratories, 5558 Ardmore Avenue, Chicago, Ill. Structural formula and nomenclature supplied by Cheronis.[12]

zolium salt. Slides were passed through water and 80 per cent ethanol for 5 minutes, washed in 3 rinses of water and mounted in glycerogel.

Forty-six of 157 C3H male mice which had had partial (two thirds) hepatectomy were used for this experiment. They were sacrificed at 21 hours, 2 to 10 days, 14 and 28 days. Sections of the liver were treated as described above. Control sections were taken from each animal during the operation. A total of 12 sections per animal were tested for succinic dehydrogenase, 6 with and 6 without phenazine methosulfate. In addition, sections from each animal were stained by hematoxylin and eosin with and without pretreatment with the n-butanol and ether mixture. Staining with Sudan black B[18] was also carried out.

Results

The specific morphologic appearance of the liver following partial hepatectomy is well known and will not be described. In general, our observations indicated a rapid demobilization of fat, its deposition in the cytoplasm of liver cells, and its disappearance after the third day. After the tenth day, the liver was restored to its original weight, and its microscopic appearance was within normal limits.

The histochemical studies revealed striking alterations in succinic dehydrogenase activity during this period without return to normal at the time the liver weight and structure was completely restored (Table I).

Table I

Comparative Mean Intensity of Succinic Dehydrogenase Activity in Livers at Various Times Following Subtotal Hepatectomy

Normal	21 hours	2 to 10 days	14 days	28 days
3.0±0.026	2.5±0.029	1.7±0.022	2.2±0.044	4.2±0.049

As indicated in the Table, the fall in the intensity of the formazan reaction indicating succinic dehydrogenase activity was significant in liver specimens at 21 hours, during the time of heavy lipid deposition in the parenchymal cells. A further significant fall was seen between the second to the tenth days. During this time, fat disappeared (after the third day), and rapid cellular growth began. This was completed by the tenth day. Succinic dehydrogenase had not returned to normal at 10 days, when the liver had regenerated, even though the cells appeared to be normal by conventional staining. A significant increase in enzyme intensity was seen on the 28th day.

Some of the most striking features observed were those of actual alteration in the enzymatic histochemical appearance. Normally, suc-

cinic dehydrogenase appears as particulate granules of formazan in the cytoplasm of liver cells around the portal areas, extending for a depth of one third of the lobule. The zone about the central vein is devoid of activity. This distribution was not changed following partial hepatectomy, with minor exceptions, but the character, size, and contour of the loci as demonstrated by formazan were altered. During the 21-hour period, the formazan was no longer particulate but appeared as large round and ovoid globular aggregates. From the second to the tenth days the aggregates became smaller until they approached their normal size. At the 28th day they were again particulate.

Microscopic Appearance

Normal. In the normal liver the cytoplasm of liver cells in the periportal region contained extremely fine granular deposits of formazan at the sites of enzymatic activity. This occupied approximately the peripheral one third of the liver lobule. The zone around the central vein was nonreactive. Bile ducts, blood vessels, and Kupffer cells exhibited no enzyme activity (Figs. 1 and 2).

Twenty-one Hours Following Hepatectomy. The general topographic disposition of succinic dehydrogenase remained as in the normal liver. Intensely positive formazan particles, with rounded and smooth contours, were present in aggregates within the cytoplasm of the cells. For the most part, these were nearly spherical and attained an average size of approximately 4 to 7 μ. They were located within areas occupied by lipid globules, usually situated in the center of the globules (Fig. 3). In many instances, the formazan particles were arranged at the periphery and within the lipid globules where they assumed "sausage shapes" (Fig. 4). Although the majority of cells contained the large aggregates, certain portions of cells exhibited fine granular formazan or a series of size gradations. In frozen sections stained for lipids, the liver at 21 hours showed large fat droplets occupying most of the hepatic cells. Where the droplets were very large, only the peripheral zone of the vacuole stained. In enzyme preparations in which lipids had been extracted, formazan granules appeared in the center and periphery of fat globules (Figs. 3 and 4).

Two Days Following Hepatectomy. During this period the general topographic distribution of enzyme activity was about the same as at the 21 hour period and in the normal liver. The size of the aggregates was slightly smaller than at 21 hours and more fine, particulate formazan was present.

Three to Four Days Following Hepatectomy. The aggregates of formazan-positive material were much smaller, averaging approxi-

mately 2 to 4 μ. The distribution was somewhat altered, and the deposits were more uniformly arranged throughout the entire extent of the lobule. However, the reaction was more intense around the portal areas (Fig. 5).

Five to Ten Days Following Hepatectomy. The aggregates were much smaller than at earlier stages, measuring 1 to 2 μ in diameter. There were fine granules in the cytoplasm of cells concentrated mainly about the portal areas. A "spotty" type of enzyme activity was evident in scattered groups of cells which contained fine formazan deposits. These groups were manifest about the portal areas and showed varying intensities of enzyme activity (Figs. 6 and 7).

Fourteen to 28 Days Following Hepatectomy. The granules of formazan were fairly uniform in size. The distribution was somewhat spotty but remained concentrated about the portal areas. The amount of enzyme activity was increased over that observed in the normal liver. The formazan deposits were fine and were distributed throughout the cytoplasm. Essentially normal enzymatic activity seemed to have been re-established (Fig. 8).

Discussion

Most of the formazans produced with the tetrazolium techniques are soluble in fat. This may lead to false interpretation when lipids are removed in the course of technical procedures. Moreover, formazans are prone to form crystals which may obscure small foci of enzyme activity. The salt used in this study, 2,2′-diphenyl-5,5′-di-(*m*-nitrophenyl)-3,3′-(4,4′-biphenylene) ditetrazolium chloride, has been shown by us[6,7] to be fine and particulate, and sections prepared with this salt can be kept for periods of 6 months or more without deterioration. A "nitro BT" salt has been synthesized by Tsou and co-workers[5] which has essentially the same characteristics. These two new tetrazolium salts have widened the potential scope of future histochemical investigations of this and other dehydrogenase systems.

The demonstration of dehydrogenases in the liver has been particularly difficult, especially in pathologic conditions in which the mobilization of fat or marked changes in metabolism have interfered with the detection or quantitation of the enzyme. We have encountered this problem in the study of succinic dehydrogenase in liver tumors produced by feeding p-dimethylaminoazobenzene.[14] The tetrazolium salt used was 2-(p-iodophenyl)-3-(p-nitrophenyl)-5-phenyl tetrazolium chloride (INT). Because of the rapid development of large formazan crystals, it was necessary to investigate its distribution immediately after incubation. Slides kept for several hours were of no value in

determining the role of succinic dehydrogenase in the tumor. In regions where fat was present, the histochemical pattern underwent rapid deterioration.

If the lipids which interfered with the reaction could be removed prior to the histochemical procedure, the resultant reaction would be of more precise nature. A number of fat solvents were applied under varying conditions, but they all destroyed the enzyme at room temperature. It was apparent that it would be necessary to remove the lipids without destroying the enzyme.

In 1950, Morton[9] was able to show that if n-butanol was used at temperatures of 0 to 2° C., the lipids would dissolve in it, and the pure enzyme could be precipitated in the water phase. It was believed that n-butanol had a unique lipophilic property and an especial affinity for phospholipids.[9,15] No attempt had been made previously to apply this histochemically. Therefore, we prepared mixtures of up to 6 per cent of n-butanol and water and utilized these under a variety of conditions. Partial success was attained, but low temperatures could not be used because of the formation of ice crystals. Our observations indicated that the limiting factor was the temperature. In a series of experiments it was found that the use of a mixture of n-butanol and ether at −65° C. for 50 minutes did not destroy the enzyme but removed lipids as determined by the Sudan black B stain. After such treatment, the preservation of the cellular structure was excellent. The removal of the lipids permitted the demonstration of the enzyme or its altered activity with clarity. Following this procedure, however, the enzyme reacted feebly or not at all to the tetrazolium salt used, and phenazine methosulfate was required for demonstration purposes. This was in keeping with Singer and Kearney's[10] concept of the "pure" enzyme. Therefore, we felt that with such a treatment, we had presumably removed some of the "other carriers" referred to by Farber and Bueding[11] from our histochemical preparations. This procedure is extremely helpful in the detection of certain enzymes in pathologic tissues containing a high lipid content.

Tsuboi and co-workers[1] have shown that marked reduction of succinic dehydrogenase follows partial hepatectomy in strain A male mice. Their observations were carried out postoperatively for periods up to 28 days. They found that there was a rapid reduction of enzyme during the first day, followed by an increase and a return to normal levels on the tenth day. For their determinations they used the homogenate method of Schneider and Potter.[16] No histochemical preparations were used. Novikoff and Potter,[17] using Sprague Dawley rats, studied succinic dehydrogenase for a period of 48 hours following partial hepa-

tectomy. Their results also indicated a reduction of enzyme activity.

Our results have shown a significant fall in succinic dehydrogenase as measured by visual formazan intensities 21 hours following partial hepatectomy. The enzyme activity was further diminished from the second to the tenth days. There was a partial restoration by the 14th day, but this was less than the activity noted at 21 hours. By the 28th day the activity was found to be above normal levels. This slow return of enzyme activity differed somewhat from that observed by Tsuboi and associates[1] who noted a return to normal at 10 days when restoration of the liver was complete. Our own data also indicate that restoration of liver weight was complete at 10 days. However, succinic dehydrogenase had not attained normal activity at this time even though cytologic structure, as demonstrated by conventional staining, was normal.

The differences in our observations from those of Tsuboi and coworkers[1] may be due to a different biologic response in our strains of animals. Tsuboi used the A strain of mice; we have used the C_3H strain. There may also be differences in the techniques that were used, since we have measured the intensity of formazan production, and the other investigators[1] utilized succinoxidase activity as a function of oxygen uptake.

The topography of succinic dehydrogenase distribution in the liver is of interest although there is little variation induced in the regenerating liver. The enzyme activity is concentrated mainly about the portal areas and extends throughout approximately the outer third of the lobule. The cells surrounding the central vein are devoid of the enzyme as demonstrated by the tetrazolium salt method. This has been a constant observation in the use of both the modified tetrazolium salt and INT. Variation in incubation time and changes in substrate concentration have not altered this phenomenon. No essential change in the distribution has been manifested in animals at 21 hours following partial hepatectomy. During the third to fourth postoperative days, the intralobular distribution of the enzyme appeared more uniform, but still maintained accentuation in the peripheral portions. From 5 to 10 days postoperatively, the pattern was essentially that of the normal liver. There were, however, spotty areas unrelated to the peripheral zone in which enzyme activity was more intense. There was a continued decrease in the intensity of formazan deposit throughout the 14th day. At 28 days the distribution was normal.

The constant nature of this distribution would seem to indicate differences in function in the various portions of the hepatic lobule, a relationship which becomes disturbed during rapid growth. Studies

under way in our laboratory of a number of other dehydrogenases in the liver (α-glycerophosphate, lactic, and malic dehydrogenase requiring DPN) indicate that their distribution differs from that of succinic dehydrogenase. The possibility that the distribution of succinic dehydrogenase may reflect an association with the production of bile has been considered but has not been tested.

One of the interesting findings which marked the course of liver regeneration was the variation in the size of the formazan-positive granules. Ordinarily, formazan produced by the salt we have used has a fine and granular appearance and a rather uniform distribution throughout the cytoplasm. During the 21 hour period following partial hepatectomy, the granules became extremely large and attained a size of 7 μ. The contours were smooth and round or occasionally oblong. They tended to aggregate in lipid deposits and were noted to be compressed and oblong at the periphery of fat globules. The remaining portion of the cytoplasm continued to exhibit fine granulation. From the second to the tenth days the aggregates became smaller and more numerous. At the 28th day there was complete restoration to the normal enzyme pattern. The fact that the deposits were larger in the presence of lipid accumulation seemed to indicate that dispersion depended upon the nature of the surrounding medium. The deposits reflected enzyme activity, were insoluble in free lipid, and formed coarse aggregates in this state. This was a reversible process under the conditions of the experiment but under certain conditions could represent a very early pathologic change.

Summary

The histochemical demonstration of succinic dehydrogenase has been difficult particularly in pathologic materials because most tetrazolium salts used produce a formazan which is lipid soluble and deteriorates upon storage of preparations. A new tetrazolium, 2,2′-diphenyl-5,5′-di-(*m*-nitrophenyl)-3,3′-(4,4′-biphenyl) ditetrazolium chloride, has been used in these studies because the formazan produced has been finely particulate and stable in storage. Interfering lipids have been removed by subjecting tissue to pretreatment in a 1:1 n-butanol and ether mixture at −65° C. This has not destroyed the enzyme.

The histochemistry of succinic dehydrogenase has been studied in livers of C_3H mice subjected to partial hepatectomy at intervals during the period of rapid regeneration. Activity, as measured by the mean formazan intensity, was found to drop significantly during the first 21 hours, and 2 to 10 days following hepatectomy. It had not returned to

normal on the tenth day although liver parenchyma appeared normal in conventionally stained sections. Restoration of activity was complete, however, by the 14th to 28th days. The enzyme activity was concentrated about the portal areas and remained there rather constantly, with minor variations. This distribution differed from that of α-glycerophosphate and other DPN dependent dehydrogenases.

The distribution of enzyme loci could be clearly demonstrated in tissue pretreated with n-butanol and ether at –65° C., especially when lipids were abundant in the liver during the first 4 days after hepatectomy. With such pretreatment, the tissues reacted feebly or not at all with tetrazolium salts unless phenazine methosulfate was added. During the first 21 hours, enzyme active regions were manifested by large globules of formazan deposit which contrasted with the fine granular appearance in the normal liver. These coarse deposits prevailed in the areas occupied by lipid. During the third to tenth days the aggregates became smaller until they returned to normal size at 14 to 28 days.

REFERENCES

1. Tsuboi, K. K.; Yokoyama, H. O.; Stowell, R. E., and Wilson, M. E. The chemical composition of regenerating mouse liver. *Arch. Biochem.*, 1954, **48**, 275–292.
2. Seligman, A. M., and Rutenberg, A. M. The histochemical demonstration of succinic dehydrogenase. *Science*, 1951, **113**, 317–320.
3. Pearson, B., and Defendi, V. Histochemical demonstration of succinic dehydrogenase in thin tissue sections by means of 2-(p-iodophenyl)-3-(p-nitrophenyl)-5-phenyl tetrazolium chloride under aerobic conditions. *J. Histochem.*, 1954, **2**, 248–257.
4. Defendi, V., and Pearson, B. Quantitative estimation of succinic dehydrogenase activity in a single microscopic tissue section. *J. Histochem.*, 1955, **3**, 61–69.
5. Tsou, K-C.; Cheng, C-S.; Nachlas, M. M., and Seligman, A. M. Synthesis of some p-nitrophenyl substituted tetrazolium salts as electron acceptors for the demonstration of dehydrogenases. *J. Am. Chem. Soc.*, 1956, **78**, 6139–6144.
6. Pearson, B. Use of nitroneotetrazolium in enhancing the permanence and effecting finer histochemical localization of succinic dehydrogenase. (Abstract.) *Fed. Proc.*, 1957, **16**, 368.
7. Pearson, B. Improvement in the histochemical localization of succinic dehydrogenase by use of nitroneotetrazolium chloride. *J. Histochem.*, 1958, **6**, 112–121.
8. Pearson, B., and Grose, F. Unpublished data.
9. Morton, R. K. Separation and purification of enzymes associated with insoluble particles. *Nature, London*, 1950, **166**, 1092–1095.
10. Singer, T. P., and Kearney, E. B. Solubilization, assay, and purification of succinic dehydrogenase. *Biochim. et biophys. acta.*, 1954, **15**, 151–153.

11. Farber, E., and Bueding, E. Histochemical localization of specific oxidative enzymes. V. The dissociation of succinic dehydrogenase from carriers by lipase and the specific histochemical localization of the dehydrogenase with phenazine methosulfate and tetrazolium salts. *J. Histochem.*, 1956, 4, 357–362.

12. Cheronis, N. Personal communication.

13. Pearse, A. G. E. Histochemistry. Theoretical and Applied. Little, Brown & Co., Boston, 1953, p. 445–446.

14. Pearson, B., and Defendi, V. Histochemical studies of succinic dehydrogenase by means of tetrazolium in rat liver tumors induced by *p*-dimethylaminoazobenzene. *Cancer Res.*, 1955, 15, 593–597.

15. Morton, R. K. Methods of Extraction of Enzymes from Animal Tissues. In: Methods in Enzymology. Colowick, S. P., and Kaplan, N. O. (eds.). Academic Press, Inc., New York, 1955, Vol. I, pp. 25–51.

16. Schneider, W. C., and Potter, V. R. The assay of animal tissues for respiratory enzymes. II. Succinic dehydrogenase and cytochrome oxidase. *J. Biol. Chem.*, 1943, 149, 217–227.

17. Novikoff, A. B., and Potter, V. R. Biochemical studies on regenerating liver. *J. Biol. Chem.*, 1948, 173, 223–232.

LEGENDS FOR FIGURES

Sections illustrated were pretreated 50 minutes in n-butanol and ether (1:1) at −65° C. They were then incubated 30 minutes at 25° C. with standard incubation solution containing nitroneotetrazolium. No counter stain was used.

FIG. 1. Normal liver, showing succinic dehydrogenase activity. The enzyme indicated by formazan deposit is localized about portal areas. Parenchyma about the central vein is devoid of enzyme. × 90.

FIG. 2. High power magnification of normal liver, showing particulate deposition of formazan representing succinic dehydrogenase in cytoplasm of liver cells. × 600.

FIG. 3. Liver at 21 hours following partial hepatectomy, showing the characteristic large ovoid formazan-positive deposits. In the lower portion of the photograph formazan-positive material may be seen within lipid globules. × 600.

FIG. 4. Liver, 21 hours following partial hepatectomy. Formazan-positive material tends to be arranged as "sausage shaped" masses at the periphery of lipid globules. × 600.

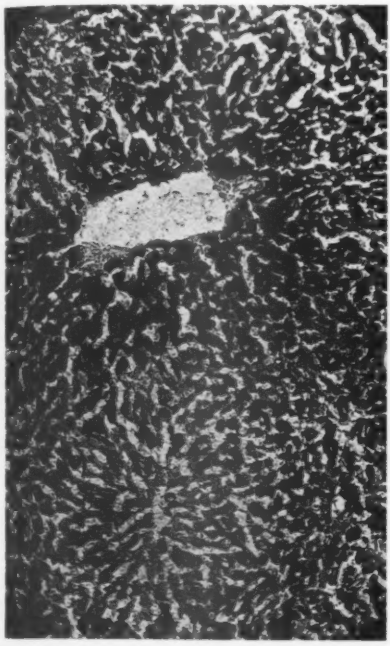

1

2

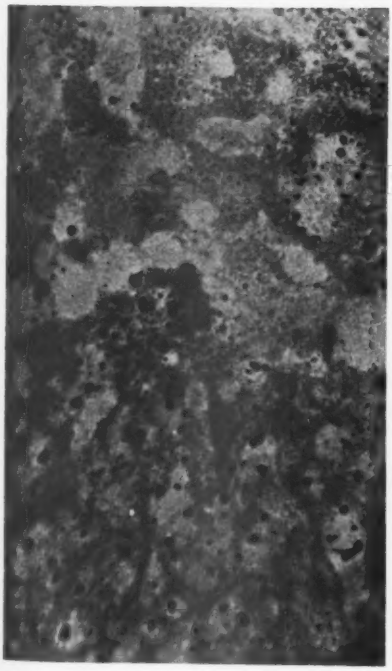

3

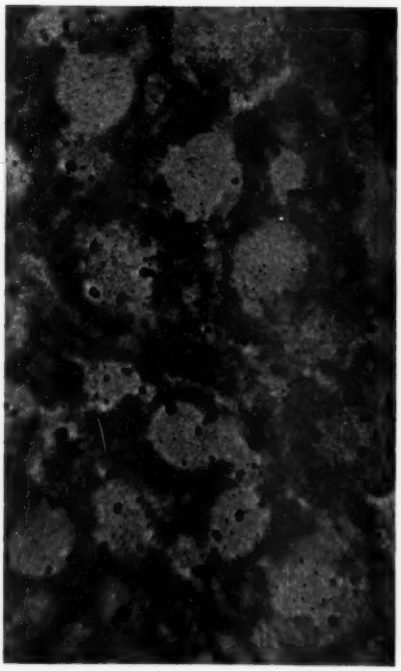

4

FIG. 5. Liver, 3 days following partial hepatectomy. An intense formazan deposition is evident. Granules are smaller than those at 21 hours. × 600.

FIG. 6. Photograph of a "light" area of liver at 7 days, showing spotty restoration of enzyme activity. × 600.

FIG. 7. Photograph of a "dark" area, showing spotty restoration of enzyme activity 10 days after operation. For the most part, enzyme is distributed as fine particles in the cytoplasm. Larger granules can be seen, however, in the upper portion of the photograph. × 600.

FIG. 8. Liver, 28 days postoperatively. Succinic dehydrogenase activity is shown by uniformly distributed fine formazan granules. × 600.

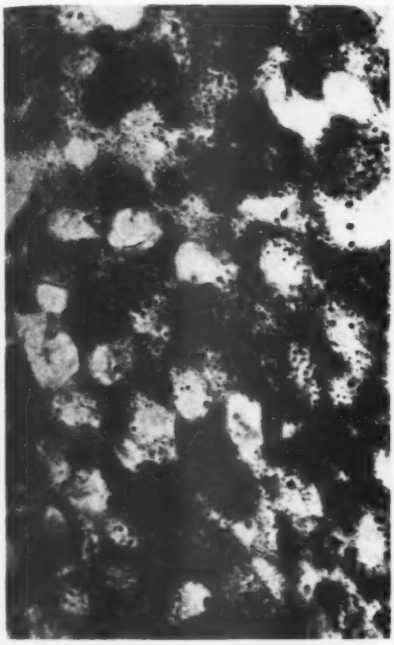

5

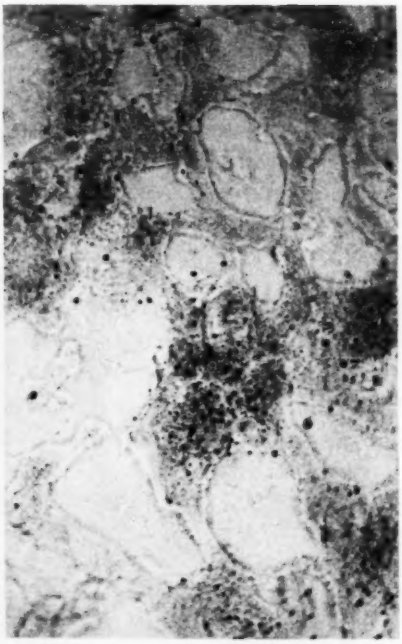

6

7

8

BOTRYOMYCOSIS *

DONALD J. WINSLOW, Lt. Col., MC, U.S. Army†
From the Armed Forces Institute of Pathology, Washington, D.C.

Botryomycosis is characterized by a chronic, suppurative, more or less granulomatous lesion in which the specific feature is the presence of fungus-like grains, or granules, within suppurative foci. These grains, unlike those of mycetomas and actinomycosis, contain non-branching bacteria which can be seen microscopically, especially when Giemsa or Gram stain has been properly applied to the tissue section. Bollinger[1] discovered this disease in the horse in 1870, and in 1884 Rivolta,[2] under the impression that it was caused by a true fungus, gave it the name botryomycosis. In 1913, Opie[3] published the first report of a human case of botryomycosis in the United States, which was also the first account of visceral involvement. In this paper he reviewed the literature up to that time. The reports which he found, added to those subsequently published by other authors,[4] constitute at present a total of about 40 human cases. There is little doubt that infection of this type is much more common than this number would indicate.

An analysis of the cases of human botryomycosis reported indicates that they fall into two broad anatomic groups: integumentary, with or without muscular and skeletal involvement; and visceral. The former distribution has been by far the more frequent. Occasionally the integumentary lesion begins as osteomyelitis which progresses to a chronic stage, with the development of fistulas and sinuses containing botryomycotic grains. Exposed surfaces of skin are more commonly affected, the hands, feet and head being the principal sites. In some cases a sequestrum or other foreign body has been associated with the lesions. Unexposed surfaces of the body, such as the breast, scrotum, labium majus, and perianal region, may also be the site of botryomycotic lesions, but often these are regions subject to trauma or bacterial contamination.

The causative agent has been identified as a micrococcus in most of the integumentary infections; the staphylococcus was cultured in 5 of 37 cases. In two instances a combination of staphylococcus and *Escherichia coli* was substantiated by culture. In one case, a granuloma of the face reported by Langeron,[5] the etiologic agent was considered to have the appearance of an actinobacillus, but no cultures were obtained.

* Received for publication, May 22, 1958.
† Pathologist, Geographic and Infectious Disease Section, AFIP.

Reports of the visceral form of the disorder have been uncommon. After Opie's[3] first description of a huge chronic botryomycotic abscess of the liver, it was 20 years until Beaver and Thompson[6] reported the first fatal instances of human actinobacillosis (botryomycosis) and described the existence of grains in the lesions. Then Fink,[7] in 1941, cited a case of fatal visceral botryomycosis involving the liver and lung, in which the etiologic agent proved to be *Staphylococcus aureus*, the organisms being identified in sections and by culture. In 1948, Auger[4] reported 4 instances, one of which was fatal and was found to have multiple renal botryomycotic abscesses. A gram-negative bacillus, which resembled *Actinobacillus lignieresi* morphologically and culturally, was recovered. In 1946, Moulonguet and Gaske[8] reported a case in which the kidneys were the seat of botryomycotic lesions. The causative agent was considered, on morphologic grounds, to be a staphylococcus.

Experimentally, lesions of botryomycotic type have been produced in animals by Magrou,[9] Aynaud,[10] and Kimmelstiel and Easley.[11] Magrou and Aynaud each used staphylococci, the former to inoculate rabbits, and the latter, sheep. Kimmelstiel and Easley fixed a fishbone in the intestine of a rabbit so that the sharp end protruded into the lumen. They were able to obtain lesions resembling those of botryomycosis in the wall of the intestine opposite the sharp point of the fishbone. Although their experiment was ingenious and produced lesions of botryomycotic type, their experimental approach did not parallel the conditions under which human botryomycosis develops in most instances.

Little is known at present of the factors which cause certain bacteria to produce lesions of the botryomycotic type. Magrou[9] was of the opinion that the essential factor was a delicate balance between the virulence of the infecting agent and the tissue resistance of the host, a sort of symbiosis developing between micro-organism and host. Henrici,[12] in working with experimental aspergillus infections in rabbits, correlated the onset of skin hypersensitivity with an alteration in the inflammatory reaction from a suppurative to a granulomatous form, and a change in the fungus to an actinomycetoid form. Drake, Sudler and Canuteson[13] have suggested that botryomycosis is the result of a relative decrease in virulence of the organisms and an increase in resistance of the host. They called attention to the observations of several workers that cultures of *Staphylococcus aureus* isolated from botryomycotic lesions have a rather low virulence for experimental animals.

Although it is difficult to locate cases of botryomycosis because they

are often incorrectly classified under another name, 8 have been found in the collections of the Armed Forces Institute of Pathology. The tissue in two cases was insufficient and unsuitable for the purposes of this study. One was an example of the fatal visceral variety, probably due to the staphylococcus, with lesions in the heart and kidney. The other was an instance of osteomyelitis of the foot, in which botryomycotic grains were found microscopically. The causative agent appeared to be a micrococcus. Six cases will be presented in order to illustrate certain features which may aid in differential diagnosis.* It will be noted that the original diagnosis in each instance was mycetoma, Madura foot, actinomycosis, or nocardiosis.

Case Reports

Case 1

A 60-year-old colored man (AFIP Acc. 811002) died with a severe, persistent, and refractory infection of the urinary tract. An organism of the Proteus group of bacteria had been recovered repeatedly from the urine. At necropsy, the kidneys and lungs contained numerous abscesses from which a Proteus micro-organism was isolated.

Original Diagnosis. Nocardiosis or actinomycosis.

Microscopically, the focal abscesses in the lung were surrounded by granulation tissue (Fig. 1). Near the center of such areas of suppuration were grains, which, under higher power, were seen to be bordered by clublike extensions of a homogeneous substance (Fig. 2). This feature of the granules may have prompted the original diagnosis. However, special stains, such as the Gomori silver methenamine, failed to demonstrate either the branching filaments of Actinomyces and Nocardia, or the broad hyphae or spores of the higher fungi. In Giemsa and Gram stained preparations, small gram-negative coccobacilli were demonstrated in and adjacent to the grains. They were seen most clearly in Giemsa stained preparations under oil immersion (Fig. 3).

Review Diagnosis. Botryomycosis, probably caused by a member of the Proteus group.

Case 2

A recurrent mass was excised for the third time from the dorsum of the foot of a 23-year-old man (AFIP Acc. 551642). Purulent material had been draining from it, but none was cultured.

* Since the completion of this paper, two additional examples of botryomycosis have been received. One affected the integument of the knee; a micrococcus was the causative agent. The other was an example of the fatal visceral form, with abscesses in the prostate, kidney and lung. The organisms in the grains were gram-negative bacilli and a postmortem culture of one of the abscesses yielded both *Pseudomonas aeruginosa* and *Staphylococcus aureus*.

Original Diagnosis. Questionable actinomycosis or mycetoma.

Microscopically, the lesions consisted of focal granulomas with central suppuration. Grains were found in many of the suppurative foci. Gram stains revealed gram-positive cocci within the grains (Fig. 4). The Gomori silver methenamine method produced deep brown to black staining of the walls of the cocci (Fig. 5). There was evidence that the micro-organisms had reproduced by fission and not by budding. Neither branching filaments nor broader hyphae were found in the grains.

Review Diagnosis. Botryomycosis, probably caused by a staphylococcus.

Case 3

A rubbery, lobulated mass arose in the distal palmar crease at the base of the right index finger of a 38-year-old white man (AFIP Acc. 797995). A "ganglion" had been excised from the same region 4 years previously.

Original Diagnosis. Mycetoma.

On microscopic examination, an epithelioid granulomatous reaction was observed around a central suppurative zone which contained grains (Fig. 6). A multinucleated giant cell of the Langhans type was present near the periphery of the granuloma. Special stains revealed gram-positive cocci but no fungi within the grains.

Review Diagnosis. Botryomycosis, probably caused by a staphylococcus.

Case 4

An 8-year-old Negro boy was admitted to a hospital because of an infected foot (AFIP Acc. 130847). At the age of 3, while he was running barefoot on his father's farm, his foot was pierced by a piece of glass. The puncture wound did not heal completely and discharged thin, watery, blood-stained pus. The foot became enlarged and distorted, and multiple draining sinuses developed. Roentgenograms revealed advanced destruction of the bones of the foot. Cultures from the pus were said to have grown a segmented mycelial fungus. The mycelia were broad and produced chlamydospores. The foot was amputated.

Original Diagnosis. Madura foot.

Microscopically, grains were seen within a suppurative lesion in a section stained with hematoxylin and eosin (Fig. 7). The Gram stain revealed many gram-positive cocci within one of the grains (Fig. 8), but other cocci did not stain well, presumably because they had degenerated or were dead. Special stains for fungi were negative, except for Gomori's silver methenamine, which stained the cocci well. The fungus

which was cultured is considered to have probably been a contaminant.

Review Diagnosis. Botryomycosis with osteomyelitis, probably caused by a staphylococcus.

Case 5

A middle-aged white man (AFIP Acc. 842995) complained of a swollen submandibular lymph node. There was no history of a recent mouth infection. Cultures were not obtained.

Original Diagnosis. Compatible with actinomycosis.

Microscopically, grains with characteristic "clubs" along the periphery were noted in hematoxylin and eosin stained preparations (Fig. 9). Special stains for fungi were negative. A Gram stain revealed minute gram-negative coccobacilli near the edge of some of the grains. The Gomori silver methenamine stain failed to demonstrate these microorganisms clearly, but a Giemsa stain revealed minute coccobacilli in abundance.

Review Diagnosis. Botryomycosis, probably caused by a gram-negative coccobacillus.

Case 6

A 24-year-old white man (AFIP Acc. 230025) injured his right foot in 1945, but open reduction of a fracture was delayed until 1948. The foot became greatly swollen and indurated. Multiple ulcers and open draining sinuses developed (Fig. 10). Roentgenograms revealed a destructive process in the third, fourth and fifth metatarsal bones. The roentgenologist's diagnosis was osteomyelitis. An amputation was performed through the right upper leg. No bacterial cultures were reported, but on Sabouraud's glucose agar at room temperature a fungus grew and produced white aerial mycelia in 6 to 12 days. Microscopically, ovoid and pyriform conidia appeared singly at the ends of long conidiophores.

Original Pathologic Diagnosis. Madura foot.

Microscopic examination revealed typical botryomycotic grains within suppurative foci. Special stains demonstrated cocci but no fungi in the lesions. This case and case 4 illustrate the necessity for correlating the structural features of the grains with the cultural findings, since both cocci and fungi are frequent contaminants in cultures.

Review Diagnosis. Botryomycosis with osteomyelitis, right foot, probably caused by a staphylococcus.

Discussion

Infections which are characterized microscopically by the presence of granules may be grouped under the general heading "granular infections." As a basis for therapy, 3 main categories of granular infec-

tions may be differentiated according to whether the causative agents are bacteria, filamentous fungi, or higher fungi with broad hyphae: (1) Botryomycoses: the granular bacterioses. Agents: fission fungi (bacteria). (2) Actinomycoses: actinomycosis; granular nocardiosis (nocardial mycetoma). Agents: filamentous fungi (branching bacteria). (3) Mycetomas: regional mycotic granulomas. Agents: higher fungi with broad hyphae.

Infections of this group may appear closely similar grossly, and errors in differential diagnosis are common on microscopic examination. It is evident that certain bacteria under proper host and environmental conditions behave like certain fungi with respect to their pathologic effects on the host. Microscopic differentiation depends on the use of special stains and high power examination of the granules to determine the existence of fungi or bacteria. If special stains, such as Gomori's silver methenamine and Gridley's stains for fungi, fail to reveal fungal elements, it seems unlikely that they are present in viable and significant form. It is known that the Gomori fungus stain is capable of demonstrating even nonviable Histoplasma. It also stains the branching filamentous fungi and certain gram-positive bacteria. Bacteria generally stain well in Giemsa preparations, and these should be supplemented by Gram stains, such as that of Brown and Brenn, to aid in identification. Correlation of the clinical, morphologic, and cultural findings will allow specific identification of the infective agent. If the grains themselves could be washed and cultured, the etiologic agent might be grown and contaminants largely eliminated. The results of cultural studies should be supported by morphologic observations.

The occurrence of "clubs," knobby or smooth shells which form around micro-organisms in certain cases, is apparently a nonspecific reaction between the agent and the host,[14] possibly related to hypersensitivity.[12] The substance is often eosinophilic and safranophilic, and responds in positive fashion to the periodic acid-Schiff reaction but in negative manner to mucicarmine and Gomori's methenamine silver stains. "Club" or shell formation has been observed with a number of different fungi,[15] bacteria,[4,6,9,11] parasites,[16] and even in response to inorganic material injected into animals.[17] It has also been demonstrated in cultures of Actinomyces.[18]

In case 1 it is believed that a micro-organism of the Proteus group was the infective agent. This opinion is based on the structural and cultural observations. No other reports of Proteus botryomycosis have been found in the literature. Etiologic agents which have been demonstrated previously, and the hosts in which they occurred are as follows:

Micrococcus: Man[3,4,11,19]; horse[1,2,9]; cattle[20]; pig[20]; sheep[10]; camel.[21] *Escherichia coli:* Man.[19,22] Actinobacillus: Man[4,6]; cattle.[23]

Although Berger, Vallée and Vézina[19] and Auger[4] have suggested the term "actinophytosis" as a substitute for botryomycosis, such a change in nomenclature is a doubtful improvement. Actinophytosis signifies a lesion characterized by ray formation, produced by any plant microorganism. Since ray formation is not a specific phenomenon and the grains of botryomycosis often do not exhibit ray formation, the prefix "actino-" is misleading. The suffix "-phytosis" is too general and does not apply specifically to a bacterial disease. The entire word, when spoken, may be confused easily with "actinomycosis." Some advantages of retaining the term "botryomycosis" would seem to be: (1) It is a term accepted and used by many authors. (2) The disorder in its various manifestations closely mimics, both grossly and microscopically, certain fungous diseases such as actinomycosis and mycetoma. (3) The prefix "botryo-" refers to the grapelike appearance of the grains; and, in the majority of cases, clusters of cocci in knob-like outgrowths may be said to give the grains this microscopic appearance. (4) The suffix "-mycosis," although originally intended to imply a true fungus source, may still, with good reason, be retained because of the similarity of botryomycosis to certain true fungous diseases and because bacteria are usually classified as fission fungi. (5) Much confusion in the literature and in indices to the literature has resulted from failure to accept and define the term botryomycosis and to differentiate it from pseudobotryomycosis, pyogenic granuloma, *granuloma telangiectaticum* and *granuloma pediculatum*.[3,19]

Summary

Six new cases of human botryomycosis have been presented. In 4 of these, the etiologic agent was probably a staphylococcus; in one a gram-negative coccobacillus, and in one a member of the Proteus group of bacteria were identified. A review of the literature has failed to uncover any previously reported human case of botryomycosis due to a Proteus organism.

In these "granular infections" the use of special stains for bacteria and fungi will allow a determination of the micro-organismal component of the characteristic granules and differentiation from other lesions due to fungi. In botryomycosis, the etiologic agents are bacteria and should be distinguished from actinomycosis and nocardiosis, in which the agents are filamentous branching fungi, and from mycetoma caused by the higher fungi with broad hyphae.

REFERENCES

1. Bollinger, O. Mycosis der Lunge beim Pferde. *Virchows Arch. path. Anat.*, 1870, **49**, 583–586 (cited by Opie[3]).
2. Rivolta, S. Del micelio e delle varietà e specie di discomiceti patogeni. *Giorn. di anat. fisiol. e patol. d. animali*, 1884, **16**, 181–198 (cited by Berger, Vallée and Vézina[19]).
3. Opie, E. L. Human botryomycosis of the liver. *Arch. Int. Med.*, 1913, **11**, 425–439.
4. Auger, C. Human actinobacillary and staphylococcic actinophytosis. *Am. J. Clin. Path.*, 1948, **18**, 645–652.
5. Langeron, M. L'actinobacillose humaine. *Ann. de parasitol.*, 1941, **18**, 270–278.
6. Beaver, D. C., and Thompson, L. Actinobacillosis of man. Report of a fatal case. *Am. J. Path.*, 1933, **9**, 603–622.
7. Fink, A. A. Staphylococcic actinophytotic (botryomycotic) abscess of the liver with pulmonary involvement. *Arch. Path.*, 1941, **31**, 103–107.
8. Moulonguet, P., and Gaske, L. Infection staphylococcique du rein. Un example de vraie botriomycome. *Compt. rend. Soc. anat., Paris*, 1946, No. 5, 37–38 (cited by Auger[4]).
9. Magrou, J. Les formes actinomycotiques du staphylocoque. *Ann. Inst. Pasteur*, 1919, **33**, 344–374.
10. Aynaud, M. La botryomycose du mouton. (Abcès du mouton. Maladie caséeuse.) *Ann. Inst. Pasteur*, 1928, **42**, 256–281.
11. Kimmelstiel, P., and Easley, C. A., Jr. Experimental botryomycosis. *Am. J. Path.*, 1940, **16**, 95–102.
12. Henrici, A. T. Characteristics of fungous diseases. *J. Bact.*, 1940, **39**, 113–138.
13. Drake, C. H.; Sudler, M. T., and Canuteson, R. I. A case of staphylococcic actinophytosis (botryomycosis) in man: The tenth reported human case. *J. A. M. A.*, 1943, **123**, 339–341.
14. Meyer, K. Sur la genèse des massues des Actinomycètes. *Compt. rend. Soc. de biol.*, 1934, **115**, 1684–1686.
15. Moore, M. Radiate formation on pathogenic fungi in human tissue. *Arch. Path.*, 1946, **42**, 113–153.
16. Hartz, P. H., and van der Sar, A. Tropical eosinophilia in filariasis. *Am. J. Clin. Path.*, 1948, **18**, 637–644.
17. Levaditi, C., and Dimancesco-Nicolau, O. Formations astéröides autour des dépots telluriques. *Compt. rend. Soc. de biol.*, 1926, **95**, 531–533 (quoted by Berger and associates[19]).
18. Bayne-Jones, S. Club formation by *Actinomyces hominis* in glucose broth, with a note on *B. actinomycetum-comitans*. *J. Bact.*, 1925, **10**, 569–577.
19. Berger, L.; Vallée, A., and Vézina, C. Genital staphylococcic actinophytosis (botryomycosis) in human beings. *Arch. Path.*, 1936, **21**, 273–283.
20. Magnusson, H. The commonest forms of actinomycosis in domestic animals and their etiology. *Acta path. et microbiol. scandinav.*, 1928, **5**, 170–245.
21. Archibald, R. G. Human botryomycosis. *Brit. M. J.*, 1910, **2**, 971–972.
22. Kimmelstiel, P., and Oden, P. W. Botryomycosis. Report of 2 cases of intra-abdominal granuloma. *Arch. Path.*, 1939, **27**, 313–319.
23. Lignières, J., and Spitz, G. Contribution à l'étude des affections connues sous le nom d'actinomycose. *Arch. de parasitol.*, 1903, **7**, 428–479.

[*Illustrations follow*]

LEGENDS FOR FIGURES

FIG. 1. Case 1. Lung. A focal abscess contains grains and is surrounded by granulation tissue. Hematoxylin and eosin stain. × 60.

FIG. 2. Case 1. Lung. Granules with peripheral "clubs." Hematoxylin and eosin stain. × 800.

FIG. 3. Case 1. Lung. Minute coccobacilli in and adjacent to granules. Giemsa stain. × 1,500.

FIG. 4. Case 2. Mass on dorsum of foot. Numerous cocci within grains. Brown and Brenn stain. × 1,500.

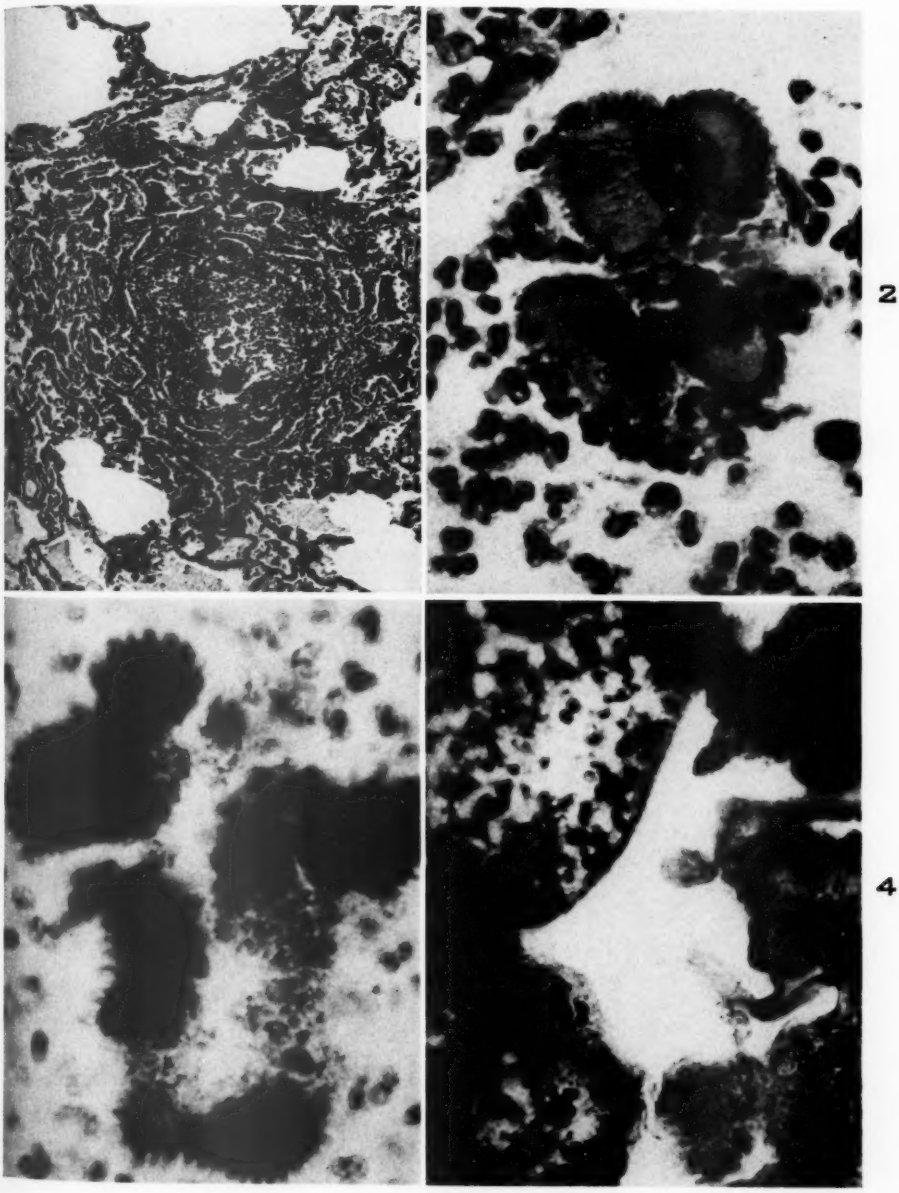

FIG. 5. Case 2. Mass on dorsum of foot. The cocci within a granule are clearly defined. Gomori methenamine silver nitrate stain. × 1,500.

FIG. 6. Case 3. Mass at base of right index finger. An epithelioid granulomatous reaction surrounds a central suppurative focus which contains grains. Hematoxylin and eosin stain. × 100.

FIG. 7. Case 4. Foot. Several grains within a suppurative focus. Hematoxylin and eosin stain. × 100.

FIG. 8. Case 4. Foot. Numerous cocci within a grain. Brown and Brenn stain. × 1,500.

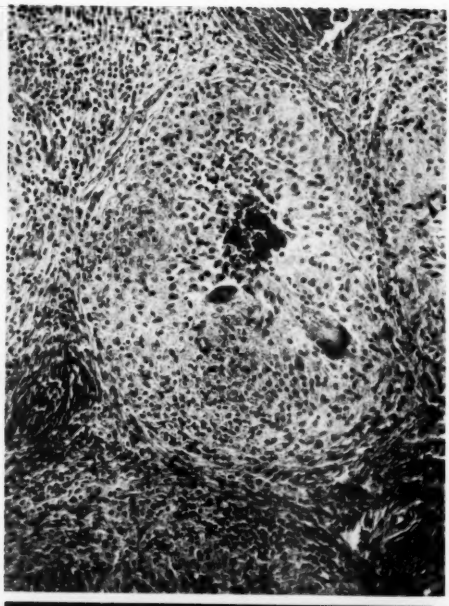

6

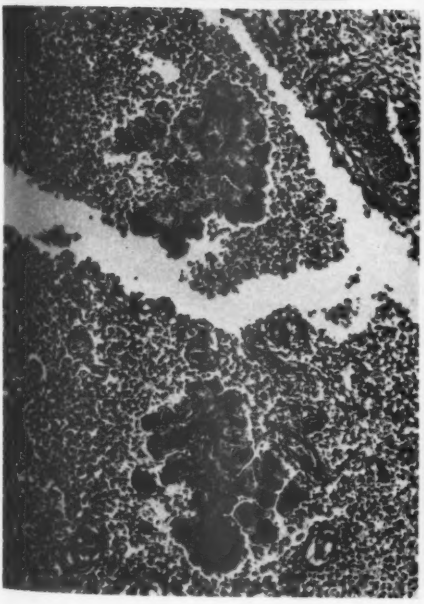

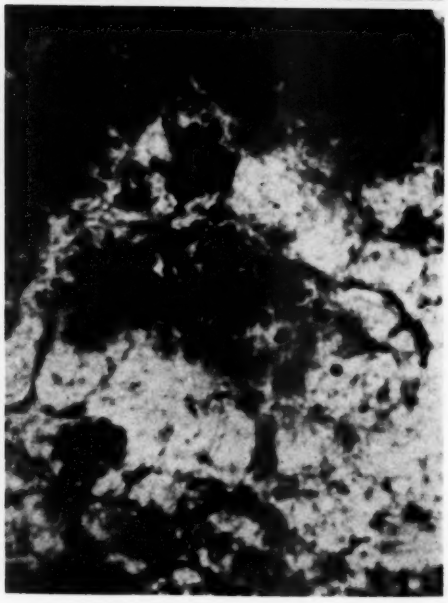

8

FIG. 9. Case 5. Submandibular lymph node. A grain with peripheral "clubs." Hematoxylin and eosin stain. × 400.

FIG. 10. Case 6. Right foot. The many ulcers and sinuses account for the clinical resemblance to Madura foot. A. Dorsal aspect. B. Lateral aspect. C. Plantar aspect.

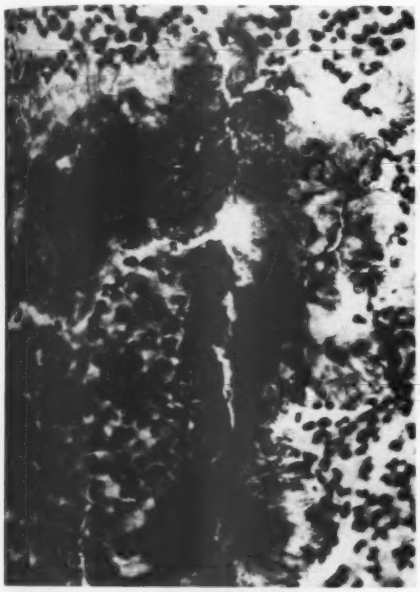

10 A

10 C

THE EFFECT OF CORTISONE AND ANTIBIOTIC AGENTS ON EXPERIMENTAL PULMONARY ASPERGILLOSIS *

HERSCHEL SIDRANSKY, M.D.,† and LORRAINE FRIEDMAN, Ph.D.
From the Departments of Pathology and Microbiology, Tulane University, School of Medicine, New Orleans, La.

For many years pathologists have encountered rare instances of human infection with classes of fungi that are widely prevalent in the environment but are generally regarded to be saprophytic. These infections are seldom encountered except in persons who are seriously debilitated as a result of other disorders. An increasing number of such human infections with "saprophytic" fungi such as Aspergillus, Mucor, and Candida have been reported recently.[1-5] These have occurred chiefly, as in the past, in chronically ill patients but particularly in patients who have been treated with cortisone or ACTH and with broad spectrum antibiotic agents during some stage of their ailments.

During the past 3 years, 18 patients with secondary fungal infections of the lungs have been observed on the Tulane Autopsy Service at Charity Hospital of Louisiana in New Orleans.[6] The causative organisms were Aspergillus, Candida, and Mucor (or Rhizopus), and most of these patients had been treated with cortisone or ACTH and antibiotic agents. In contrast, during the preceding 5-year period, only 4 similar instances of pulmonary infection were observed.

Some insight into the mechanisms by which antibiotic agents and cortisone might increase host susceptibility to fungal infections has been gained by experimental studies. It appears that antibiotic drugs can exert such an effect by acting on either the fungi themselves,[7-9] the host,[10,11] or both. Cortisone, however, is believed to act chiefly by inhibiting certain of the host defenses against infection.[12]

Our own observations of secondary fungal infections of the lungs in chronically ill patients treated with steroid hormones or antibiotic agents led us to investigate the possible effects of these substances on the susceptibility of mice to pulmonary infection by air-borne fungi. Under similar circumstances, altered susceptibility to Aspergillus,[13] Mucor,[14,15] and Candida[13,16-22] has been shown to exist in experimental animals. In most instances the method of inoculation with the fungus has not simulated conditions of natural exposure. In our experiments

* Supported in part by a Training Grant from the National Cancer Institute (CRT 5025) and a Research Grant from the National Institute of Allergy and Infectious Diseases (E 1224), the United States Public Health Service.
Received for publication, June 4, 1958.
† Present address: Laboratory of Pathology, National Cancer Institute, National Institutes of Health, Bethesda, Md.

mice were treated with cortisone and antibiotic drugs and then subjected to inhalation of aerosols containing dry, viable spores of *Aspergillus flavus*. This method of exposure probably simulates more closely the mechanism by which human beings acquire fungal infections of the lungs.

Experimental Method

Mice are normally resistant to infection with aspergillus and other "saprophytic" fungi. Hence they are suitable animals for testing the possible role of cortisone and antibiotic drugs in reducing resistance. White female mice of the Carworth Farms CF1 strain were used in all experiments except one, in which male Taconic Farms mice were used. The mice were inoculated subcutaneously with 5 mg. of an aqueous suspension of cortisone acetate (Cortone Acetate, Merck Sharp & Dohme) and intramuscularly with 30,000 units of long-acting penicillin (Bicillin,® Wyeth) two days before exposure to spores of *Aspergillus flavus*. Another antibiotic agent, tetracycline hydrochloride (Achromycin,® Lederle) was added to the water (5 mg. per 100 ml.) which the animals drank freely throughout the course of the experiment. At least two control groups were investigated simultaneously. One received spores but no cortisone or antibiotic agents, and the other received cortisone and antibiotic agents but no spores.

The exposure chamber consisted of a closed bell jar containing a cylindrical wire mesh (Fig. 1). One outlet was available to provide fresh air when necessary and another for escape of excess air. Spores, obtained by vacuum suction from dried cultures of *Aspergillus flavus*, were sprayed into the chamber with a powder atomizer. The strain used was originally cultured from a human lung which was the seat of aspergillosis.

Mice were exposed to low, medium, or high concentrations of spores for 10 to 30 minutes and were observed for 3 weeks or until death. In some experiments designed to study the sequence of the pathologic lesions and the fate of the inhaled spores, mice were sacrificed at intervals following exposure.

The approximate number of spores retained in the lungs was determined by sacrificing 2 or 3 mice of each group immediately after exposure. The left lungs were removed and individually homogenized in sterile saline. Plate counts were then performed using suitable dilutions of the homogenates. Mice exposed to 3 different concentrations of spores retained approximately 360,000, 60,000 or 24,000 viable spores per left lung.

In order to determine whether cortisone and antibiotic agents given separately and in combination influenced the susceptibility of mice to

lethal pulmonary aspergillus infection, two experiments were performed (Table I). In each, mice were divided into 4 experimental groups, all of which were exposed to high concentrations of spores. One group received cortisone and antibiotic agents, a second received cortisone alone, a third received antibiotic drugs, and a fourth received no supplementary treatment.

TABLE I

Seven-Day Mortality in Mice Inhaling Aspergillus flavus Spores

No. of mice in group	Treatment			Mortality at end of 7 days
	Spores*	Cortisone†	Antibiotic agents‡	
16	+	+	+	14/16 (88%)
15	+	+	o	10/15 (67%)
7	+	o	+	0/7 (0%)
22	+	o	o	0/22 (0%)
20	o	+	+	0/20 (0%)
20	o	+	o	0/20 (0%)
7	o	o	+	0/7 (0%)
20	o	o	o	0/20 (0%)

* Approximately 360,000 viable spores retained per left lung.

† 5 mg. cortisone acetate, 2 days before exposure to spores.

‡ 30,000 units Bicillin,® 2 days before exposure to spores; tetracycline hydrochloride, 5 mg. per 100 ml. in water bottles.

One experiment was performed to learn whether the inhalation of a large number of dead spores would produce a pneumonitis. Mice with and without treatment by cortisone and antibiotic agents were exposed to spores previously heated at 103° C. for 24 hours. Their nonviability was confirmed by failure to grow on an agar medium. Some mice were sacrificed at intervals up to one week and others were observed for 10 weeks.

Two experiments were designed to determine whether multiple doses of cortisone would increase susceptibility to infection with lower concentrations of spores. In these experiments the mice were given injections of cortisone (2.5 mg.) at intervals throughout the 2 to 3 week period of observation in addition to the regular pretreatment with 5 mg. of cortisone 2 days before exposure. In one experiment (# 323, Table III) the mice inhaled a low concentration of spores and were given supplementary injections of cortisone at 2, 5, 8, 11, 14, and 17 days after exposure to the spores. In a second experiment (# 321, Table III) the animals inhaled a medium concentration of spores and the supplementary injections of cortisone were given 2 and 5 days after exposure.

All animals were necropsied. Portions of lung were cultured, and other portions were fixed in 10 per cent formalin. Sections were stained with hematoxylin and eosin and with the Gridley stain.[23]

Results

No mice died after treatment with cortisone alone, antibiotic agents alone, or a combination of the two. No mice died after receiving spores alone or in combination with antibiotic drugs. When mice treated with cortisone or with cortisone and antibiotic agents were exposed to spores, a high mortality resulted. Table I summarizes the data obtained when cortisone and antibiotic therapy were given individually or in combination to mice exposed to a high concentration of spores. The group that received cortisone and antibiotic drugs had an 88 per cent mortality by the seventh day while the group that received cortisone had a 67 per cent mortality at 7 days. This difference is not statistically significant. In this experiment and those mentioned next, no deaths occurred in any of the animals beyond the seventh day, and any mice which survived beyond 7 days were apparently healthy at the end of the 3 week period of observation.

The results obtained in 3 experiments in which mice were exposed to 3 different concentrations of spores are presented in Table II. No mice died after treatment with cortisone and antibiotic agents alone or after receiving spores alone. When mice treated with cortisone and antibiotic drugs were exposed to spores, a high mortality resulted, the rate being dependent upon the dose of spores. At 7 days, mice exposed to the high concentration of spores had an 88 per cent mortality; mice exposed to the medium concentration, a 50 per cent mortality, and mice exposed to the lowest concentration, a 30 per cent mortality.

The lungs from all of the control animals in these experiments were normal in appearance at the time of sacrifice, 3 weeks after inhaling spores. The lungs from the experimental mice which died following exposure to spores and treatment with cortisone and antibiotic agents were diffusely hyperemic, the seat of consolidation, and contained numerous hemorrhagic areas. Extensive hemorrhagic bronchopneumonia was demonstrable microscopically (Fig. 2). In Gridley stained sections masses of hyphae could be seen filling the lumens of small bronchi and invading through bronchial walls into the neighboring soft tissue and blood vessels. In the blood vessel lumens, thrombi made up of fibrin and a feltwork of interlacing hyphae were often evident. The hyphae appeared to breech anatomic barriers in their spread and often extended indiscriminately through such structures as bron-

chial cartilage and arterial walls (Figs. 3 and 4). The infiltration by hyphae in many instances failed to elicit any detectable tissue response. In complete necropsy examinations on mice with extensive hemorrhagic bronchopneumonia and numerous mycelial thrombi in pulmonary blood vessels, evidence of extrapulmonary embolic spread of the fungus was not encountered.

In the two experiments in which mice with and without cortisone

TABLE II

The Effect of Cortisone and Antibiotic Drug Administration on Fatal Pulmonary Aspergillosis in Mice Inhaling Varying Concentrations of Aspergillus flavus Spores

Experiment and group no.	Treatment: Spores*	Cortisone†	Antibiotic agents‡	No. of mice	Day of death after exposure: 1	2	3	4	5	6	7	Mortality at end of 7 days
320 A	Low dose	+	+	10			1	1			1	3/10 (30%)
B	Low dose	o	o	10								o/10 (o%)
C	o	+	+	8								o/8 (o%)
D	o	o	o	10								o/10 (o%)
318 A	Medium dose	+	+	8					4			4/8 (50%)
B	Medium dose	o	o	9								o/9 (o%)
C	o	+	+	9								o/9 (o%)
D	o	o	o	10								o/10 (o%)
317 A	High dose	+	+	8	3	3					1	7/8 (88%)
B	High dose	o	o	8								o/8 (o%)
C	o	+	+	10								o/10 (o%)
D	o	+	o	10								o/10 (o%)
E	o	o	o	10								o/10 (o%)

* Low dose: approximately 24,000 viable spores per left lung; medium dose: approximately 60,000 viable spores per left lung; high dose: approximately 360,000 viable spores per left lung.

† 5 mg. of cortisone acetate 2 days before exposure to spores.

‡ 30,000 units of Bicilllin,® 2 days before exposure to spores; tetracycline HCl, 5 mg. per 100 ml., in water bottles.

and antibiotic treatment were exposed to high concentrations of spores and sacrificed at varying intervals, the following observations were made. Mice from both groups sacrificed immediately after exposure to spores showed no lung lesions. However, on microscopic examination many spores were seen on the mucosal cells of bronchi and bronchioles. These were unaccompanied by inflammatory reaction. Mice of both groups sacrificed one day after exposure were found to have bronchitis and early bronchopneumonia (Fig. 5). The only detectable difference was that spores alone were seen in the lungs of the control animals,

while in the lungs of the experimental animals hyphae as well as spores were present. This observation suggests that the cortisone and antibiotic treatment may have an effect on the organisms as well as the host. After 4 days the bronchopneumonia was found to be undergoing resolution and many macrophages were present in the lungs of the control mice (Fig. 6). Spores, many within macrophages, were readily identified, but no hyphae were present. At this time the lungs of the experimental mice showed an extensive hemorrhagic bronchopneumonia (Fig. 7). Hyphae were seen throughout, and no macrophages were demonstrable in the pulmonary exudate. At 7 days the lungs of the control animals were essentially normal whereas 88 per cent of the experimental animals had died. In the lungs of the control mice, spores could be identified in the tissue and in macrophages until the seventh day, and even though they were not detected microscopically after longer time intervals, a few could be cultured after two weeks. In no instance were hyphae observed in the lungs of the control mice.

In the experiment in which mice were exposed to massive clouds of heat-killed spores, no animals died, either in the group treated with cortisone and antibiotic agents or in the untreated group. No gross or microscopic lesions were observed in the mice sacrificed 4 or more days after inhaling spores. In mice of both groups sacrificed 1 to 3 days after exposure, spores were seen in the bronchi, but no cellular response was manifest.

Table III summarizes the results of the two experiments which were designed to determine whether continuation of cortisone treatment after inhalation of spores would further increase susceptibility. Mice inhaling the low concentration of spores (Experiment 323) and receiving multiple injections of cortisone continued to die throughout the 3 week period of observation, with a final mortality of 86 per cent. Among those which inhaled the medium concentration of spores (Experiment 321), the cumulative mortality was 92 per cent. These results are in contrast to the much lower mortality observed in the mice receiving only one injection of 5 mg. of cortisone 2 days before exposure to approximately the same low or medium concentration of spores (Table II). The pathologic lesions in these experiments were similar to those described in the preceding studies.

Discussion

The experiments indicate that normal mice can inhale large numbers of spores of *Aspergillus flavus* and suffer only a mild self-limiting bronchitis and pneumonitis. However, pretreatment with cortisone

TABLE III

The Influence of Multiple Doses of Cortisone Acetate on Fatal Pulmonary Aspergillosis in Mice Exposed to Low or Medium Concentrations of Aspergillus flavus Spores

Experiment and group no.	Treatment			No. of mice	Day of death after exposure																				Mortality at end of 3 weeks
	Spores*	Cortisone	Antibiotic agents†		1	2	3	4	5	6	7	8	9	10	11	12	13	14	15	16	17	18	19	20	21	
323 A	Low dose	+‡	+	14				1	3			1						1	1	1	1	1			2	12/14 (86%)
B	Low dose	o	o	13																						0/13 (0%)
C	o	+‡	+	15														2								2/15 (13%)
D	o	o	o	12																						0/12 (0%)
321 A	Medium dose	+§	+	13	1	1			4	1	3	1		1												12/13 (92%)
B	Medium dose	o	o	16																						0/16 (0%)
C	o	+§	+	13																						0/13 (0%)
D	o	o	o	8																						0/8 (0%)

* Low dose: approximately 24,500 viable spores per left lung; medium dose: approximately 49,000 viable spores per left lung.
† 30,000 units of Bicillin,® 2 days before exposure to spores; tetracycline HCl, 5 mg. per 100 ml., in water bottles.
‡ 5 mg. of cortisone acetate, 2 days before exposure to spores, and 2.5 mg. cortisone acetate on 2nd, 5th, 8th, 11th, 14th and 17th days after exposure.
§ 5 mg. cortisone acetate 2 days before exposure to spores, and 2.5 mg. cortisone acetate on 2nd and 5th days after exposure.

and antibiotic drugs renders the mice highly susceptible to fatal pulmonary aspergillosis. It is apparent from the results listed in Table I that cortisone rather than the antibiotic treatment is chiefly responsible for the enhanced susceptibility.

Two independent observations suggest that even extremely low concentrations of air-borne spores may be sufficient to induce severe pulmonary infection in occasional cortisone-treated animals. Sági and Lapis,[24] while treating rats with cortisone and studying tumor transplants, found that many of their animals died with pulmonary aspergillosis. They attributed this to the cortisone treatment. Moreover, in our own experiments, on one occasion a leak developed in the exposure chamber and a small number of spores escaped into the room air. Subsequently, several mice in a control group which had received cortisone and antibiotic agents but no spores died (animals originally in Experiment 321 C, Table III, but not listed). At necropsy these animals were found to have pulmonary aspergillosis, attributed to infection with spores which had escaped into the air of the room.

The pathologic events disclosed by sacrificing mice at varying time intervals are of interest. The control animals which inhaled spores in large numbers developed a transient purulent bronchitis and bronchopneumonia within a day, but the pneumonia was resolved by the fourth day, and at 7 days the lungs were histologically normal. Spores but no hyphae were demonstrable within the lungs throughout this period. Though many of the spores remained viable for several weeks, as demonstrated by culture, they appeared to be unable to germinate into hyphae. The inhibition of germination may be attributed to some aspect of the host's natural resistance. Phagocytosis of the spores by macrophages may be one of many protective mechanisms involved. In animals exposed to spores and treated with cortisone and antibiotic drugs, a bronchitis and bronchopneumonia developed within a day. This was at first indistinguishable from that present in the controls. However, it progressed to a hemorrhagic bronchopneumonia and produced a high mortality within 7 days. In these animals hyphae developed within 24 hours and were soon seen invading throughout the lungs. Under the conditions of our experiments cortisone failed to inhibit the acute inflammatory response. This is in agreement with the observations of some workers[25,26] but contrary to those of others.[27-29] However, the macrophage response found in the untreated mice after a few days was not seen in any of the cortisone- and antibiotic-treated mice, either in those which died or those which were sacrificed. This indicates that the macrophage response in the lungs may be partly or completely

inhibited by cortisone. Such a conclusion is consistent with the observations of others.[27,29]

The gross and histologic lesions in the lungs of cortisone-treated mice exposed to spores of *Aspergillus flavus* closely resemble those found at necropsy in human cases of pulmonary aspergillosis.[6] Although terminal pulmonary aspergillosis is a relatively rare complication even in chronically ill patients, our experiments suggest that cortisone and antibiotic treatment may increase susceptibility to this and possibly other serious fungus infections in human subjects.

Summary

Untreated mice and those receiving cortisone and antibiotic drugs were exposed to inhalation of aerosols containing dry, viable spores of *Aspergillus flavus*. Untreated mice and those given antibiotic agents and subsequently exposed to spores in large numbers developed only transient nonfatal pneumonitis. The administration of cortisone and antibiotic drugs or of cortisone alone rendered animals that inhaled spores highly susceptible to fatal pulmonary aspergillosis. The number of spores inhaled and the duration of cortisone treatment influenced the mortality.

Inhaled spores rapidly germinated into hyphae which penetrated throughout the lungs in mice treated with cortisone and antibiotic agents, but did not germinate into hyphae in the lungs of control mice. Heat-killed spores produced no evident lesions in control or experimental mice.

The increased susceptibility of cortisone- and antibiotic-treated mice to air-borne spores of *Aspergillus flavus* strengthens the hypothesis that a similar increase in susceptibility to air-borne saprophytic fungi may develop in certain chronically ill patients receiving these agents.

REFERENCES

1. Zimmerman, L. E. Fatal fungus infections complicating other diseases. *Am. J. Clin. Path.*, 1955, **25**, 46–65.
2. Keye, J. D., Jr., and Magee, W. E. Fungal diseases in a general hospital. *Am. J. Clin. Path.*, 1956, **26**, 1235–1253.
3. Baker, R. D. Pulmonary mucormycosis. *Am. J. Path.*, 1956, **32**, 287–313.
4. Baker, R. D. Mucormycosis—a new disease? *J. A. M. A.*, 1957, **163**, 805–808.
5. Torack, R. M. Fungus infections associated with antibiotic and steroid therapy. *Am. J. Med.*, 1957, **22**, 872–882.
6. Sidransky, H., and Friedman, L. Pulmonary aspergillosis associated with cortisone and antibiotic administration; human and experimental studies. (Abstract.) *Am. J. Path.*, 1958, **34**, 585–586.

7. Huppert, M.; MacPherson, D. A., and Cazin, J. Pathogenesis of *Candida albicans* infection following antibiotic therapy. I. The effect of antibiotics on the growth of *Candida albicans*. *J. Bact.*, 1953, **65**, 171–176.

8. Huppert, M., and Cazin, J., Jr. Pathogenesis of *Candida albicans* infection following antibiotic therapy. II. Further studies of the effect of antibiotics on the *in vitro* growth of *Candida albicans*. *J. Bact.*, 1955, 70, 435–439.

9. Campbell, C. C., and Saslaw, S. Enhancement of growth of certain fungi by streptomycin. *Proc. Soc. Exper. Biol. & Med.*, 1949, 70, 562–563.

10. Stevens, K. M. The effect of antibiotics upon the immune response. *J. Immunol.*, 1953, **71**, 119–124.

11. Slanetz, C. A. The influence of antibiotics on antibody production. *Antibiotics & Chemother.*, 1953, 3, 629–633.

12. Kass, E. H., and Finland, M. Adrenocortical hormones in infection and immunity. *Ann. Rev. Microbiol.*, 1953, 7, 361–388.

13. Mankowski, Z. T., and Littleton, B. J. Action of cortisone and ACTH on experimental fungus infections. *Antibiotics & Chemother.*, 1954, 4, 253–258.

14. Baker, R. D.; Schofield, R. A.; Elder, T. D., and Spoto, A. P., Jr. Alloxan diabetes and cortisone as modifying factors in experimental mucormycosis (Rhizopus infection). (Abstract.) *Fed. Proc.*, 1956, **15**, 506.

15. Bauer, H.; Wallace, G. L., Jr., and Sheldon, W. H. The effects of cortisone and chemical inflammation on experimental mucormycosis (*Rhizopus oryzae* infection). *Yale J. Biol. & Med.*, 1957, **29**, 389–395.

16. Pappenfort, R. B., and Schnall, E. S. Moniliasis in patients treated with aureomycin. Clinical and laboratory evidence that aureomycin stimulates the growth of *Candida albicans*. *A. M. A. Arch. Int. Med.*, 1951, 88, 729–735.

17. Foley, G. E., and Winter, W. D., Jr. Increased mortality following penicillin therapy of chick embryos infected with *Candida albicans* var. *stellatoidea*. *J. Infect. Dis.*, 1949, **85**, 268–274.

18. Seligmann, E. Virulence enhancing activities of aureomycin on *Candida albicans*. *Proc. Soc. Exper. Biol. & Med.*, 1952, **79**, 481–484.

19. Seligmann, E. Virulence enhancement of *Candida albicans* by antibiotics and cortisone. *Proc. Soc. Exper. Biol. & Med.*, 1953, **83**, 778–781.

20. Syverton, J. T.; Werder, A. A.; Friedman, J.; Roth, F. J., Jr.; Graham, A. B., and Mira, O. J. Cortisone and roentgen radiation in combination as synergistic agents for production of lethal infections. *Proc. Soc. Exper. Biol. & Med.*, 1952, 80, 123–128.

21. Friedman, J.; Werder, A. A.; Roth, F. J.; Graham, A. B.; Mira, O. J., and Syverton, J. T. The synergistic effects of roentgen radiation and cortisone upon susceptibility of mice to pathogenic microorganisms. *Am. J. Roentgenol.*, 1954, 71, 509–519.

22. Roth, F. J., Jr.; Friedman, J., and Syverton, J. T. Effects of roentgen radiation and cortisone on susceptibility of mice to *Candida albicans*. *J. Immunol.*, 1957, **78**, 122–127.

23. Gridley, M. F. A stain for fungi in tissue sections. *Am. J. Clin. Path.*, 1953, **23**, 303–307.

24. Sági, T., and Lapis, K. Unter dem Einfluss der Cortisonbehandlung entstehende Lungenaspergillose bei Ratten. *Acta microb. Hung.*, 1956, 3, 337–340.

25. Moon, V. H., and Tershakovec, G. A. The trigger mechanism of acute inflammation. (Abstract and discussion.) *Am. J. Path.*, 1951, **27**, 693–695.

26. Lattes, R.; Blunt, J. W., Jr.; Rose, H. M.; Jessar, R. A.; Vaillancourt, De G., and Ragan, C. Lack of cortisone effect in the early stages of inflammation and repair. *Am. J. Path.*, 1953, **29**, 1–19.

27. Michael, M., Jr., and Whorton, C. M. Delay of the early inflammation response by cortisone. *Proc. Soc. Exper. Biol. & Med.*, 1951, **76**, 754–756.

28. Menkin, V. The significance of the accumulation of cortisone in an inflamed area. *Brit. J. Exper. Path.*, 1953, **34**, 412–419.

29. Spain, D. M.; Molomut, N., and Haber, A. Studies of the cortisone effects on the inflammatory response. I. Alterations of the histopathology of chemically induced inflammation. *J. Lab. & Clin. Med.*, 1952, **39**, 383–389.

[*Illustrations follow*]

LEGENDS FOR FIGURES

FIG. 1. Exposure chamber consisting of a closed bell jar containing a cylindrical wire mesh. The powder atomizer used to spray dried spores is at upper right.

FIG. 2. Lung of mouse exposed to spores and treated with cortisone and antibiotic drugs, showing hemorrhagic bronchopneumonia with vascular thrombosis (lower left). Hematoxylin and eosin stain. × 100.

FIG. 3. Lung of mouse exposed to spores and treated with cortisone and antibiotic agents, showing hyphae invading through bronchus and into adjacent blood vessel (upper right). The double membrane in the vessel (upper right) is the elastic lamina. Gridley stain. × 55.

FIG. 4. Higher magnification of blood vessel in Figure 3, showing hyphae penetrating the elastic lamina. Gridley stain. × 900.

1

2

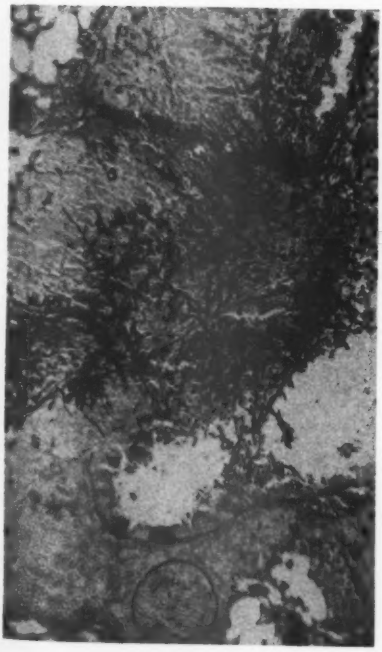

3

4

FIG. 5. Lung of mouse treated with cortisone and antibiotic drugs and sacrificed one day after exposure to aerosols containing viable spores. Lung shows acute bronchitis and early bronchopneumonia. Control mice at this time interval showed the same lesion. Hematoxylin and eosin stain. × 145.

FIG. 6. Lung of control mouse sacrificed 4 days after exposure to aerosols containing viable spores, showing extensive macrophage response surrounding a bronchus. Hematoxylin and eosin stain. × 145.

FIG. 7. Lung of mouse treated with cortisone and antibiotic agents and sacrificed 4 days after exposure to aerosols containing viable spores. There is extensive bronchitis and bronchopneumonia. An artery contains a thrombus (lower left). Hematoxylin and eosin stain. × 145.

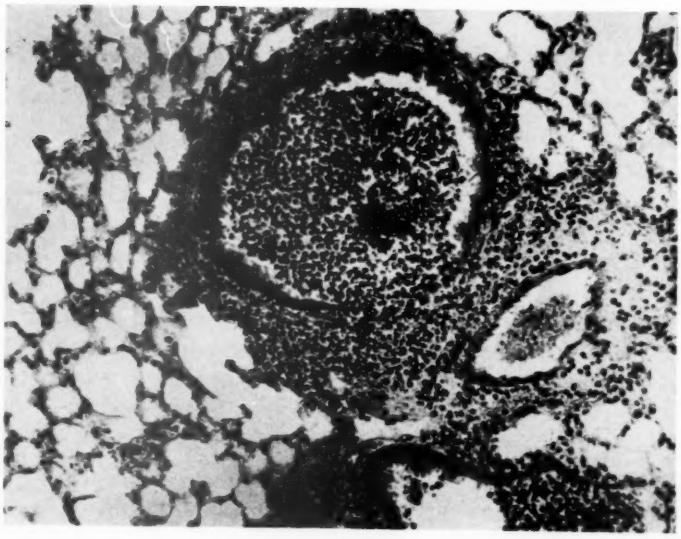

5

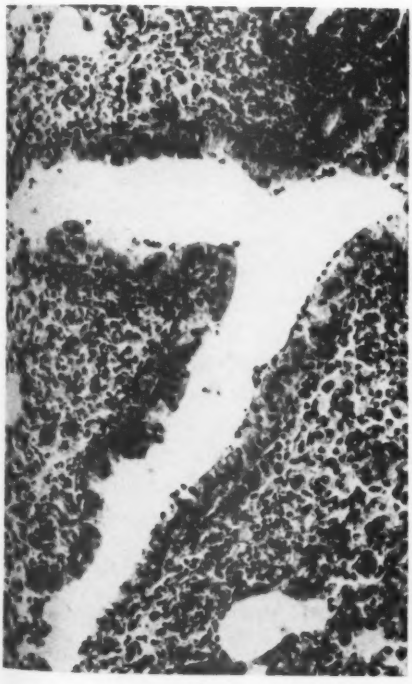

6

7

EXPERIMENTAL INFECTION OF MICE AND MONKEYS BY ACANTHAMOEBA*

C. G. Culbertson, M.D.; J. W. Smith, Ph.D.; H. K. Cohen, D.V.M., and J. R. Minner, M.S.

From The Lilly Research Laboratories, Eli Lilly and Company, Indianapolis, Ind.

Acanthamoeba castellanii[1-4] and *Vahlkampfia debilis*[5,6] are members of related genera of the family of *Amoebidae*.[1] Such amebas have been characterized as "free living," "coprozooic," or as "parasitic" upon fungi and have not been found pathogenic for any species of animal.[1,6,7] Both types have been found in cultures of fungi or yeasts.[3,6] They also produce lysis of plate cultures of selected fungi or bacteria.[3,6,8,9] Acanthamoeba has been found in monkey kidney tissue cultures by two groups of investigators.[10,11]

This report describes observations on Acanthamoeba first observed by us in tissue sections procured from monkeys and mice which had been inoculated with fluid from tissue cultures thought to contain an unidentified virus.[12] Since the suspected virus was not neutralized by available antiviral serums against any of the known agents, it was believed to represent a new agent. The unknown agent appeared in the course of tissue culture safety tests of poliomyelitis vaccine. It was encountered in both uninoculated cultures and in those inoculated with the vaccine. Since unknown agents under these circumstances must, in the interest of safety, be carefully studied, a series of procedures which include animal pathogenicity tests are required. Sixteen monkeys received intracerebral, intraspinal, and intramuscular injections of unfiltered, uncentrifuged, and undiluted tissue culture fluid. They were also given a single dose of 50 mg. of cortisone acetate according to the standard test utilized.[13] All monkeys died in 4 to 7 days with a prostrating illness but with no evidence of paralysis. Forty 20-gm. Swiss white mice were also given intracerebral injections of .03 to .05 ml. of the same fluid, but received no cortisone. These died in 3 to 4 days.

The brains and spinal cords of these animals were sectioned and studied histologically and were found to exhibit both severe chorio-meningitis and severe destructive lesions with suppuration at the sites of injection. There were many organisms which were identified as amebas lying in the inflammatory exudate and also in otherwise normal-appearing nervous tissue. Following these observations, samples

* Presented at the Fifty-fifth Annual Meeting of the American Association of Pathologists and Bacteriologists, Cleveland, O., April 26, 1958.

Received for publication, May 9, 1958.

of the fluid which had been preserved were examined microscopically, and the motile amebas were easily identified, mixed with floating tissue culture cells. Further studies on fluid from which the amebas were removed, both by tissue culture and animal inoculation, revealed no evidence of viral or bacterial agents which might have been associated with the amebas.

The observation pertaining to the severe damage to the central nervous system and the fact that the amebas did not all remain at the sites of injection but showed the ability to migrate *in vivo* led to the additional studies reported in this paper.

The strain isolated was sluggishly motile in the tissue culture or other artificial medium at room temperature and showed characteristic spine-like pseudopods. The ameba exhibited a contractile vacuole, and a single nucleus containing a large karyosome was easily observed in the fresh state. The motility was greatly enhanced when the ameba was suspended in saliva or tears or in sterile preparations of hog gastric mucin. The reasons for this increase in motility have not been explained. The amebas did not phagocytize red cells but did cause a plaque-like clearing on cultures of *Salmonella typhosus*, and, as in the case of other amebas of this group previously reported, caused clearing of plate cultures in the case of some organisms but failed to do so in others. The trophozoites were readily soluble in bile and one per cent deoxycholate. Culture methods for their detection in biological materials such as blood, pus, etc., were not studied or developed. The organism divided by mitosis and in culture often appeared joined together after division by intracellular septums somewhat reminiscent of an organoid arrangement. The rounded amebas measured approximately 30 μ. In unstained tissue culture preparations, the amebas bore a superficial resemblance to "damaged" tissue culture cells.

The cysts and precysts, which appeared in the tissue cultures but were not readily demonstrable in the trypticase soy medium, formed clusters which on superficial examination were quite suggestive of groups of yeast cells, but the uniform size, the absence of budding forms, the presence of typical nuclei, and the pore-like structure in the cyst wall differentiated them from yeast cells. Further studies permitting more definitive classification are to be published in a subsequent paper.

The structure of the ameba in stained sections was quite characteristic in fresh lesions, but as the defense process altered the features of the ameba, recognition became increasingly difficult. Hematoxylin and eosin stained preparations were preferable to any other method thus far used, but there was often little or no differentiation in the staining

qualities of the tissue cells and the amebas. It thus became necessary to detect the organisms by the pattern of their nuclei since the cytoplasm of the amebas often was identical in appearance to that of mononuclear phagocytes. The round nucleus with a large karyosome, which usually stained purple or slightly red in formalin-fixed tissue, was the only distinctive feature. The ameba was almost always surrounded by a clear zone, which often helped to locate it on low power magnification. Bizarre forms resembling some of the cysts described in the literature have been seen, but these have not been identified with certainty.

Material and Methods

Cultures of Acanthamoeba used experimentally were subcultures made by inoculation of 40 ml. of monkey kidney cell culture fluid into Povitsky bottles containing one liter of trypticase soy broth (Baltimore Biological Laboratory), pH 7.3, and grown 7 to 10 days at 37° C. on a reciprocating rocker platform such as is used for cultivation of Maitland type kidney cultures in the production of poliomyelitis virus. It has now been learned that virulent cultures of this organism can also be produced by serial transfer on trypticase broth for 3 generations. Ameba counts were performed, utilizing a white blood cell counting chamber. Usually the cultures contained from 200,000 to one million organisms per ml.

Animal Inoculation

Mice. Swiss white mice weighing 15 gm. were anesthetized with ethyl ether to a point of falling. Intranasal inoculation was effected by holding the mouse back down, nose slightly up, and placing .01 to .03 ml. of the fluid over the nares; respiratory efforts caused it to enter the respiratory tract. For intravenous inoculation, 0.5 ml. of fluid was injected into the tail vein. Intracerebral inoculation was accomplished by injecting .03 ml. of fluid into the brain, and intraspinal inoculation by introducing .03 ml. of fluid into the meningeal space lateral to the cord through a transverse skin incision in the mid-dorsal region.[14] Inoculums of 0.2 ml. of fluid were also injected subcutaneously into various sites in the midline over the mid-dorsal region. In addition, 0.5 ml. of fluid was injected intraperitoneally in some mice.

Monkeys. Intravenous inoculation was carried out by the injection of 15 ml. of culture fluid into the anticubital vein of two 4-pound rhesus monkeys. The monkeys, which were observed daily, were bled from the femoral vein for antibody studies before inoculation and at weekly intervals thereafter. Two ml. of culture was introduced into the right ventricle of four 4-pound rhesus monkeys anesthetized with amo-

barbitol sodium ('Amytal,' Lilly). Two of these received 50 mg. of cortisone acetate each day for 3 days. The monkeys were bled at 9 days and sacrificed 16 days after inoculation.

Complement Fixation Tests

Antigen was made by concentrating the trypticase culture fluid containing amebas killed with 1:4,000 formalin solution. The suspension was concentrated by centrifugation; supersonication was carried out for 5 minutes, and the sediment diluted to a concentration equivalent of roughly one million organisms per ml. Whole live amebas were not sufficiently antigenic to be employed as antigen. The complement fixation method of Bengston[15] was used with one hour incubation at 37° C.

Results

The intravenous mouse inoculation experiments were followed by pulmonary granulomas containing many amebas and caused death of the mice only when very large doses were given.

In mice, the more interesting lesions followed intranasal inoculation. With large inoculums (2,000 to 4,000 amebas in .03 ml. of fluid), a spectacular lesion was induced. The nasal mucosa was penetrated and destroyed, and by direct extension the olfactory bulbs were invaded and also extensively damaged. The lungs were the seat of consolidation, and the amebas invaded pulmonary veins causing severe destruction. They were carried to the systemic circulation and could be demonstrated in renal glomeruli, spleen, and heart. There was considerable tendency to migrate into tissue about the blood vessels.

The minimum infectious intranasal dose of amebas has not been determined after several attempts. In some cases large inoculums (3,000 to 5,000 amebas) were not followed by a high percentage of invasions, and in other instances as few as 75 amebas invaded and killed over half the mice inoculated. Small doses tended to cause death by pulmonary involvement while larger doses were followed by brain invasion. The latter were often accompanied by pulmonary lesions, and death usually occurred rapidly. Studies in several mice sacrificed at 24 and 48 hours following instillation indicated that the amebas could traverse the mucosa and enter the olfactory bulb via the olfactory nerve within 24 hours.

Attempts to infect mice by intragastric instillation were not successful. Intraperitoneal and subcutaneous inoculation did not produce death of the animals, and histologic studies 2 weeks after inoculation showed no lesions. Pathologic studies at shorter intervals after inoculation have not been made. Intraspinal injection was followed by invasion of the cord and paralysis.

In order to determine antibody response to live amebas in monkeys, two of four 4-pound rhesus monkeys were given intravenous injections of tissue culture fluid (15 ml.) containing an uncounted number of amebas (estimated in retrospect as approximately 20,000 per ml.). The test and control animals were observed for a period of 5 weeks. No clinical signs were manifest. Necropsy findings were grossly negative in all 4 animals. On microscopic examination, the brains of the monkeys showed lymphocytic choriomeningitis and mild granulomatous inflammation of the cerebral meninges, but no amebas could be identified in these lesions. There were no significant lesions in other tissues or in the control monkeys.

The results of the complement fixation tests (Table I) suggested that an antigenic stimulus had been applied and withdrawn with a rapid disappearance of the specific antibody. This was somewhat

TABLE I

Results of Complement Fixation Tests after Intravenous Injection of Live Acanthamoeba

Monkey no.	Intravenous inoculum (ml. culture)	Complement fixation titer*				
		Prior to inoculation	14 days	21 days	28 days	35 days
F-5635	15	—	16	8	4	2
F-5636	15	—	8	8	4	2
F-5639	0	—	—	—	—	—
F-5640	0	—	—	—	—	—

* Reciprocal of highest serum dilution giving at least a 2+ reaction.

reminiscent of the decline of reagin in patients with early syphilis under intensive treatment. The failure to demonstrate amebas in the tissues would seem to indicate that the positive complement fixation test was dependent upon the continued presence of the amebas in the animal tissues.

In order to study the lesions which might be produced in monkeys when the amebas were distributed via the systemic circulation, 2 ml. of a culture containing about 200,000 amebas per ml. was introduced intracardially into the left ventricle of four 4-pound rhesus monkeys. Two animals were given cortisone as described and were sacrificed in 16 days. Lesions appeared only in the brain in these two animals. In monkey C-889 a yellowish lesion, approximately 1 cm. in diameter, was found in the meningeal surface of the right parietal lobe. This proved to be a superficial brain abscess over which was a severe but localized meningitis. In monkey C-896 no meningeal lesion was encountered, but a similar abscess was found in the left occipital lobe.

Amebas were demonstrated in the abscess contents by smear in both cases. Histologic examination showed no alterations except in relation to the abscesses; there were necrosis and a marked acute inflammatory exudate containing numerous amebas. The other two monkeys received no cortisone and remained symptomless. They were sacrificed on the 38th day. Gross and microscopic examination in these animals revealed neither lesions nor amebas, but it is suspected that more detailed investigation might have demonstrated them.

Table II shows the results of complement fixation tests in these monkeys. No correlation can be made between the presence of lesions and the antibody titer. Cortisone did not suppress the development of antibody except possibly in one of the test monkeys. The variation in

TABLE II

Results of Complement Fixation Tests after Intracardial Injection of Live Acanthamoeba

Monkey no.	Cortisone (50 mg.)	Ameba inoculated (2 ml.)	Lesions observed	Complement fixation titer*		
				3/20	3/27	4/1
C-889	3/9–10–11	3/11	Brain abscess 3/27	—	—	—
C-896	3/9–10–11	3/11	Brain abscess 3/27	8	128	—
C-895	None	3/11	None	8	4	4
C-897	None	3/11	None	4	256	128

* Reciprocal of highest serum dilution giving at least a 2+ reaction.

response suggests the possibility that some monkeys were previously sensitized. Unfortunately, pre-inoculation blood samples were not obtained. It cannot be determined, therefore, whether or not the animals had pre-existing complement fixing antibodies before inoculation. We have found on testing approximately 100 "normal" monkeys that occasional monkeys have antibody titers as high as 1 to 8.

DISCUSSION

The possibility of concomitant pathogenic virus, bacteria, or fungus was considered early in the study; thus far none has been demonstrated. Other observers have had little success in growing bacteria or fungi, once phagocytosis by amebas has occurred. Admittedly, it is very difficult to eliminate the contributory significance of a virus by any method. There is no question, however, that the Acanthamoeba is able to enter the body by its own power and may be able to do so in nature as well. The potentiality of repeated damage to organs and the possibility of a true or mechanical vector role are suggested by these experiments. By its capacity to penetrate the mucous membrane, this

ameba might conceivably assist microbial infectious agents in breaking through the natural barriers.

The Acanthamoeba, like that reported by Negroni and Fischer,[6] is bile soluble. This may explain its failure to infect when ingested. The great increase in motility which is seen when the organism is placed in saliva, tears, and sterile gastric mucin might contribute to its invasive capacity in the nasal cavity. There is evidence to suggest that the ameba may multiply in the mucus of the nasal cavity; thus a small inoculum may grow into a larger one before invasion occurs. One cannot be certain, in the absence of effective investigative methods, whether very few amebas could indeed invade the mucous membrane. If this were the case, however, entrance into the animal body, occurring naturally, would be followed by limited lesions.

The histologic similarity of the organisms to degenerated mononuclear cells in ordinary preparations makes it difficult to detect them in lesions. A specific staining method for this purpose has not yet been devised. Since the numbers involved in any natural infection may be quite small, it is likely that immunologic methods, such as the fluorescent antibody technique and hypersensitivity tests, may be necessary for evaluation of the role of the ameba in diseases of animals other than mice.

This paper has dealt only with the phenomenon of invasion and the acute phase of the reaction to Acanthamoeba. Its importance in chronic disease is yet to be determined. Further study of related strains of Acanthamoeba are indicated, and the distribution of pathogenic forms in nature require investigation.

Conclusions

A strain of Acanthamoeba similar to that described by Castellani, Douglas, and others has been isolated from monkey kidney tissue culture. This proved to be pathogenic for mice and to a limited extent for monkeys.

The implications of these observations have been outlined and future investigation suggested in order to determine whether Acanthamoeba and related genera are of importance in naturally occurring disease processes.

REFERENCES

1. Kudo, R. R. Protozoology. Charles C Thomas, Springfield, Ill., 1954, ed. 4, 966 pp.
2. Volkonsky, M. Hartmannella castellani Douglas et classification des Hartmannelles. (Hartmennellinae nov. subfam., Acanthamoeba nov. gen., Glaeseria nov. gen.) *Arch. de Zool. Exper. et Gén.*, 1931, **72**, 317–339.

3. Castellani, A. An amoeba growing in cultures of a yeast: second note. *J. Trop. Med.*, 1930, **33**, 188–191.
4. Douglas, M. Notes on the classification of the amoeba found by Castellani in cultures of a yeast-like fungus. *J. Trop. Med.*, 1930, **33**, 258–259.
5. Jollos, V. Untersuchungen zur Morphologie der Amöbenteilung. *Arch. f. Protistenk.*, 1917, **37**, 229–275.
6. Negroni, P., and Fischer, I. Ensayo sobre la biología de *"Vahlkampfia debilis,"* Jollos, 1917. Amoeba parásita de una levadura y fenómenos de lisis semejantes a la bacteriofágica. *Prensa med. argent.*, 1941, **28**, 279–300.
7. Van Rooyen, C. E. Observations on the clearing effect of *Amoeba (Hartmannella) Castellanii* on bacterial cultures: a phenomenon simulating bacteriophagy. *J. Trop. Med.*, 1932, **35**, 259–266.
8. Shinn, L. E., and Hadley, P. B. Note on the spontaneous contamination of a bacterial culture by an organism resembling *Hartmannella castellanii*. *J. Infect. Dis.*, 1936, **58**, 23–27.
9. Hewitt, R. Natural habitat and distribution of *Hartmannella castellanii* (Douglas), reported contaminant of bacterial cultures. *J. Parasitol.*, 1937, **23**, 491–495.
10. Jahnes, W. G.; Fullmer, H. M., and Li, C. P. Free living amoebae as contaminants in monkey kidney tissue culture. *Proc. Soc. Exper. Biol. & Med.*, 1957, **96**, 484–488.
11. Culbertson, C. G.; Smith, J. W., and Minner, J. R. Acanthamoeba: Observations on animal pathogenicity. *Science*, 1958, **127**, 1506.
12. Hull, R. N.; Minner, J. R., and Mascoli, C. C. New viral agents recovered from tissue cultures of monkey kidney cells. III. Recovery of additional agents both from cultures of monkey tissues and directly from tissues and excreta. *Am. J. Hyg.*, 1958, **68**, 31–44.
13. Technical Committee on Poliomyelitis Vaccine (Shannon, J. A., chairman), and Subcommittee on the Monkey Safety Test (Bodian, D., chairman). The monkey safety test for poliomyelitis vaccine. *Am. J. Hyg.*, 1956, **64**, 104–137.
14. Powell, H. M., and Culbertson, C. G. Mouse immunity tests of trivalent poliomyelitis vaccine. *Proc. Soc. Exper. Biol. & Med.*, 1955, **88**, 563–564.
15. Bengston, I. A. Complement fixation in the rickettsial diseases—technique of the test. *Pub. Health Rep.*, 1944, **59**, 402–405.

LEGENDS FOR FIGURES

FIG. 1. Roller tube monkey kidney tissue culture. Two separate groups of Acanthamoeba are seen at the margin of partially destroyed portions of the cell sheet. Unstained. × 400.

FIG. 2. Acanthamoeba trophozoites from trypticase soy medium suspended in mucin preparation. The organisms have very active motility when thus suspended. Unstained. × 4,000.

(Figs. 3 to 9, inclusive, represent lesions observed in mouse no. 19209-3.)

FIG. 3. Nasal mucosa. Ameba invading mucous membrane. Three organisms are near the surface and two others are deeply embedded. Hematoxylin and eosin stain. × 1,000.

FIG. 4. Nasal mucosa. Ameba beneath epithelium. Mouse inoculated 24 hours before necropsy. Spinous pseudopods are seen. Hematoxylin and eosin stain. × 1,000.

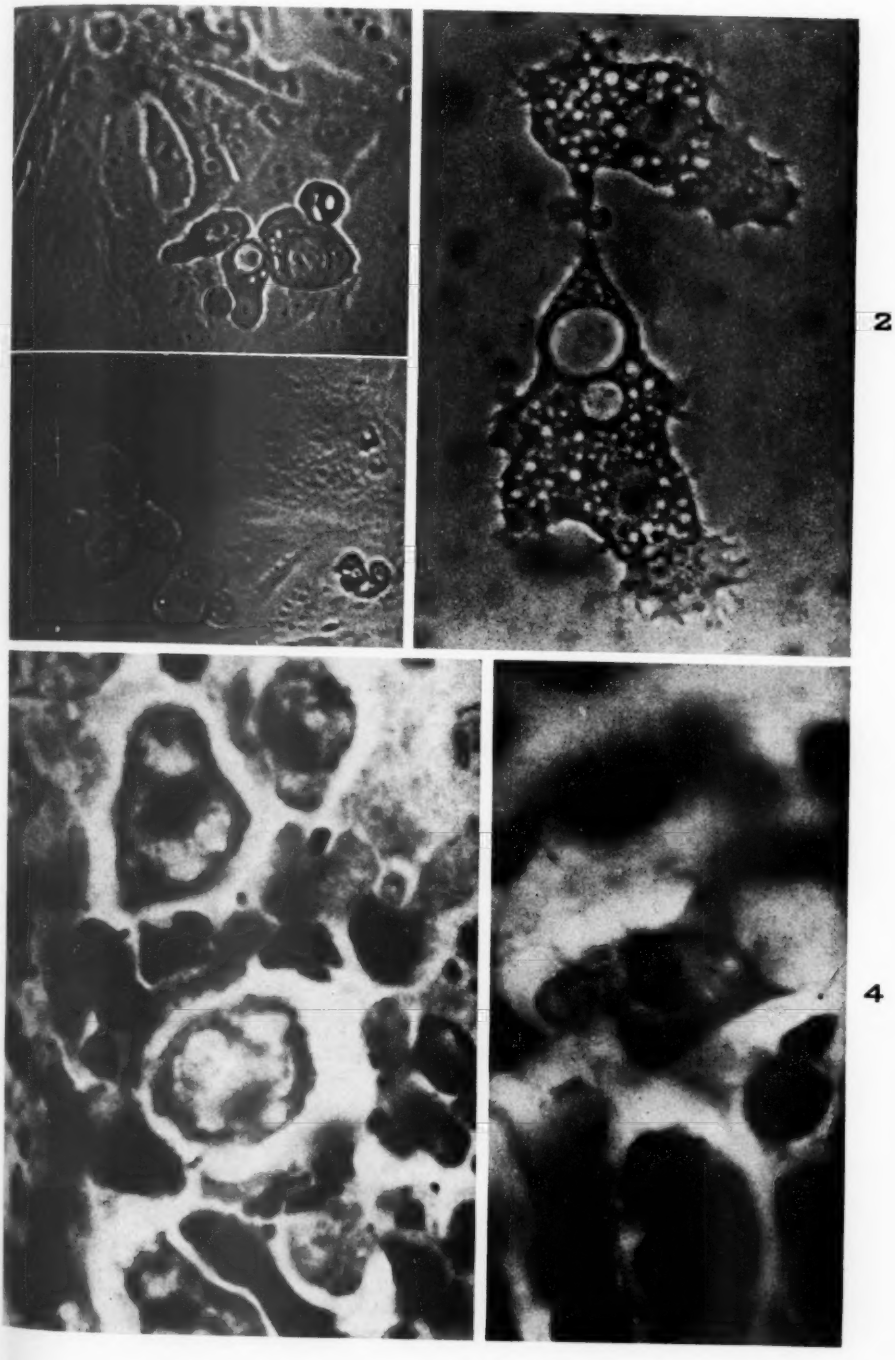
1
2
3
4

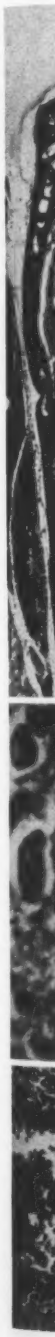

FIG. 5. Mouse head, frontal section at level of eyes. Forebrain is hemorrhagic unilaterally over a zone of destroyed nasal mucosa. Hematoxylin and eosin stain. × 50.

FIG. 6. Mouse forebrain. Approximately midline in the less severely affected frontal lobe shown in Figure 5. A collection of amebas is seen in the brain substance. This process caused death of the mouse in 4 days after intranasal instillation. Hematoxylin and eosin stain. × 500.

FIG. 7. Mouse lung, showing consolidation with many amebas in pulmonary alveoli. Pulmonary vein is invaded and lumen contains amebas. Hematoxylin and eosin stain. × 100.

5

6

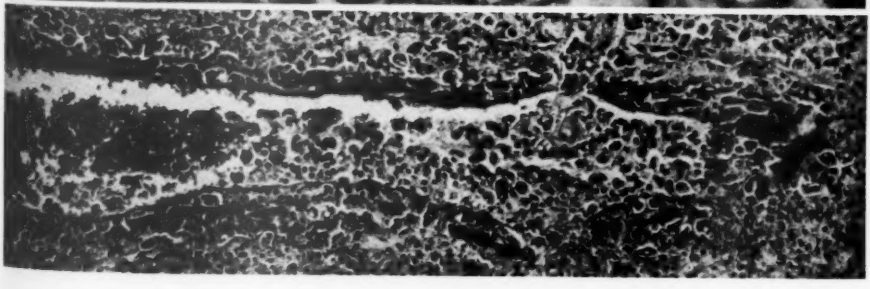

7

FIG. 8. Mouse lung, pulmonary vein. Two amebas are seen beneath the endothelium and several can be seen in the lumen. Hematoxylin and eosin stain. × 1,000.

FIG. 9. Mouse kidney. Two amebas are seen in glomerular capillaries. Hematoxylin and eosin stain. × 400.

FIG. 10. Monkey no. C-896, brain. Occipital lobe of brain showing a recent abscess in which Acanthamoebas were demonstrated. The lesion followed intracardial inoculation and cortisone treatment.

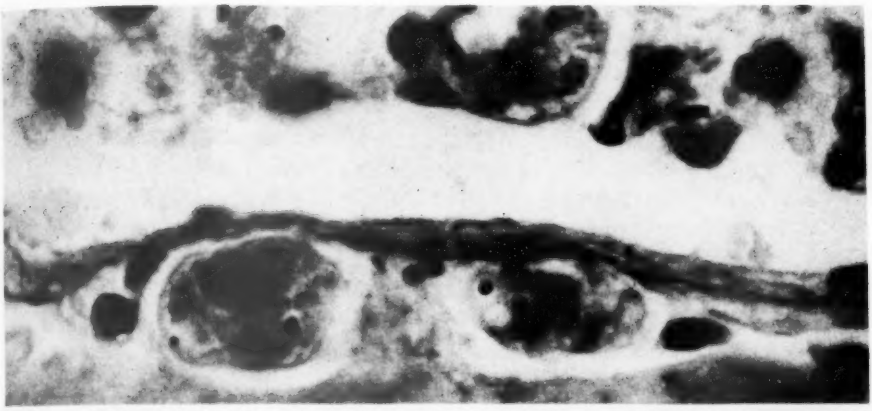

8

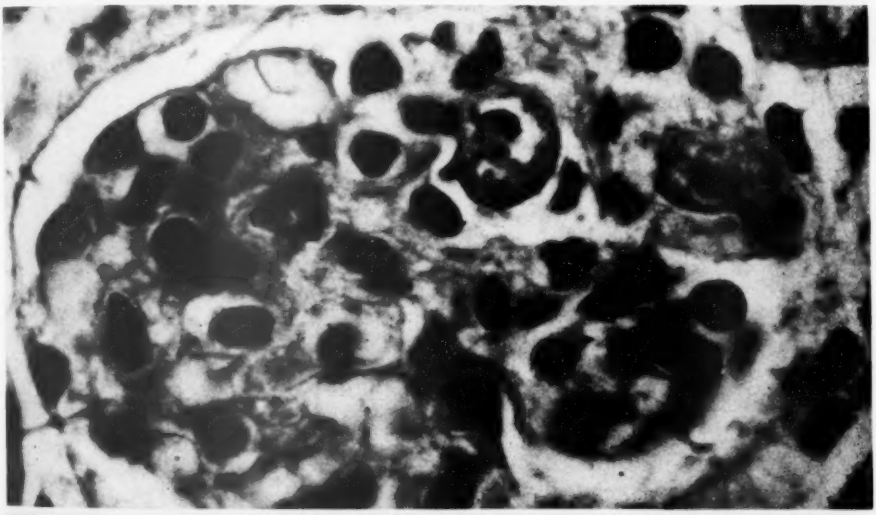

9

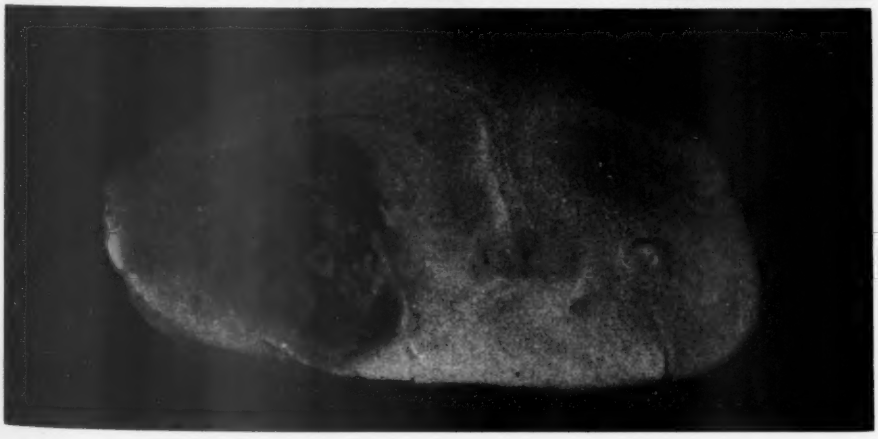

10

OXIDIZED TANNIN-AZO METHOD FOR PROTEIN IN TISSUES*

KENDAL C. DIXON, M.D., Ph.D.

From the Department of Pathology, Cambridge University, Cambridge, England.

Tannic acid can combine with protein present in sections of fixed tissues.[1-4] The tanned sections have a whitish appearance.[4] This bound tannin is readily detected by development of an inky black color with ferric salts.[1-4] The addition of 0.1 N HCl to the solution of tannic acid substantially augments the capacity of the tissues to bind tannin; this indicates that positively charged basic groups in proteins are the principal loci responsible for binding tannic acid.[4] If these basic amino groups of the tissue proteins are masked by fixation in formaldehyde, little tannic acid can be attached subsequently; fixation by agents not containing formaldehyde is thus a prerequisite for the detection of cellular protein by utilizing its tannophilic powers.

By treatment with ferric salts after attachment of tannin, Salazar[3] and Amado[5] studied the distribution of tannophilic substances in the hypophysis, thyroid, stomach, pancreas and kidney. More recently Dixon[4] showed that the chromophilic Purkinje cells of the cerebellum, which contain substantially more protein than the chromophobic Purkinje cells, also contain much more tannophilic material detectable by immersion in tannic acid and subsequent treatment with ferric chloride.

Metallic salts of low solubility may, however, be precipitated in the tissues remote from the original location of their anionic components. Colloidal nuclei in the tissues or cells may determine the sites of precipitation;[6,7] artifacts of this kind vitiated much of the early work on the cellular location of hydrolytic enzymes. An attempt was therefore made to locate the tannin attached to tissue proteins by making the bound tannin participate in covalent union to form a colored dye as opposed to utilizing an ionic interaction with metallic salts. The method described below was devised with this object.

MATERIAL AND METHODS

The tissues studied included cerebral cortex (rabbit), cerebellum (rabbit), skin (rabbit, 5 to 9 days old), liver (rat) and kidney (rat). Immediately after death of the animal, small slices or strips of tissue were removed and immersed in Carnoy's fluid.

Following fixation in Carnoy's fluid for 2 hours the tissues were

* Received for publication, July 3, 1958.

transferred to ethanol. After passage through 3 changes of ethanol (duration, 4 to 6 hours in all), the tissues were immersed overnight in chloroform; they were then transferred to wax (3 changes over 6 hours). Sections 5 μ in thickness were cut, placed on slides, and incubated in an oven at 60° C. overnight. This treatment firmly attached the sections to the slides. Sections used for the oxidized tannin-azo method (as well as for other methods involving the use of tannic acid) were thus affixed to slides without employing any adhesive.

Reagents for Oxidized Tannin-azo Method

Tannic acid-HCl: Dissolve 10 gm. of tannic acid (British Drug Houses, Ltd.) in distilled water; add 25 ml. N HCl (concentrated HCl, specific gravity 1.1800, diluted to 10 times its volume with distilled water), and make up to 250 ml. with distilled water.

Periodic acid: 0.5 per cent (weight per volume) $HIO_4 \cdot 2H_2O$ in distilled water.

Diazotized o-dianisidine: Dissolve 100 mg. of brentamine fast blue B salt (Imperial Chemical Industries, Ltd., Dyestuffs Division) in 100 ml. of ice-cold buffer solution (pH = 4.0) made by mixing 82 ml. of 0.2M aqueous acetic acid and 18 ml. of 0.2M aqueous sodium acetate. This solution contains free diazonium ions liberated from the stabilized product of diazotization of o-dianisidine. The solution should be kept in the refrigerator and used on the day it is prepared.

Oxidized Tannin-azo Method

1. Remove wax from sections with xylene. Wash briefly in ethanol and then in running tap water for 5 minutes. Wash in distilled water.
2. Immerse sections in tannic acid-HCl in a Coplin jar for 10 minutes. The sections become white in color.
3. Wash with 3 changes of distilled water.
4. Place sections on staining rack and flood with two changes of aqueous periodic acid; allow this to act for 5 minutes. During this stage the sections become brownish yellow in color (if sections are cleared and mounted at this juncture, they appear pale yellow).
5. Wash with 3 changes of distilled water.
6. Immerse for 10 minutes in ice-cold diazotized o-dianisidine at 5 to 8° C. in the refrigerator. During this stage the sections become dark salmon red.
7. Wash in distilled water (3 changes) or in running tap water, followed successively by ethanol and xylene. Mount in D.P.X. neutral mountant.

Sections of each tissue studied, treated as above but with stage 4 omitted, were also examined. These unoxidized sections served as controls; they developed only a feeble color.

Use of Formaldehyde to Mask Reactive Groups in Tissue Proteins

After stage 1 in the foregoing method, sections are immersed overnight in 3.6 per cent aqueous formaldehyde and are then washed thoroughly in running tap water and distilled water. The sections are subsequently treated by all the other stages of the oxidized tannin-azo method. These sections give only a very faint coloration.

Tannin and Oxidized Tannin Detected by Ferric Chloride

Oxidized tannin (as well as tannin) held in the tissues can also be detected by treatment with ferric chloride, as opposed to being coupled with diazotized o-dianisidine.

Sections treated directly with ferric chloride after tanning and washing (i.e., after stage 3 above) become inky black in color.[4] For this purpose, a solution containing 10 gm. of $FeCl_3 \cdot 6H_2O$ dissolved in water and made up to 100 ml. (not 250 ml. as inadvertently stated previously[4]) with water, is allowed to act for 1 minute.

After tanning followed by oxidation with periodic acid (i.e., after stage 5 above), subsequent treatment for 1 minute with 10 per cent (weight per volume) aqueous $FeCl_3 \cdot 6H_2O$ gives a conspicuous olive green color to the sections. These sections, when washed in distilled water and passed through ethanol and xylene, give good permanent preparations on mounting in D.P.X. neutral mountant.

Solutions Used for Observations on Oxidation of Tannic Acid in Vitro

Dilute tannic acid: Tannic acid-HCl as prepared above, diluted 1:10 with distilled water.

Periodic acid: As prepared above.

Ferric chloride: 10 gm. of $FeCl_3 \cdot 6H_2O$ made up to 100 ml. with distilled water.

Sodium hydroxide: N NaOH in aqueous solution.

Baryta: 0.1 N $Ba(OH)_2$ in aqueous solution.

Diazotized o-dianisidine: As prepared above.

Oxidized tannic acid: Dilute tannic acid treated with an equal volume of periodic acid. For comparison with this "oxidized tannic acid," dilute tannic acid was diluted further with an equal volume of water so as to contain an equivalent concentration of phenolic acid.

Results

Oxidized Tannin-azo Method

Tanned sections became faint yellowish brown on treatment with periodic acid; when subsequently immersed in diazotized o-dianisidine, the color of the sections rapidly changed to deep salmon red.

Figure 1 shows a section of rabbit cerebellum treated in this manner. The cortex is stained more strongly than the white matter, and the chromophilic Purkinje cells, which are known to be specially rich in protein,[4] are colored with conspicuous intensity. Figure 2 illustrates, at higher magnification, 3 chromophilic and one chromophobic Purkinje cells (also shown in Fig. 1); the chromophilic cells are stained much more darkly than the chromophobic cell. This method also demonstrated the presence of abundant protein in the neuropil of the molecular layer and in the glomeruli of the granule cells of the cerebellar cortex. In cerebral cortex the chromophilic neurones were stained more darkly than the chromophobes; the neuropil of the cortical gray matter of the cerebral hemispheres was also strongly colored.

Figure 3 shows cells from the liver (rat) similarly stained by the oxidized tannin-azo method. The granules of chromatin in the nuclei and the nuclear membranes react strongly. The cell membranes are also prominent. In the cytoplasm small intensely stained particles are visible, as well as larger more feebly colored masses. The dark particles appear to correspond with the basophilic components of hepatic cytoplasm which are so readily stainable by hematoxylin.

Subcutaneous fat from a 5-day-old rabbit is illustrated in Figure 4; the lipocytes shown in this figure may be contrasted with the hepatic cells of Figure 3. In the lipocytes an intense reaction with the oxidized tannin-azo method is confined to the peripheral films of cytoplasm, which enclose spherical empty spaces previously occupied by globules of fat.

Figure 5 shows a section of skin from a 9-day-old rabbit. The deeper layers of the epidermis are colored with intensity. The nuclei of the prickle cells are paler than the cytoplasm which is strongly stained; the cell membranes are also prominent. The *stratum corneum* is feebly colored and the keratinized portions of hairs are unstained; the medullary cells of the hairs, however, give a definite reaction (Fig. 5).

Omission of Various Stages in Oxidized Tannin-azo Method

Tanned sections not treated with periodic acid gave only a very faint coloration on subsequent immersion in diazotized o-dianisidine. When tanned sections were mounted after oxidation with periodic acid and without subsequent coupling with the diazo reagent, they were

very faint yellow in color. Tanned sections oxidized with periodic acid and then treated with sodium hydroxide changed to dark red brown, but the darkly colored material rapidly dissolved out of the tissues and entered the fluid in which they were immersed. Treatment of untanned sections with diazotized o-dianisidine, even after oxidation with periodic acid, gave hardly any detectable coloration.

Masked Active Groups

Sections of cerebrum, cerebellum, liver and skin were immersed overnight in 3.6 per cent aqueous formaldehyde. These sections were then treated by the oxidized tannin-azo method. Coloration was very substantially inhibited, although other sections, stained simultaneously, but not pretreated with formaldehyde, gave the usual deep salmon red coloration. Coloration of tanned sections by ferric iron was similarly inhibited by pretreatment with formaldehyde.

Oxidized Tannin Detected by Ferric Iron

Tanned sections treated with ferric chloride (after stage 3) became blue black in color. After tanning and subsequent oxidation with periodic acid (i.e., after stage 5), some sections were treated with ferric chloride instead of diazotized o-dianisidine. These sections rapidly assumed an olive green color. Figure 6 shows a chromophilic and a chromophobic Purkinje cell in the cerebellar cortex stained by this method. The deep olive green of the chromophilic Purkinje cell was a conspicuous feature. The ferric salt of oxidized tannin was olive green in contrast to the blue black color of ferric tannate itself.

Some Properties of Oxidized Tannic Acid

Tannic acid-HCl, the prime reagent for the oxidized tannin-azo method, is brownish yellow in color. This solution gave a deep brown precipitate on treatment with an equal volume of periodic acid. When diluted 1:10 with water, the tannic acid-HCl reagent was scarcely colored. This diluted solution was used for investigating the oxidation of tannic acid by periodic acid with the following results:

On treatment with an equal volume of periodic acid, dilute tannic acid became pale golden brown in color; this golden brown solution will be referred to as oxidized tannic acid. For comparison with oxidized tannic acid, the dilute tannic acid was further diluted with an equal volume of water. This latter solution will be referred to as tannic acid.

Ferric chloride (1 drop) gave a deep indigo blue color with tannic acid (2 ml.), but with freshly prepared oxidized tannic acid (2 ml.) a

dark olive green precipitate was formed on the addition of ferric chloride (1 drop). In tanned sections, as we have seen, after oxidation with periodic acid, a similar olive green color was given by treatment with ferric chloride.

Tannic acid turned yellow on addition of an equal volume of N NaOH; the resultant solution slowly darkened at its surface in contact with air. Oxidized tannic acid immediately became deep golden red in color on similar addition of sodium hydroxide.

The addition of barium hydroxide to tannic acid (in equal volumes) gave a blue green precipitate, but with oxidized tannic acid a red brown precipitate followed similar mixture with baryta.

An equal volume of diazotized o-dianisidine gave a pale salmon red color on addition to tannic acid. Oxidized tannic acid became deep salmon red in color when similarly treated with diazotized o-dianisidine; within a minute of mixture a dark red precipitate became visible. This intensely colored red precipitate flocculated in about 15 minutes, leaving a colorless supernatant fluid.

Discussion

Tannic acid bound to the tissues is oxidized by periodic acid to form a yellowish compound which may then be coupled with diazotized o-dianisidine to form an intense salmon red dye. In this way tannic acid held by tissue protein may be visualized by covalent union to form a conspicuously colored compound.

Previous methods for locating tannic acid attached to tissues involve the formation of colored ferric salts[1-4] or the reduction of complex diamine silver ions to metallic silver.[8] The oxidized tannin-azo method avoids some of the potential artifacts introduced by possible dissociation of metallic salts or the precipitation of metals and salts at sites remote from their point of formation. This method depends on coupling oxidized tannic acid to a diazonium compound by covalent linkage to form an azo dye, as opposed to forming a colored salt by the more readily reversible attachment of a metallic ion. The site of tanning in the tissues is thus located with greater precision.

Nature of Tannophilic Loci in the Tissues

Tannic acid is most effectively bound at acid pH; this suggests that positively charged amino groups in the tissue proteins are the loci responsible for attachment of tannin.[4] This view was substantiated by the observations on sections pretreated with formaldehyde. These sections gave a relatively poor coloration either with the oxidized tannin-azo method or with the tannate-iron technique. Formaldehyde

combines with both $-NH_2$ and –NH groups in tissue proteins; it is likely that the former are mainly concerned in rapid tanning as applied to sections.[4] The combination of formaldehyde with amino groups in the protein may thus mask their capacity to bind tannin. Elimination of amino groups by the action of nitrous acid is known to diminish the power of hide powder to take up tannin.[9] The effect of formaldehyde, in inhibiting the development of a strong color in sections treated by the oxidized tannin-azo method, probably depends on similar inactivation or masking of the tannophilic loci in the tissues.

It is thus probable that the oxidized tannin-azo technique detects positively charged loci in the tissue proteins. As these loci include the amino groups of the tissue proteins, the necessity for avoiding fixatives containing formaldehyde is comprehensible.

Composition of Oxidized Tannin

Without oxidation by periodic acid the tannin held in the tissues does not effectively couple with diazotized o-dianisidine to form a highly colored compound. It is therefore relevant to consider the nature of the product of oxidation, which is subsequently coupled to form the intense salmon red dye.

When tannic acid in solution is oxidized with periodic acid, a brown color develops. The resulting yellow brown solution gives reactions with ferric iron, NaOH, $Ba(OH)_2$ and with diazotized o-dianisidine which differ markedly from those given by the original unoxidized tannic acid. It is apparent that a new compound is formed. Similarly the tannic acid bound to tissues is converted into a new derivative by oxidation with periodic acid; this oxidized product in the tissue sections gives an olive green ferric salt and a red brown color with alkali, and it also couples with diazotized o-dianisidine to form an intensely colored dye which is firmly held to the tissues.

The tannic acid bound to tissue sections when oxidized by periodic acid, thus has properties similar to those of oxidized tannic acid in solution. It is likely, therefore, that oxidation by periodic acid causes the same change in the constitution of bound tannic acid as is effected in solution.

Some of the color reactions of oxidized tannic acid are similar to those described for ellagic and luteic acids, which can be formed from tannic acid by oxidation with arsenate. Another possibility, however, is that oxidation of tannic acid, which itself contains o-quinol hydroxyl groups, gives rise to an o-quinone. Ramachandran and Sarma[10] treated various dyes containing o-quinol groupings (including alizarin red S and ellagic acid) with alkaline periodate; they noted a change of

color and concluded from absorptiometric observations on the resultant solution that o-quinones are formed as the products of oxidation. It seems likely that tannic acid, which also contains hydroxyl groups in o-quinol position, may be oxidized similarly to an o-quinone by periodic acid. Such a quinone derived from tannic acid would still contain one hydroxyl group in each aromatic nucleus, since tannic acid is a vicinal trihydroxy compound. Hydroxy quinones can, moreover, be coupled in acid solution with diazonium salts to form azo dyes.[11,12] This would account for the formation of an intensely colored azo dye on the addition of diazotized o-dianisidine to oxidized tannic acid.

According to this view, the rapid change in color of the tanned sections from white to brownish yellow on treatment with periodic acid was due to the oxidation of the tannin bound in the tissues to an o-quinone; this latter compound, which was still held by the tissue proteins, could then be coupled with diazotized o-dianisidine to form an intensely colored azo dye. Tannic acid in solution was similarly oxidized, and the resulting compound was also convertible to a red insoluble dyestuff by treatment with diazotized o-dianisidine. The constitution of the dye formed is still uncertain, but its formation from tannic acid held in the tissues affords a convenient and rapid method for revealing the location of cellular protein.

Summary

Tannic acid can be bound to proteins in sections of fixed tissues. This bound tannic acid is oxidized by periodic acid to a brownish yellow compound which can then be coupled with diazotized o-dianisidine to form an intensely colored salmon red azo dye. The sequence of reactions enables the site of cellular protein to be located with precision.

Without oxidation by periodic acid, tanned sections are only feebly colored on treatment with diazotized o-dianisidine. Observations on tanned sections, as well as on tannic acid in solution, indicate that the oxidized tannin-azo method depends on the covalent union of a product of oxidation of the tannic acid held by the tissues with a diazonium salt. The resulting azo dye is firmly attached to the tissue proteins.

The product of oxidation of tannic acid by periodic acid, which may be an o-quinone, can also be detected in the tissues by its capacity to form an olive green ferric salt.

Treatment of tanned sections with formaldehyde inhibits subsequent coloration by oxidation and coupling. This observation confirms the view that amino groups in cellular proteins are the loci revealed by the oxidized tannin-azo method. Pretreatment with formaldehyde effectively masks these reactive groups.

The oxidized tannin-azo method demonstrates abundant protein in cells of the liver, kidney, epidermis, cerebrum and cerebellum. The chromophilic and chromophobic Purkinje cells of the cerebellum are well differentiated by disparity in their content of protein.

REFERENCES

1. Salazar, A. L. Méthodes pour la coloration des éléments tannophiles: tannin-osmium; tannin-osmium-fer. *Compt. rend. Soc. de Biol.*, 1921, **84**, 991–994.
2. Salazar, A. L. La méthode tanno-ferrique: mordançage tanno-acétique. *Anat. Rec.*, 1923, **26**, 60–64.
3. Salazar, A. L. La technique de tannin-fer. *Stain. Technol.*, 1944, **19**, 131–135.
4. Dixon, K. C. Differentiation of chromophilic and chromophobic neurones. *J. Anat.*, 1958, **92**, 425–432.
5. Amado, P. O método tano-férrico de Salazar no estudo da estrutura renal. *Gaz. med. port.*, 1954, **7**, 287–290.
6. Lison, L. Histochimie et Cytochimie Animales. Gauthier-Villars, Paris, 1953, ed. 2, pp. 507–509; 513–514.
7. Pearse, A. G. E. Histochemistry, Theoretical and Applied. J. & A. Churchill, Ltd., London, 1953, p. 256.
8. Gatenby, J. B., and Beams, H. W. (eds.) The Microtomist's Vade-mecum (Bolles-Lee). A Handbook of the Methods of Animal and Plant Microscopic Technique. J. & A. Churchill, Ltd., London, 1946, pp. 548–549.
9. Thomas, A. W., and Foster, S. B. The behaviour of deaminized collagen. Further evidence in favor of the chemical nature of tanning. *J. Am. Chem. Soc.*, 1926, **48**, 489–501.
10. Ramachandran, L. K., and Sarma, P. S. Periodate oxidation of dyes containing the hydroquinone grouping. *J. Sci. Indust. Res.*, 1951, **10B**, 147–148.
11. Kehrmann, F., and Goldenberg, M. Ueber Azochinone. *Ber. deutsch. chem. Gesellsch.*, 1897, **30**, 2125–2130.
12. Kvalnes, D. E. An optical method for the study of reversible organic oxidation-reduction systems. IV. Arylquinones. *J. Am. Chem. Soc.*, 1934, **56**, 2478–2481.

The author wishes to thank A. J. King for very valuable technical assistance and S. W. Patman for the photomicrography. Brentamine fast blue B salt, for preparing diazotized o-dianisidine, was kindly given by Imperial Chemical Industries, Ltd. (Dyestuffs Division).

[*Illustrations follow*]

LEGENDS FOR FIGURES

FIG. 1. Cerebellum of rabbit stained by oxidized tannin-azo method. The cortex is strongly stained. The chromophilic Purkinje cells are colored intensely; chromophobic Purkinje cells are also visible. × 114.

FIG. 2. Cerebellum of rabbit stained by oxidized tannin-azo method. Higher magnification of part of the same field shown in Figure 1, illustrating 3 intensely stained chromophilic Purkinje cells and one chromophobic Purkinje cell. × 450.

1

2

FIG. 3. Liver of rat stained by oxidized tannin-azo method. × 1,070.

FIG. 4. Subcutaneous fat of rabbit stained by oxidized tannin-azo method. × 450.

FIG. 5. Abdominal skin of young rabbit stained by oxidized tannin-azo method. The cells of the malpighian layer of the epidermis are colored intensely. × 420.

FIG. 6. Cerebellum of rabbit colored olive green by ferric chloride after tanning and subsequent oxidation with periodic acid. A chromophilic Purkinje cell is stained much more strongly than an adjacent chromophobic Purkinje cell. × 410.

3

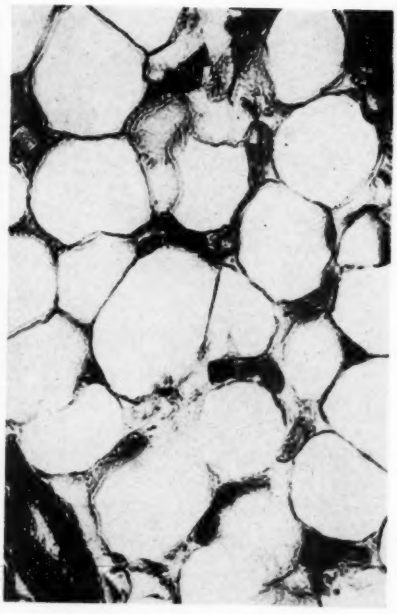

4

5

6